

Sphingosine-1-phosphate dynamically regulates GLUT activity through PP2A in normal and diabetic red blood cells

Inaugural-Dissertation

zur Erlangung des Doktorgrades
der Mathematisch-Naturwissenschaftlichen Fakultät
der Heinrich-Heine-Universität Düsseldorf

vorgelegt von

Nadine Thomas

aus Düsseldorf

Düsseldorf, Mai 2024

aus dem Institut für Molekulare Medizin III
der Heinrich-Heine-Universität Düsseldorf

Gedruckt mit der Genehmigung der
Mathematisch-Naturwissenschaftlichen Fakultät der
Heinrich-Heine-Universität Düsseldorf

Berichtersteller:

1. Prof. Dr. Bodo Levkau
2. Prof. Dr. Jürgen Scheller

Tag der mündlichen Prüfung:

04.09.2024

Table of contents

1	Abstract	I
2	List of Abbreviations	II
3	List of Figures	VI
4	List of Tables	VII
5	Introduction	1
5.1	Sphingolipids and their metabolism	1
5.2	Sphingosine-1-phosphate signalling and its role in cellular processes	5
5.2.1	Shingosine-1-phosphate signalling – receptor dependent	5
5.2.2	Shingosine-1-phosphate signalling – receptor independent	8
5.2.3	Shingosine-1-phosphate regulation and transport	9
5.3	Sphingosine-1-phosphate related medication	10
5.4	Red blood cells - specialized suppliers for the body	14
5.4.1	Shingosine-1-phosphate in blood and red blood cells	15
5.5	Glucose transport as an important distributor of energy source	16
5.5.1	Glucose in red blood cells and disorder due to hyperglycaemia	18
5.6	PP2A - more than just a tumour suppressor	20
6	Aim of this study	23
7	Material and Methods	25
7.1	Materials	25
7.1.1	Devices	25
7.1.2	Consumables	32
7.1.3	Chemicals & Reagents	33
7.1.4	Commercial Kits	39
7.1.5	Laboratory animal diet	39
7.1.6	Cell culture media	40

7.1.7	Antibodies for Western blot.....	40
7.1.8	Antibodies/ Proteins for flow cytometry.....	40
7.1.9	Primers for quantitative Real-Time PCR.....	41
7.2	Methods.....	42
7.2.1	Human samples	42
7.2.2	Mouse models	42
7.2.3	Culturing of HEK293-Mfsd2b cells.....	42
7.2.4	Transient transfection of HEK293 cells with SphK1	43
7.2.5	Stable transfection of HEK293 cells with Sphk1	44
	Bacterial strains and plasmid preparation.	44
	Cloning.....	44
	Transfection.....	45
	Selection	45
7.2.6	RBC isolation and preparation.....	45
7.2.7	Sphingolipid loading	45
7.2.8	Efflux assay	46
7.2.9	LC-MS/MS measurement	46
7.2.10	Glucose uptake	47
	Glucose uptake assay with RBCs	48
	Glucose uptake assay with HEK293 cells.....	49
7.2.11	PP2A activity.....	49
7.2.12	GLUT activity.....	50
	Liposome reconstitution.....	51
	Phosphate assay (quantification of phospholipids)	51
	Liposome [³ H] glucose uptake	52
7.2.13	RBC ghost preparation.....	52

7.2.14	Lipid raft isolation	53
7.2.15	Western blot analysis	53
	Protein determination	53
	Protein separation with sodium dodecyl sulfate–polyacrylamide gel electrophoresis (SDS-Page).....	54
	Western blot.....	54
7.2.16	Quantitative Real-Time PCR	55
	RNA isolation	55
	cDNA synthesis	55
	Quantitative Real-Time PCR	55
7.2.17	GLUT4 surface measurement	57
	Preparation and validation	57
	Measurement	58
7.2.18	GLUT1 surface measurement	58
7.2.19	Hba1c measurement	58
7.2.20	Lipid peroxidation measurement	59
7.2.21	Statistics.....	59
8	Results.....	61
8.1	Glucose uptake in erythrocytes determined by dynamic regulation of intracellular S1P levels	61
8.2	The S1P exporter Mfsd2b impacts the extent of RBC glucose uptake	68
8.3	FTY720-P decreases glucose uptake	72
8.4	S1P reduces the amount of GLUT on the surface of RBCs.....	74
8.5	S1P regulates glucose uptake through modulation of PP2A activity	76
8.6	S1P regulates cell surface GLUT1 expression, glucose uptake and PP2A activity in human RBCs.....	79

8.7	RBCs from chronically hyperglycemic mice have higher S1P levels and increased Sphk1 and PP2A activities.....	81
8.8	Patients with diabetes mellitus type 2 exhibit high S1P and increased PP2A activity in RBCs	82
8.9	Lack of Mfsd2b prevents the pathological HbA1c increase in chronic hyperglycemia	84
9	Discussion	87
9.1	S1P regulates glucose uptake in human and mice RBCs under normoxic conditions 87	
9.2	Glucose uptake rescue happens via the export of S1P through the transporter Mfsd2b.....	88
9.3	Phosphorylated Fingolimod, like S1P, regulates glucose uptake in RBCs	90
9.4	The activity of GLUT protein is not regulated by S1P concentration in the plasma membrane	90
9.5	S1P leads to increased internalization of GLUT transporter at the cell surface of RBCs	91
9.6	S1P activates PP2A, resulting in internalization of GLUT in mice and human RBCs	93
9.7	S1P has a protective effect on RBCs under hyperglycemic conditions	94
10	Summary and outlook	96
11	Graphical abstract.....	98
12	References	99
13	Erklärungen.....	111
13.1	Eidesstattliche Versicherung.....	111
13.2	Bemerkung / Remark	112

1 Abstract

This study reveals the crucial role of red blood cells (RBCs) as carriers of sphingosine-1-phosphate (S1P) in the bloodstream and demonstrates a direct dependency on the glucose uptake of these cells. Through genetic and pharmacological interventions, it was possible to modulate the S1P levels within RBCs, thereby influencing glucose uptake and metabolic activity. This modulation occurs via S1P-triggered activation of the catalytic protein phosphatase 2 (PP2A) subunit, which in turn regulates the abundance and activity of cell-surface glucose transporters (GLUTs). The study demonstrates that this regulatory mechanism is capable of dynamically adjusting to metabolic changes in the environment, boosting S1P synthesis, enhancing PP2A activity, and consequently reducing the phosphorylation and surface expression of GLUTs. Consequently, glucose uptake in red blood cells (RBCs) from diabetic individuals is diminished, offering a protective effect against lipid peroxidation associated with hyperglycaemia and diabetes. Experimental evidence, including observations in diabetic mice and humans, as well as in mice lacking the S1P exporter *Mfsd2b*, supports the effectiveness of this mechanism. Notably, these mice exhibit resistance to the elevation of HbA1c levels in diabetic individuals and reduced generation of thiobarbituric acid reactive substances (TBARS) in diabetic red blood cells (RBCs). Interestingly, this regulatory role of S1P on glucose uptake was not exclusive to RBCs but was also observed in nucleated cells like HEK293 cells. Moreover, the findings of this study indicate that pharmacological agents such as fingolimod, which mimic S1P activity, could potentially replicate these therapeutic effects. These results suggest a broader applicability of the revealed mechanism beyond red blood cells, potentially extending to insulin-independent tissues.

2 List of Abbreviations

°C	degree Celsius
µg	microgram
µL	microliter
µM	micromolar
2DG	2-deoxyglucose
2DG6P	2-Deoxyglucose-6-phosphate
A2B	adenosine receptor 2B
ABC-Transporter	ATP binding cassette-Transporter
AC	adenylate cyclase
ADP	adenosine diphosphate
APC	adenomatous polyposis protein
ApoE	apolipoprotein E
ATP	adenosine triphosphate
BSA	bovine serum albumin
C1P	ceramide 1-phosphate
Ca ²⁺	calcium
cDNA	complementary deoxyribonucleic acid
CO ₂	carbon dioxide
CT	threshold cycle
DGK	diacylglycerol kinase enzyme
DMEM	dulbecco's Modified Eagle's Medium
DMSO	dimethyl sulfoxide
DNA	deoxyribonucleic acid
DOP	4-Deoxypyridoxin
ECL	enhanced chemiluminescence
EDTA	ethylenediaminetetraacetic acid
EGFP	enhanced green fluorescent protein
EGTA	ethylene glycol-bis(β-aminoethyl ether)-N,N,N',N'-tetra acetic acid
ELISA	enzyme linked immunosorbent assay

List of Abbreviations

ER	endoplasmic reticulum
ERK	extracellular-signal regulated kinases
EtOH	ethanol
FTY720	fingolimod
FTY720-P	fingolimod-phosphate
g	gravitational force equivalent
GAPDH	glycerin aldehyde 3-phosphate dehydrogenase
GDP	guanosine diphosphate
GLU1-4	glucose transporter 1-4
GPCR	G-Protein coupled receptor
h	hour/s
HbA1a	hemoglobin A1a
HbA1b	hemoglobin A1b
HbA1c	hemoglobin A1c
HDL	high density Lipoprotein
HRP	horseradish peroxidase
HTLV	human T lymphotropic virus
Ip	immunoprecipitation
kcal	kilocalories
KO	knockout
L	liter
LB-media	lysogeny broth media
LDL	low density Lipoprotein
LS-MS/MS	liquid chromatography-mass spectrometry /mass spectrometry
M	molar
MAPK	mitogen-activated protein kinase
MCV	mean corpuscular volume
MeOH	methanol
MFS	major facility superfamily
Mfsd2b	major facilitator superfamily transporter 2b
mg	milligram

List of Abbreviations

min	minute/s
Mio	million
ml	milliliter
mM	millimolar
mRNA	messenger RNA
MS	multiple sclerosis
MSA	malondialdehyde
n	count (number of replicated)
NADH	nicotinamide adenine dinucleotide
NADPH	nicotinamide adenine dinucleotide phosphate
ng	nanogram
NGS	normal goat serum
nm	nanometer
NP-40	nonyl phenoxy polyethoxy ethanol
OD	optical density
PA	phosphatidic acid
PBS	phosphate-buffered saline
PC	phosphatidylcholine
PCR	polymerase chain reaction
PFA	perfluoro alkoxy alkanes
Pi	phosphate
PI3K	phosphoinositol-3-Kinase
PLC	phospholipase C
pM	picomolar
pmol	picomole
PP1	protein phosphatase 1
PP2	protein phosphatase 2
PP2A	protein phosphatase 2A
PPP	pentose phosphate pathway
PVDF	polyvinylidene difluoride
q-rtPCR	quantitative real time PCR

List of Abbreviations

RBC	red blood cell
RDW	red cell distribution width
RNA	ribonucleic acid
Rpm	rounds per minute
RT	room temperature
s	second/s
S1P	sphingosin-1-Phosphat
S1PR1-5	sphingosin-1-Phosphat-Rezeptor 1-5
SD	standard derivation
SDS	sodium Dodecyl Sulfate
SGLT	sodium-driven glucose symporters
Sgpl	sphingosin-1-Phosphat Lyase
SLC	solute carrier
SM	sphingomyelin
Sph	sphingosine
SphK1	sphingosine kinase 1
SphK2	sphingosine kinase 2
SPNS2	spinster homologue 2
SRF	Serum response factor
T2DM	type 2 diabetes mellitus
TBA	thiobarbituric acid
TBS	tris-buffered saline
TCA	trichloroacetic acid
TBARS	thiobarbituric acid reactive substances
TMB	3,3,5,5-Tetramethylbenzidin
UK	United Kingdom
USA	United States of America
V	volt
VLDL	very low density Lipoprotein
WT	wildtype

3 List of Figures

Figure 1: Simplified overview of sphingolipid metabolism.	4
Figure 2 Schematic S1P receptor signaling pathways.	6
Figure 3: Phosphorylation of FTY720 to FTY720-P generates a structural analog to S1P... ..	11
Figure 4: Drugs based on the mode of action of S1P receptor modulation.	13
Figure 5: Schematic structure of holoenzyme PP2A.	21
Figure 6: Plasmid construct of EGFP-C1-Sphk1 plasmid.....	44
Figure 7: Principle of Glucose uptake-glow assay Kit (Promega, Madison, USA).	48
Figure 8: S1P loading of RBCs by sphingosine leads to lower glucose uptake. S1P-unloading with BSA or a S1P neutralizing antibody restores glucose uptake.....	62
Figure 9: Effect of S1P and sphingosine on RBC integrity.	64
Figure 10: Elevated intracellular S1P decreased RBC glucose uptake in mice RBCs <i>in vivo</i>	66
Figure 11: Low intracellular S1P increases glucose uptake in murine RBCs <i>in vivo</i>	67
Figure 12: Mfsd2b activity controls glucose uptake in RBCs by modulating intracellular S1P levels.	69
Figure 13: Mfsd2b activity controls glucose uptake in stable transfected HEK293 cells....	70
Figure 14: Mfsd2b activity controls glucose uptake in transient transfected HEK293 cells.	71
Figure 15: FTY720 and FTY720-P transport in RBC occurs independently of Mfsd2b with FTY720-P but not FTY720 suppressing glucose uptake.	73
Figure 16: S1P content of liposomes has no influence on glucose uptake in GLUT4 reconstituted liposomes.....	74
Figure 17: S1P has no influence on GLUT4 protein distribution on lipid rafts of RBCs.....	75
Figure 18: S1P regulates cell surface GLUT4 on mouse RBCs	76
Figure 19: S1P regulates glucose uptake by activating PP2A <i>in vitro</i> and <i>in vivo</i>	78
Figure 20: S1P regulates human RBC glucose uptake, PP2A activity and cell surface GLUT1.	80
Figure 21: RBC from chronically hyperglycemic mice have higher S1P levels and increased PP2A activity.	82

Figure 22: RBC from patients with diabetes mellitus type 2 have higher S1P levels and increased PP2A activity. 84

Figure 23: RBC from chronically hyperglycemic *Mfsd2b*^{-/-} mice have no changes in HbA1c level..... 86

Figure 24 Illustrative description of the uncovered role of S1P in regulation of glucose uptake in red blood cells. 98

4 List of Tables

Table 1: Media and supplements for cell cultivation. 40

Table 2: Primers for different genes used for RT qPCR. 41

Table 3: Mobile phase gradient settings. 47

Table 4: Pipetting scheme for 12%/4% SDS-PAGE gels, 1.5 mm..... 54

Table 5: Protocol for quantitative Real-Time PCR..... 57

5 Introduction

5.1 Sphingolipids and their metabolism

Sphingolipids, also known as sphingophospholipids, together with phosphoglycolipids belong to the phospholipids, which represents one of the main classes of eukaryotic lipids. Johann Ludwig Wilhelm Thudichum, a German pathologist, biochemist and physiologist was the first who isolated sphingolipids from brain tissue in 1884. He entitled the name sphingosine after the mythical creature, the Sphinx [1]. Years later, the bioactive functions of the sphingolipids were discovered and defined, first for sphingosine, followed by ceramide and S1P. The newfound significance in regulating various aspects of cell growth has propelled sphingolipids into a distinct category of bioactive lipids. Today more than 300 different sphingolipids are known [2-6]. Sphingolipids represent a diverse class of lipids that play crucial roles in cellular structure and signaling across various species. While the basic structure and function of sphingolipids are conserved, variations in types and abundance exist among different organisms. For instance, plants and fungi also possess sphingolipids, albeit with less diversity compared to animals. In plants, glucosylceramides contribute to membrane structure, inositol phosphorylceramides are implicated in stress responses and signaling, and phytoceramides play a role in plant development [7]. Fungi, like plants, have inositol phosphorylceramides serving similar functions. In addition, the lipid manosyl-inositol phosphorylceramides is decisive for maintaining cell wall integrity in fungi [8, 9]. Sphingolipids found in animal organisms exhibit greater complexity. Sphingosine (Sph), ceramide, and sphingosine-1-phosphate (S1P) stand thereby out as biologically crucial. Several studies in recent years have identified a multitude of physiological and pathophysiological processes highlighting the critical role of bioactive sphingolipids in most, if not all, major cell biological reactions, including all crucial cell signaling pathways. They emphasize a connection between sphingolipid metabolism and significant human diseases. The wide range of functions currently ascribed to bioactive sphingolipids is enormous and encompasses almost every important aspect of cell biology. This includes their involvement in cell growth, the cell cycle, cell death, cellular senescence,

Introduction

inflammation, immune responses, cell adhesion and migration, angiogenesis, nutrient uptake, metabolism, responses to stress stimuli, and autophagy [5].

It is therefore not surprising that sphingolipids are pivotal in numerous both common and rare diseases. Common diseases in which sphingolipids play a role include oncogenesis, cardiovascular diseases, immune disorders, diabetes, obesity, osteoporotic diseases, and a number of neurodegenerative syndromes [10-16]. A rare disease that has been described in connection with a malfunction of the sphingolipid metabolism is the Niemann-Pick-Disease, where patients have different degrees of lipid storage and foam cell infiltration in tissues. The disease can have various genetic causes and is classified in Type A, B & C whereas the first two types are caused by deficient activity of the enzyme acid sphingomyelinase (ASM) and is therefore also known as acid sphingomyelinase deficiency. Type C is caused by a dysfunction of cholesterol transport [17].

The characteristic structure of sphingolipids consists of a sphingosine backbone [(2S, 3R, 4E)-2-Amino-1,3-dihydroxy-4-trans-octadecene] and a fatty acid molecule attached via an amide bond at the C-2. This structure forms the ceramide. Ceramides naturally occur with fatty acids consisting of two to 28 carbon atoms, in saturated or monounsaturated forms [18, 19]. The *de novo* synthesis (Figure 1) of sphingolipids begins with the condensation of the amino acid L-serine with the activated fatty acid palmitoyl-CoA, which is catalyzed by serine palmitoyltransferase in the endoplasmic reticulum (ER). The product, 3-ketosphinganine, is then reduced to dihydrosphingosine through the action of 3-ketosphinganine reductase, followed by an acylation to form ceramide. The dihydrosphingosine is acylated by a fatty acyl-CoA molecule, resulting in dihydroceramide formation, catalyzed by dihydroceramide synthase. In a following desaturation step the insertion of a trans-4,5 double bond via the dihydroceramide desaturase leads to the final formation of ceramide [20-22]. Ceramides have an important role in regulation of the cellular phosphoproteome by activating protein phosphatase 1 (PP1) and protein phosphatase 2 families (PP2). [10, 23, 24]. Among many other biological functions, ceramides have been linked to mitochondrial apoptosis [25]. The complexity of the ceramides is remarkable, but they are mainly an intermediate in synthesis of complex sphingolipids. The enzyme sphingomyelin synthase catalyses the conversion of ceramide in

Introduction

the membrane phospholipid sphingomyelin. According to this, ceramides are present in cell membrane only to a small extent [26]. The conversion of sphingomyelin to ceramide is catalyzed by sphingophosphomyelinases. Ceramide can also be formed by the acylation of sphingosine through one of six ceramide synthases. These six synthases are categorized into acidic (N-acylsphingosine amidohydrolase 1), neutral (N-acylsphingosine amidohydrolase 2, 2B and 2C) and alkaline ceramidases (Alkine Ceramidase 1, 2 and 3), which hydrolyze ceramides to sphingosine [27, 28]. Two sphingosine kinases, Sphingosine kinase 1 (SphK1) and Sphingosine kinase 2 (SphK2) phosphorylate sphingosine at its primary hydroxyl group to S1P. Three lipid-phosphate phosphatases as well as two S1P-phosphatases are able to dephosphorylate S1P back to sphingosine. The hydrolysis of the phosphate residue mediated by the mentioned S1P phosphatase is a reversible process. Sphingosine is formed, which can be converted back to S1P through the action of sphingosine kinases or hydrolyzed to ceramide via ceramide synthases [29]. Therefore, metabolism of ceramide, sphingosine and S1P is not a one-way street, but a complex and reversible system in which ceramide serves as a building block for the synthesis of other sphingolipids; except the irreversible cleavage of S1P to ethanolamine phosphate and hexadecenal that is caused by the S1P lyase [30, 31].

During their metabolic pathway, sphingolipids traverse various compartments within the cell. The synthesis of sphingolipids initiates in the ER and continues in the Golgi apparatus. Sphingolipids serve as crucial components of cellular membranes, particularly acting as key constituents of so-called membrane rafts. Their degradation primarily occurs in lysosomes. Thus, it is clear that sphingolipid transport must occur within the cell, where inter-organelle routes primarily involve vesicular-mediated pathways, but can also occur through non-vesicular mechanisms [32, 33]. Ceramide is transported to the Golgi through either the vesicular pathway or the ceramide transport protein, CERT. Ceramide transported by CERT is employed in the synthesis of ceramide 1-phosphate (C1P) or sphingomyelin (SM). C1P and SM are then transferred from the Golgi to the plasma membrane through the ceramide 1-phosphate transfer protein and vesicular trafficking, respectively. Internally generated S1P is able to undergoes export facilitated by either sphingolipid transporter Spinster

Introduction

homologue 2 (SPNS2) or ABC family transporters [32]. Cells are involved not only in the production and export of sphingolipids but also in the uptake of sphingolipids from the cytoplasm into the cell. Complex sphingolipids like ceramide and S1P scarcely enter cells. The phosphorylated form S1P is dephosphorylated by cell surface lipid phosphate phosphatases to Sph, which then enters into cells via the acyl-CoA synthetases [34]. Recent studies have also shown that S1P can be taken up through a phospholipid phosphatase-independent pathway. The results suggest that the channel-like transporters SPNS2 and the ABC family transporter belonging major facilitator superfamily transporter 2b (MFsd2b), which export S1P, can to some extent also import S1P into the cell [35].

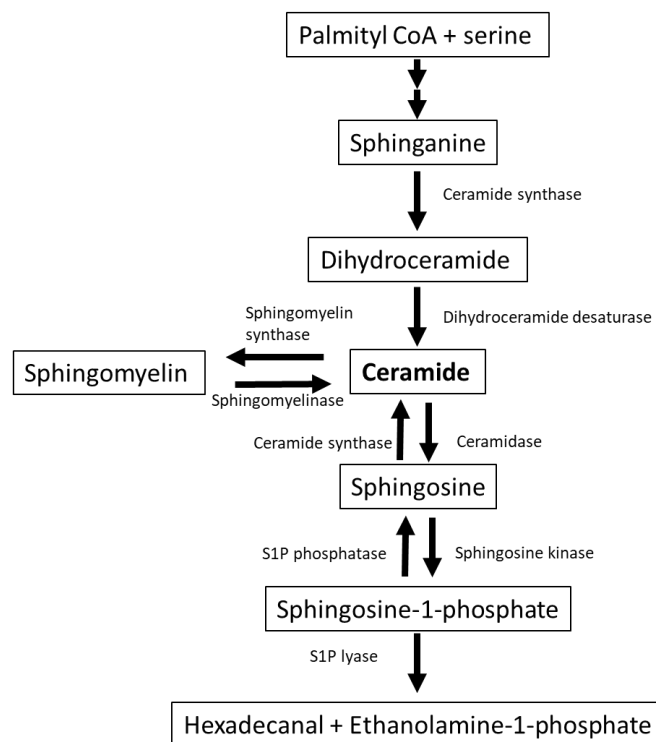


Figure 1: Simplified overview of sphingolipid metabolism.

Condensation of serine with palmitoyl-CoA initiates de novo synthesis of sphingolipids, resulting in 3-ketosphinganine, which is reduced to sphinganine. Subsequently, sphinganine is acylated to dihydroceramide by ceramide synthase. Dihydroceramide is converted to ceramide by the insertion of a trans-4,5 double bond. Ceramide can be reversibly converted to sphingomyelin by sphingomyelin-synthase or deacylated to sphingosine by ceramidase. Sphingomyelin serve as a reservoir for sphingolipids as the enzyme sphingomyelinase catalyze the cleavage of the phosphodiester bond of sphingomyelin, which belongs to the sphingolipid group. This produces ceramide and phosphorylcholine. Sphingosine is phosphorylated at the primary hydroxyl group by one of the two existing sphingosine kinases (kinase 1 and 2) to form sphingosine-1-phosphate (S1P). The degradation of S1P occurs either by reversible dephosphorylation back to sphingosine by S1P specific phosphatases or irreversible degradation by S1P lyase to hexadecanal and ethanolamine phosphate.

5.2 Sphingosine-1-phosphate signalling and its role in cellular processes

Sphingosine-1-phosphate (S1P), is one of the best discovered sphingolipids and is recognized as a critical regulator of many physiological and pathophysiological processes [11]. It is a bioactive signaling lipid which was discovered in the 1880s [36]. S1P regulation is important for cardiovascular health and disease, autoimmune and inflammatory processes, bone growth as well as for neurological, oncological and fibrotic diseases [12, 14, 37]. It is not only responsible for many physiological functions but can also be used as a therapeutic agent.

5.2.1 Shingosine-1-phosphate signalling – receptor dependent

S1P acts both as an intracellular messenger and as ligand via five G-protein-coupled receptors [38, 39]. Like all five G-protein-coupled receptors they are characterized by seven α -helical transmembrane domains, with an extracellular amino terminus and intracellular carboxyl group. The receptors are composed of a receptor part and a heterotrimeric G-protein [40]. All five different receptors are involved in various physiological and pathophysiological processes, whereby they are activating, inhibiting or modulating a variety of signaling cascades via the different G-proteins. This results in an active phospholipase C (PLC), active extracellular-signal regulated kinases (ERK) and Phosphoinositid-3(PI3) kinase pathway, as well as inhibit adenylate cyclase and active Rac and Rho GTPases [41]. In more detail: the S1P receptor 1 (S1PR1) and S1P receptor 2 (S1PR2) mediates S1P-induced mitogen-activated protein kinases (MAPK) activation, adenylyl cyclase (AC) inhibition, PLC activation and Ca^{2+} mobilization. S1P receptor 2 stimulation leads to activation of serum response factor (SRF), MAPK, AC and, PLC as well as Ca^{2+} mobilization, and Rho activation. The third S1P receptor (S1PR3) appears to resemble S1PR2, except for regulation of Rac and S1P receptor 4 (S1PR4) mediates no S1P-induced SRE activation in contrast to S1PR2. The S1P receptor 5 (S1PR5) mediates S1P-induced AC inhibition and Ca^{2+} mobilization like the other S1P receptors [41].

Introduction

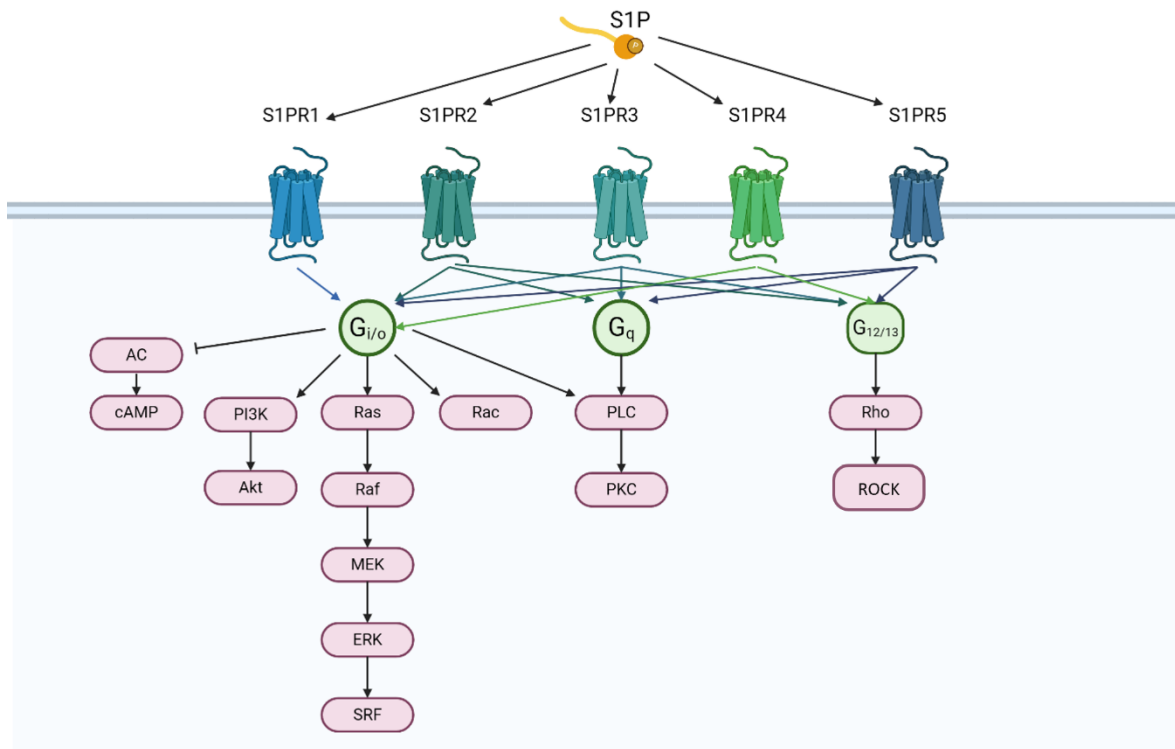


Figure 2 Schematic S1P receptor signaling pathways.

Extracellular S1P binds to specific S1P receptors (S1PR), each of which interacts with different G proteins, initiating various downstream signaling cascades. S1PR1 predominantly binds to Gi/o, whereas S1PR2 binds to G12/13, Gi/o, and Gq. S1PR3 primarily binds to Gq, with additional interactions with Gi/o and G12/13. Both S1PR4 and S1PR5 bind to Gi/o and G12/13. Gi/o activation leads to the stimulation of protein kinase B (Akt) via phosphatidylinositol 3-kinase (PI3K) pathway, signal-regulated kinase/ serum response factor (ERK/SRF), Rac, and phospholipase C/ protein kinase C (PLC/PKC) pathways while inhibiting Cyclic adenosine monophosphate (cAMP) production via adenylyl cyclase (AC) inhibition. Gq activation specifically triggers the PLC/PKC pathway, while G12/13 activation induces Rho activation, initiating the downstream Rho/Rho-associated kinase (Roh/ROCK) pathway.

S1PR1 to S1PR5 do not only operate in different ways, but they are also expressed on several cell types and are responsible for a variety of physiological functions. Regarding receptor expression, the receptors S1P1-3 are ubiquitous, whereas S1P4 has been identified exclusively in the lung, the hematopoietic and lymphoid tissues [42]. The S1P5 receptor has only been detected in the brain, skin and spleen thus far [43].

The physiological and pathophysiological functions are diverse. Activation of S1PR1, for example, is particularly important in regulating the migration of immune cells such as T lymphocytes from the thymus into the bloodstream and their distribution into lymphoid tissues such as lymph nodes and spleen. This regulation is crucial for efficient immune surveillance and response to infections or other immunological challenges. In addition, the

Introduction

S1P1 receptor influences inflammatory responses and contributes to the maintenance of immunological tolerance by preventing autoreactive immune cells from entering tissues where they could cause damage [11, 44, 45]. Due to the important physiological functions of the S1P1 receptor, especially for the immune system, its dysregulation can be associated with a variety of diseases. A key aspect is its role in autoimmune diseases, where dysfunction of the S1P1R can impair immunological tolerance, which can lead to increased activation of autoreactive lymphocytes and consequently to autoimmune reactions. In addition, changes in the S1P1R are associated with inflammatory diseases such as rheumatoid arthritis and inflammatory bowel disease, where they can increase inflammatory reactions. In the context of cancer, the S1P1 receptor is considered a potential factor in tumor progression, as its activation can promote tumor cell migration and invasion [11, 46-48].

S1PR2 mediates lots of different cellular functions depending on the cell type where it is expressed. In endothelial cells for example it is involved in the permeability of vessels [49, 50]. In addition, metabolic functions in the liver and pancreas can be attributed to receptor 2 [51, 52], as well as important regulatory functions in the muscular system [53-55], the neuronal system [56] the kidney [57, 58] and the regulation of cancer growth [59-61]. Even if its role is rather subordinate compared to the S1P1 receptor, its importance becomes apparent in a S1PR2-knockout. First it was shown that the deletion of S1PR2 in mice leads to a defect in the *Stria Vascularis*, which is responsible for the blood supply to the inner ear. S1PR2 knockout mice lose their hearing and balance approximately 14 days after birth due to the degeneration of hair cells in the Corti's organ of the cochlea and neuronal degeneration of the spiral ganglion [62-64]. Later, it was also shown that S1PR2-knockout mice have an osteopenic bone phenotype and are obese, which is related to the S1P2R regulated activation and differentiation of osteoblasts and osteoclasts [12]. This highlights the important role of S1P in conjunction with S1PR2 in bone metabolism and bone health.

S1PR3 plays a critical role in immune response and inflammation. Among other things, it could be shown that the S1PR3 expression in dendritic cells is important for switching immune reactions to T helper cell response [65]. Furthermore, the S1P3 receptor is important in the regulation of inflammatory reactions by influencing the release of

Introduction

inflammatory mediators and the migration of immune cells into inflamed tissue [66]. S1PR3 activation and its expression patterns in cardiac tissue is clearly associated with Bradycardia and hypertension [67]. Its's role in cardiovascular functions can be observed during sepsis. S1PR3 is thereby released in the circulating bloodstream which leads to lower blood vessel resistance and increasing vessel permeability [68], which is associated with the role of S1PR3 in vasoconstriction and vasodilation. In addition, it was shown that receptor 3 expression is closely related to the development and growth of various tumor types [69-71].

The S1P receptor 4 is mainly expressed in hematopoietic cells and most discovered functions of this receptor are related to this system [72].

S1P receptor 5 is highly expressed in oligodendrocytes and their precursors in the brain. It is also found within natural killer cells, where it has the essential role to direct their egress into the lymphatic system [73]. Another role is the maintenance of the blood-brain barrier. Studies have shown that activation of S1P receptor 5 is associated with increased tight junction density and thus reduced permeability of the blood-brain barrier [74]. Similar to other S1P receptors, there are also studies for S1P receptor 5 that show associations with tumor and cancer cell proliferation and migration [72, 75, 76].

5.2.2 Shingosine-1-phosphate signalling – receptor independent

Additionally, to receptor related signaling S1P mediates as intracellular second messenger. The receptor-independent pathway of S1P signaling involves the direct interaction of S1P with various intracellular proteins and enzymes without the need for binding to specific S1P receptors. This pathway can occur in different cell types and influences a variety of cellular processes. First indication on a receptor independent signaling was found in systems where no S1P receptors are expressed. In yeast for example, high intracellular S1P levels lead to suppressed cell growth even if the yeast genome does not encode for any S1P receptor and extracellular given S1P has no impact [77-79]. In mammalian cells it was demonstrated, that intracellular S1P is able to bind and inhibit the ceramide synthases without participation of S1P receptors [80]. An further example of the receptor-independent pathway is the regulation of intracellular calcium concentration by S1P. S1P can stimulate calcium release from intracellular stores and promote calcium influx into the

Introduction

cell, which influences various cellular functions such as smooth muscle cell contraction or the activation of signal transduction pathways [81, 82]. Other examples include the manipulation of enzymes such as phospholipase C and phospholipase D as well as the modulation of protein kinases such as protein kinase C and protein kinase D [83-87]. Overall, the receptor-independent pathway contributes to the diversity of biological functions of S1P, especially in cells that rely on rapid and precise responses to extracellular signals.

5.2.3 Shingosine-1-phosphate regulation and transport

Since S1P level influences intracellular pathways, it is important that S1P content is regulated in cells. This is done by several enzymes that produce or degrade S1P. Like mentioned before the direct precursor of S1P, sphingosine gets phosphorylated by SphK1 and 2 to form S1P [88] whereas S1P phosphatases and the S1P lyase are responsible for its degradation [89, 90]. SphK1 as well as SphK2 phosphorylates sphingosine adenosine triphosphate (ATP) dependent and they are grouped with mammalian diacylglycerol kinase enzymes (DGKs), other eukaryotic lipid kinases and prokaryotic enzymes of the bacterial DgkB class into the DAGK_cat family [91]. SphK1 consists of two domains whereby the N-terminal domain has the binding site for the nucleotide and a C-terminal hosting the sphingosine binding site. Its catalytic center is located in a cleft formed at the interdomain junction [91]. SphK2 is located in the nucleus of cells and its N-terminal domain binds to sulfatide and phosphoinositides. This domain appears to be important for correct sub-cellular localization and may exert allosteric control over enzyme activity [92].

Not only does the production and degradation of S1P influence intracellular S1P levels, but S1P transport also regulates S1P content. Due to its polar nature S1P is unlike sphingosine not able to cross through membranes without any transporter [72]. Besides the suggestion that transporters belong to the ATP-binding cassette family that can participate in S1P translocation, two specialized S1P transporters are defined. Spinster homologue 2 (SPNS2) transporter in vascular endothelial cells and Mfsd2b mostly expressed in red blood cells (RBCs) and platelets; both proteins belong to the major facilitator superfamily (MFS) and are responsible sources for circulating S1P [93]. Mfsd2b is identified as S1P transporter in

the hematopoietic system. It belongs to a group of solute carrier proteins (SLCs) termed major facilitator superfamily (MFS) transporters. It is homolog to Mfsd2a, the lysophosphatidylcholine transporter [94]. A typical characteristic of SLCs is that they are secondary active transporters. They use energy from coupled ions or facilitative diffusion to move substrates via coupled transport, exchange or uniport [95]. One third of all SCLs belong to the MFS family, which is characterized through its diversity. It has members in several organisms, like bacteria, yeast, insects and mammals [96-100]. Members of this protein family consist of a single polypeptide (16) and are usually composed of 400-600 amino acids [101]. MFS transporters are transporting their substrates via the rocker-switch mechanism [102] through the membrane. Here, the transporter undergoes a sequence of conformational changes that transport the substrate across the membrane. Mfsd2b belongs, like all MFSDs to the atypical SLCs of MFS type proteins. This means that they are evolutionarily classified as the SLCs, but cannot be clearly grouped into an existing SLC family so far [103]. In 2017, the transport of S1P via Mfsd2b was discovered [104]. It could be shown that RBCs take up sphingosine which is phosphorylated by SphK1 to S1P which can be transported out of the RBC by Mfsd2b. Thus, Mfsd2b provides 50% of plasma S1P [104, 105]. In RBCs and platelets of Mfsd2b knockout mice (Mfsd2b^{-/-}) a high S1P accumulation can be found, compared to cells from wild type mice. This accumulation is due to a disturbed or blocked S1P export and fits with the fact that S1P levels in plasma are lower in these animals than in controls [104].

5.3 Sphingosine-1-phosphate related medication

Since S1P is involved in many physiological and pathophysiological processes, it is an interesting target for drug treatment of numerous diseases. At this time, there are several drugs on the market that affect the S1P signalling pathway system, especially for the treatment of multiple sclerosis (MS), a chronic autoimmune disease.

The most famous one is based on the S1P analogue FTY720, also known as Fingolimod and is commercially available under the trade name Gilenya® by Novartis. It is used to treat highly active form of MS in patients aged 10 years and older. FTY720 has a strong structural

Introduction

similarity to sphingosine (Figure 3) and is primarily phosphorylated via SphK2 to its active form FTY720 phosphate (FTY720-P) [106]. The effect of FTY720-P occurs due to its binding of four of the five known S1P receptors (S1P receptor 1, 3, 4 and 5) [107]. Different experimental setups indicated the inhibition of lymphocyte recirculation by FTY720-P (fingolimod phosphate) by acting as a functional antagonism at the S1PR1 [108]. Gräler and Goetzl documented a decrease in S1P receptor levels following treatment with fingolimod [109], while others demonstrated a reduction in membrane expression of S1P1 on lymphocytes in vivo following fingolimod treatment [110]. This is aligned with observations that mutant mice expressing S1P1 with impaired internalization exhibit delayed lymphopenia kinetics in response to fingolimod [111], and that lymphocytic knock-down of S1P1 also hinders their egress from the thymus [112].

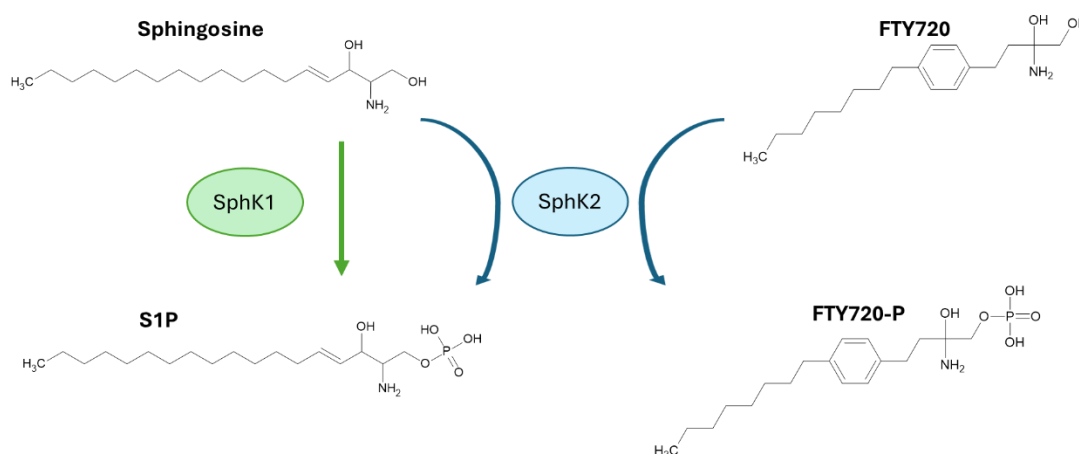


Figure 3: Phosphorylation of FTY720 to FTY720-P generates a structural analog to S1P.

FTY720 also known as fingolimod, exhibits strong structural similarity to sphingosine and undergoes phosphorylation by sphingosine kinase 2 (SphK2), however, not by sphingosine kinase 1. FTY720 functions as a prodrug, converting into FTY720-P, which then interacts with S1P receptors, leading to the activation of intracellular targets associated with S1P signaling. Based on Brunkhorst et al, 2014 [108].

Another commercially approved drug is since 2020 the S1P receptor modulator Siponimod, which is a further development of Fingolimod and available under the trade name Mayzent® by the company Novartis. It is also used for the treatment of MS, more accurate for adult patients with secondary progressive MS. The active substance selectively binds to the G-protein-coupled receptors S1P receptor 1 and S1P receptor 5. As Fingolimod,

Introduction

Siponimod acts as a functional antagonist on the S1P receptor 1 of the lymphocytes and thus prevents the migration of lymphocytes from the lymph nodes. This reduces the recirculation of T cells into the CNS and limits inflammation there. After crossing the blood-brain barrier, Siponimod also binds directly to the S1P receptor 5 on oligodendrocytes and astrocytes, thereby counteracting harmful immunological processes in the brain tissue [113-115]

It is foreseeable that in the course of this year, a further active substance acting as S1PR1 and S1PR5 modulator for MS treatment will be launched on the German market. With Zeposia® containing the active ingredient ozanimod the US pharmaceutical company Bristol-Myers Squibb show effectively reduces in the number or relapse in patients with MS [116, 117].

The drug ponesimod (trade name Ponvory®) from the company Janssen Pharmazeutika, which has been approved in Germany since 2021 for adults with active relapsing-remitting multiple sclerosis, is comparable in its mode of action and use to the drugs mentioned here before [118, 119].

Introduction

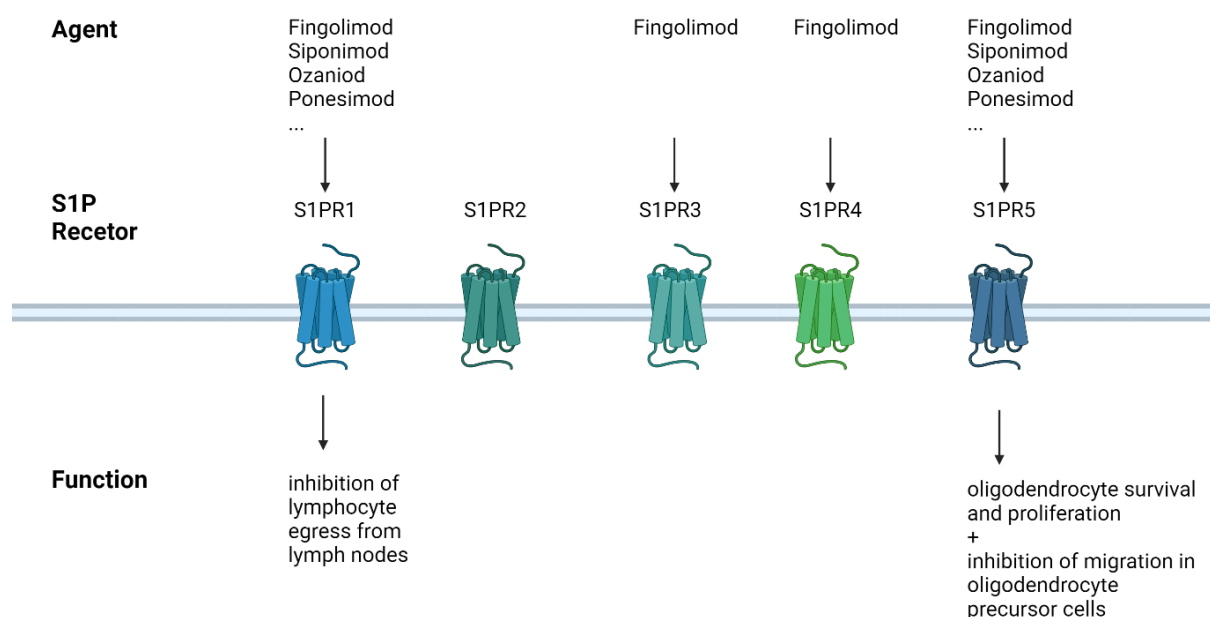


Figure 4: Drugs based on the mode of action of S1P receptor modulation.

The agents fingolimod, siponimod, ozanimod and ponesimod interact with S1P receptor 1 (S1PR1) and lead to inhibition of lymphocyte egress from lymph nodes. Fingolimod also interacts with receptors 3, 4 and 5 (S1PR3-5). Siponimod, ozanimod and ponesimod also interact with S1P receptor 5 which lead to oligodendrocyte survival and proliferation as well as inhibition of migration in oligodendrocyte precursor cells. The list of drugs is not exhaustive, and the described function is limited to one main function to which the effect of the medication is attributable.

In addition to the modulation of S1P receptors, other sites in the S1P metabolism also offer great potential for the development of effective drugs. Safingol [(2S, 3S)-2-aminoctadecane-1,3-diol] is, among other clinical benefits, an inhibitor of SphK1 and is in clinical phase to be used as a drug in combination with conventional chemotherapeutic agents [120-122]. The active substance with the name ABC294640, also called opaganib or Yeliva, is a selective inhibitor of both SphK2 and the dihydroceramide desaturase 1. Thus, ABC294640 inhibits the synthesis of S1P, which may eventually lead to the induction of apoptosis and inhibition of cell proliferation in cancer cells overexpressing SphK2 [122-125]. SKI-II is a highly selective inhibitor for both Sph kinases and also used in clinical trials. *In vitro* studies have shown that SKI-II decreases cancer cell proliferation by inducing apoptosis [126-128] as well as autophagy [128, 129] and other signs of stress like oxidative stress, endoplasmic reticulum stress and cell cycle arrest [122, 130-132]. By inhibiting the

Sph kinases, S1P levels are decreased, and ceramide levels thereby increased, leading to activating of several signaling pathways [126, 127, 129, 131, 133].

5.4 Red blood cells - specialized suppliers for the body

Most of the cells in blood are red blood cells (RBCs). Of the total blood volume, 40 -45% are red blood cells, just one percent are white blood cells and the rest is composed of platelets and blood plasma. Mature RBCs are biconcave, flexible disks packed with hemoglobin. Their function is to transport oxygen and carbon dioxide through the body [134] which makes them indispensable to the respiration of vertebrates. RBCs transport the oxygen, deliver it to the tissue and at the same time absorb the CO₂ produced by the tissue to transport it into the lungs [135]. Due to their shape, RBCs have a large surface area and their flexibility enables them to get into narrow blood vessels, the capillaries. Like all the other cellular components of the blood, RBCs are generated by stem cells in red bone marrow, particularly in the ribs, sternum, pelvis, vertebrae, and long bones of the extremities. The production of red blood cells is controlled by a hormone called erythropoietin which is primarily produced by the kidneys. In humans, the lifespan of an erythrocyte is about 120 days, before they are recycled by macrophages within the spleen, liver and lymph nodes. In mice the lifespan is about 45 days [136, 137]. The human body produces around 2.4 million RBCs per second, so that despite their relatively short lifespan, there are always enough cells available [138]. In most mammalian species, including mice and humans, the cell nucleus and other organelles such as mitochondria are lost during the RBC maturation process [134]. Therefore, RBCs are specialized to obtain energy only through glycolysis and pentose phosphate pathway (PPP) making them depend on glucose as sole energy source. Consequently, the transport of glucose is closely linked to red blood cell physiology. A defect in glucose metabolism or transport activity is associated with impaired red blood cell morphology and deformability leading to reduced lifespan [135]. Additionally, glycolysis is not only important for producing ATP, but also yields nicotinamide adenine dinucleotide (NADH), a powerful reducing agent that prevents oxidation of haem and thus keeps iron in the reduced Fe²⁺ state [135]. Glucose is mainly transported through glucose transporters. In human RBCs, the facilitative glucose transporter 1 (GLUT1) is expressed

Introduction

most abundantly, while in other mammals, like mice, GLUT1 is lost during RBC maturation and there is a switch to high expression of glucose transporter 4 (GLUT4) [139].

5.4.1 Shingosine-1-phosphate in blood and red blood cells

It is known that the main source of S1P in plasma are hematopoietic cells, mainly RBCs. However, also endothelial cells from vascular and lymphatic systems synthesize and release S1P [140, 141]. In humans, different studies discovered S1P plasma concentrations of 100 to 200 nM [31, 142-144]. The S1P plasma concentration in wild type mice under normal chow is comparable. It is between 100 nM and 800 nM [145, 146]. Since, as already mentioned, the main source of S1P in the blood are the RBCs, the S1P levels in whole blood is higher as in pure plasma, at approximately 5 μ M [147]. In contrast to platelets, it could be shown that RBCs not only store a large part of S1P in blood, but also secrete it. This secretion of S1P into plasma could not be observed in serum-free medium, which shows that S1P release depends on a plasma factor [148]. In blood, the fraction of S1P, which is not located in RBCs, is mostly bound to high-density lipoproteins (HDL) in plasma. HDL bound S1P is biologically active and showed impressive influence on the effect of HDL. Low HDL-S1P is associated with impaired HDL function and has been linked to diseases like atherosclerosis, coronary artery disease, myocardial infarctions and diabetes mellitus [149]. The remaining S1P in plasma, which is not bound to HDL (about 30%) is associated to albumin as well as low-density lipoprotein (LDL) and very-low density lipoprotein (VLDL) [150].

Since RBCs lose their nucleus during maturation process, no nuclear localized SphK2 just cytosolic localized SphK1 can be found in these cells [151, 152]. Therefore, they are able to phosphorylate sphingosine to S1P via SphK1. High S1P levels in RBCs can be explained by the fact that no S1P-degrading enzymes such as S1P lyase or S1P phosphatases are available in RBCs [153]. Therefore, RBCs are good S1P stores and suitable for S1P transport through the organism. Mfsd2b is responsible for the S1P efflux from RBCs [104]. Obstruction of this transport leads to increased S1P levels in RBCs and to morphological changes in these cells [104]. The S1P level in RBCs could be influenced by other pharmacological and genetic modifications. For example, administration of 4-deoxyypyridoxine (DOP), a pharmacological

Introduction

inhibitor of the S1P lyase, leads to an increase in S1P levels in the RBC [148]. If, on the other hand, SphK1 is knocked out, animals show lower S1P level in blood, as sphingosine cannot be phosphorylated anymore [141]. It could be shown, that the intracellular S1P level in RBCs have an impact on its function. A study from 2016 showed, that people spending time on high altitude (>5000 m) have elevated S1P levels in their erythrocytes. Together with investigations on a mouse model under hypoxic conditions a connection between hypoxia, elevated RBC SphK1 activity, elevated S1P levels and an improved supply of oxygen to the tissue could be proven [154]. In connection with this study, a link between S1P and glycolysis in the RBCs was established. It could be shown that hypoxia induced SphK1 activity in RBCs which leads to induction of RBC glycolytic enzyme activity and in the end to an increased glycolysis in these cells [154].

5.5 Glucose transport as an important distributor of energy source

For the majority of mammalian cells, glucose is an important metabolic substrate that serves as both, an energy source and a signalling molecule. Glucose transport is therefore important for supplying cells with energy. There are three different families of solute carriers that have been identified to be able to transport glucose through membranes. Specialized glucose transporters of the MFS family (GLUTs), the sodium-driven glucose symporters (SGLTs) and the SWEET transporters, a family of transporters for glycosides that typically use a uniport transport mechanism [155-158]. In mammalian cells GLUTs are the most present and important glucose transporters. They are ubiquitously distributed and catalyse the diffusion of glucose down its concentration gradient. GLUTs, also known as SLC2a, are encoded by the *SLC2* genes, and are members of the solute carrier family (SLCs) [156]. GLUTs are regulated in their expression, localisation, synthesis, and half-life by a variety of factors. These factors include stress hormones, a variety of metabolic stressors such as cellular energy demand, metabolic toxins, inflammation and chronic diseases [159]. GLUT transporters are separated in 14 different isoforms whereas GLUT4 often plays a particularly important role in research [156]. GLUT4 also known as SLC2A4 is mostly responsible for mediating glucose uptake in insulin sensitive tissues like skeletal muscle, adipose tissue or cardiac muscle due to its response to insulin [160]. Due to this

Introduction

characteristic it has been intensively studied in relation to the pathophysiology of type 2 diabetes mellitus [161]. GLUT4 is not permanently located at the membrane surface and available for glucose transport. A constant turnover between the cell surface and specialized membrane vesicles changes the locality and thus the activity of the transporter. The GLUT4 translocation to the cell surface in vesicles is initiated by insulin signalling [162]. But it could be shown that not only the insulin signalling influences GLUT4 localization and activity, also an insulin-independent activity of the GLUT transporter is known. Glucose transport activity is controlled by the phospholipid composition of the membrane. With help of liposomes containing different lipid composition Hresko and his team could prove that anionic and conical lipids increase the transporter activity of GLUT4 and GLUT3 [163]. It was shown that anionic phospholipids, like phosphatidic acid (PA) stabilize the glucose transporters which is required for their activity. Furthermore, conical, or non-bilayer lipids increase transporter activity dramatically in the presence of these anionic phospholipids [163]. This is based on various mechanisms that ensure improved glucose uptake in the reconstituted liposomes. The anionic phospholipids stabilize GLUT by its charged headgroup, whereas conical lipids have no influence on protein stability, indicating direct interaction of only anionic phospholipids with the transporter. Moreover, a kinetic analysis indicated that both lipids do not change the affinity of the transporters for their substrate D-glucose but change either the turnover rate or the fraction of active transporters [163].

There are also studies for other GLUT isoforms showing that the activity of the transporter can depend on many factors. In addition to GLUT4, also GLUT1 is known to have distinct regulatory characteristics that reflect its specific role in cellular and whole-body glucose homeostasis. GLUT1 (SLC2A1), is a transport protein in the cell membrane of pancreatic β -cells, endothelial cells of the blood-brain barrier in mammals, human erythrocytes and many other tissue types that facilitates the transport of glucose. The glucose transport through GLUT1 is thereby insulin independent [156, 164].

It could be shown that there is a nutrient dependent regulation of glucose transport in adipocytes. A decreased extracellular glucose concentration leads to an increase in GLUT1 activity in 3T3-L1 adipocytes [165-167] which could be linked to the localisation of GLUT1 within the plasma membrane [165]. Kumar et al. showed that active GLUT1 is accumulated

Introduction

in certain plasma membrane regions, the lipid rafts [165]. Lipid rafts, also called membrane rafts or glycolipid enriched membrane domains are membrane structures of eukaryotic cells described based on their low solubility in certain detergents and their low density. Lipid rafts are rich in sphingolipids, cholesterol, highly saturated phospholipids and the ganglioside GM1 [168].

Furthermore, a correlation between lipids of the sphingolipid metabolism and the localization of GLUT on the membrane could be observed. In the lab of Sarah Spiegel, the internalization of GLUT1 triggered by the sphingosine analogue (SK1-I) was demonstrated [169]. Others could further show a loss of surface GLUT1 induced by sphingosine analogue FTY720 [170]. Further studies indicated that sphingolipids and its analogous can trigger this nutrient transporter internalization by activating of protein phosphatase 2A (PP2A) [171].

5.5.1 Glucose in red blood cells and disorder due to hyperglycaemia

Glucose is the major energy source of RBCs. However, it must be noted that mature cells are lacking the oxidative enzymes relevant for mitochondrial glucose metabolism. According to this RBCs are not able to perform aerobic glycolysis but depend on anaerobic glycolysis to produce their energy [172, 173]. Under normoxic conditions and under normal physiological circumstances, glucose is catabolized anaerobically to pyruvate or lactate by the Embden-Meyerhof pathway, in which ATP as well as nicotinamide adenine dinucleotide (NADH) are produced. NADH has an important role in the RBC, as it can be used by the cytochrome b5 reductase to reduce methaemoglobin to haemoglobin [173].

The transport of glucose across the membrane of red blood cells is well studied. It is remarkable how high the capacity of glucose uptake in this is, compared to its glucose consumption. Like described before, the transport through GLUT transporter is not an active system and its influx and efflux kinetics are not symmetric. The influx is facilitated compared to the efflux [174]. In human RBCs there are estimations of 300 000 glucose transporters per single red blood cell [175] which is surprisingly high compared to other transporters. Experiments of other research groups indicated more than thousand times less sodium-potassium (Na^+ - K^+) pumps on the surface of human red blood cells [176].

Introduction

Glucose is the unique energy source for RBCs and defects in glucose metabolism or transport activity is closely linked with disturbed cell morphology and a reduced deformability which leads to reduced lifetime of the cell [135, 177, 178]. Mutations that lead to a lack of glycolytic enzymes in the RBC, can result in hemolytic anemia as well as non-hematopoietic consequences, such as a fatal neuronal disease [112]. In patients having glucose transporter type 1 deficiency syndrome (Glut1DS), glucose uptake is disturbed. As the name implies, a genetic disorder leads to the deficiency of GLUT1. As a result, glucose transport activity is reduced by approximately 50% in RBCs of these patients. Typical symptoms are infantile-onset epilepsy, deceleration of head growth, impaired neurological growth and development and complex movement disorders [179]. However, since not only the glucose uptake in RBCs is disturbed but also glucose uptake through the blood-brain barrier, it is difficult to determine which of the symptoms is due to decreased glucose uptake in RBCs. Nevertheless, the decreased glucose uptake in RBCs is an important finding for this disease as it can easily serve as a diagnostic tool for it [179]. Another disease that affects glucose transport and thus the vitality of RBCs is diabetes mellitus, which is characterized by elevated glucose concentration in plasma [180]. This chronic hyperglycemia causes long-term complications like retinopathy, neuropathy, and nephropathy, among other things [181, 182]. Hyperglycemia induces an increase in glycated hemoglobin also called hemoglobin A1c, or HbA1c, which is the main biomarker used to assess long-term glycemic control in individuals with diabetes [183, 184]. Hemoglobin from healthy individuals contains hemoglobin A which is approximately 6% glycated, the major component being hemoglobin A1c (HbA1c) (5%), with minor components of hemoglobin A1a (HbA1a) and hemoglobin A1b (HbA1b) (1%) [185]. The HbA1c glycosylation level is dependent on the concentration of the blood glucose level as well as the erythrocyte lifespan and results from glycation, the covalent binding of glucose to N-terminal valine of the hemoglobin β -chain [185, 186]. High intracellular glucose levels are harmful for cells and so also for RBCs. In patients with diabetic disease, the erythrocytes are in a constant environment of increased extracellular glucose due to increased blood glucose levels and it has been shown that diabetic patients have increased disturbances in the morphology of their RBCs, which has been linked to vasculopathy, critical sheer stress and increased aggregation [187, 188]. Furthermore, a positive correlation between mean

Introduction

corpuscular volume (MCV) and red cell distribution width (RDW) with HbA1c levels could be established [187]. MCV is a measure of the average volume of a red blood cell, whereas RDW is a calculated coefficient of MCV variability. Accordingly, higher RDW values reflecting greater heterogeneity in MCV, which usually indicates inconsistency in erythrocyte size, which in turn can provide the first indications of anemia [189]. Higher RDW levels are also associated with increased risk of cardiovascular disease and kidney disease [190], which shows a relation between hyperglycemia, red blood cell morphology and the diseases mentioned. In diabetic patients, not only the size is disturbed, but they also show reduced deformability of RBCs. The subsequent rigidity complicates the pass through microvessels which leads to microcirculation disturbance [191]. Among all these things, high glucose concentration in red blood cells lead to lipid peroxidation, loss of activities of erythrocyte enzymes and hemolysis [187, 192]. In general, red blood cells play a significant role in glucose transport and glucose metabolism. The Disturbance of the glucose balance of the RBC can lead to considerable disturbances of the cell and thus to far-reaching physiological problems.

In addition, S1P levels are known to be lower in the plasma of diabetic patients [193-195]. Further, previous studies reported a possible protection mechanism of high plasma S1P and the development of diabetes [196-199]. However, the influence of hyperglycemic conditions on the RBC S1P level is unknown yet and need to be investigated.

5.6 PP2A - more than just a tumour suppressor

Protein phosphatase 2A (PP2A) is a serine/threonine phosphatase which is present as heterotrimeric enzyme in eukaryotic cells [200]. Its holoenzyme structure contains a catalytic C-subunit, a regulatory B-unit and a stabilising A-unit [200, 201].

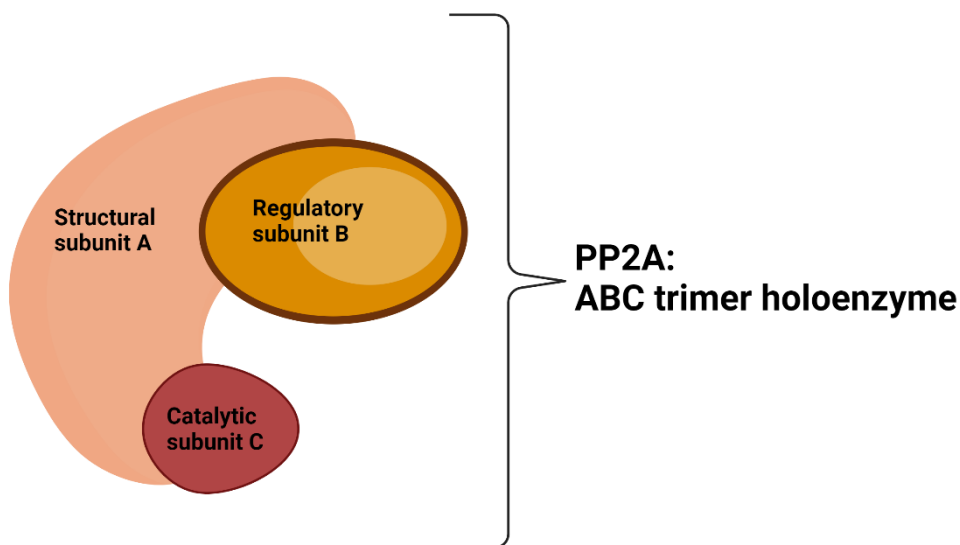


Figure 5: Schematic structure of holoenzyme PP2A.

The enzyme protein phosphatase 2A (PP2A) contains three subunits. The stabilizing, structural subunit A, the regulatory subunit B and the catalytic subunit C. PP2A is therefore classified as ABC trimer holoenzyme.

PP2A regulates multiple cell signalling cascades and achieved great attention in tumour research. The role of PP2A in cancer development and progression and its associated role as a possible tumour suppressor has been repeatedly demonstrated [202-205]. In addition, deregulation of PP2A function is linked to a variety of other diseases including neurodegenerative disorders and heart failure [206, 207]. The activity of the enzyme can be regulated through changes directly in the catalytic subunit or by specific interplay between the holoenzyme and its specific inhibitor proteins [200]. Different ceramides were shown to activate PP2A [208-211] whereby both the direct activation of the catalytic unit [210] and the activation via binding of the PP2A inhibitor SET could be demonstrated [212]. In addition to various ceramides, PP2A activation through the S1P and sphingosine analogues FTY720-P and FTY720 was demonstrated, respectively [200, 213, 214]. The use of a chemical sphingosine analogue (SH-BC-893) also showed increased PP2A activity followed by mis localization of PI(3,5)P2 generation by the lipid kinase PIKfyve which triggers cytosolic vacuolization and blocks lysosomal fusion as a consequence [142, 171]. Thereby, PP2A activity was mainly used as a readout for altered membrane trafficking as

Introduction

increased PP2A activity was found to be associated with the loss of nutrient transporters at the cell surface.[171, 211]

Furthermore, there is evidence of a link between hyperglycaemia and increased PP2A activation. Studies showed hyperactivated PP2A in bovine aortic endothelial cell under glucotoxic conditions [215]. Moreover, hyperactivation of PP2A in retina and aorta isolated from diabetic rats compared to control animals was described [215]. However, these findings can be attributed to disturbed insulin secretion which was monitored by the investigation of the regulatory effects of insulin on PP2A activity and expression in muscle cells isolated from human patients with type 2 diabetes mellitus and age-matched controls. This data indicated a significant reduction in the expression of PP2A following insulin treatment in skeletal muscle from control subjects. However, the insulin-mediated effects on these metabolic indices were not seen in muscle preparations from type 2 diabetes mellitus subjects [216].

As the glucose uptake of RBCs is insulin independent, it has not been studied yet how PP2A is involved in the process of glucose uptake in this cell type and whether hyperglycaemia has an impact of PP2A activation.

6 Aim of this study

Glucose transport by GLUTs is intimately linked to RBC physiology. It has been shown that RBCs are sensitive to elevated intracellular glucose levels, as in the case of hyperglycaemia. Although several membrane phospholipids affect GLUT function, the relevance of the bioactive sphingolipid S1P, of which RBC carry the highest content of all cells, for glucose transport is unknown. Therefore, the aim of this study is to investigate how S1P influences the glucose uptake in RBCs under normoxic conditions. It is to be examined how intracellular S1P concentration determines the glucose uptake in murine and human RBCs *in vitro* and *in vivo*. To this end, several pharmacological and genetic approaches are being used to modulate the S1P content of erythrocytes by altering S1P precursor uptake, S1P synthesis and S1P efflux.

Initial experiments indicated that RBC glucose uptake is affected by incubation with the S1P precursor sphingosine. This will be further investigated in the following experiments, by analysing glucose uptake in murine erythrocytes with altered S1P levels induced by incubation with sphingosine or additionally with the S1P acceptor bovine serum albumin (BSA). In addition, glucose uptake in RBCs that have altered S1P levels will be analysed *in vivo*. For this purpose, mice with increased intracellular S1P levels due to pharmacological or genetical inhibition of the S1P degrading enzyme S1P lyase, as well as mice with decreased intracellular S1P due to genetical deletion of SphK1 will be used. By using mice lacking the main S1P transporter in RBCs, *Mfsd2b*, as well as by using a cell line overexpressing this transporter, it will be investigated how glucose uptake is affected by modified S1P transport. Furthermore, the influence of S1P and sphingosine analogues FTY720-P and FTY720 will be studied. Finally, the question arises whether the influence of S1P on glucose uptake in RBCs is limited to murine RBCs or whether it also applies to human RBCs. To clarify this, human RBCs are isolated, loaded with S1P and glucose uptake rate is determined. Since it is known that RBCs are sensitive to elevated intracellular glucose levels, it is important to investigate the relationship between elevated intracellular glucose levels and S1P. For this purpose, RBCs from hyperglycaemic mice and humans with type 2 diabetes mellitus are analysed. By addressing this question, it brings the following results into a medically relevant context.

Aim of this study

The results of this work will provide new insights into S1P-regulated insulin-independent glucose uptake in RBCs from healthy and hyperglycaemic individuals. These will be the first results on whether and how S1P affects glucose uptake in RBCs under normoxic conditions. Furthermore, there are no known data on S1P levels in diabetic RBCs and how their glucose uptake is influenced. This study forms the basis for new potential studies to further investigate glucose uptake regulation by S1P in other insulin-independent cell types as well as for investigations with the aim of regulating intracellular glucose levels in RBCs of patients with diabetic mellitus.

7 Material and Methods

7.1 Materials

7.1.1 Devices

Camera at cell culture microscope EP50	OLYMPUS, Tokyo, Japan
Cell counter EVE TM Plus	NanoEntek, South Korea
Cell culture microscope CK53	OLYMPUS, Tokyo, Japan
Centrifuge 1K15	Sigma/ Sigma-Aldrich, St. Louis, USA
Centrifuge 5810 R	Eppendorf, Hamburg, Germany
CO2 Incubator HERAcell vios 250i	Thermo Fisher Scientific, Waltham, USA
Flow Cytometer Gallios	Beckman Coulter, Brea, USA
Column oven	Shimadzu Deutschland GmbH, Duisburg, Germany
Degassing Unit	Shimadzu Deutschland GmbH, Duisburg, Germany
HLC Heating-ThermoMixer	DITABIS, Pforzheim, Germany
Incubator	Thermo Fisher Scientific, Waltham, USA
Mass spectrometer LCMS-8050	Shimadzu Deutschland GmbH, Duisburg, Germany
Mercury Burner at cell culture microscope	OLYMPUS, Tokyo, Japan
Microplate reader, CLARIOstar Plus	BMG Labtech, Ortenberg, Germany
Mini centrifuge	Biozym Scientific, Hessisch Oldendorf, Germany
Mini-Exdruder	Avanti Polar Lipids, Alabaster, USA

Material and Methods

Multipette E3	Eppendorf, Hamburg, Germany
Nanodrop One	Thermo Fisher Scientific, Waltham, USA
Nitrogen generator	CMC Instruments, Eschborn, Germany
PH meter, pH Level2	WTW Ivolab/ Xylem Analytics, Weilheim, Germany
Pipettes	Eppendorf, Hamburg, Germany
Power PAC 200	BioRad, Hercules, USA
Real-Time System CFX96™	BioRad, Hercules, USA
Rotary Pump with noise reduction cover	Shimadzu Deutschland GmbH, Duisburg, Germany
Scintillation Counter	Packard Instrument Company/ PerkinElmer, Waltham, USA
Solvent delivery Unit	Shimadzu Deutschland GmbH, Duisburg, Germany
System controller	Shimadzu Deutschland GmbH, Duisburg, Germany
Thermal Cycler C100™	BioRad, Hercules, USA
UHPLC autoinjector	Shimadzu Deutschland GmbH, Duisburg, Germany
Vet abc Plus	Scil, Viernheim, Germany
Western Blot Imaging System ChemiDoc™ XRS	BioRad, Hercules, USA
Western Blot System	BioRad, Hercules, USA
Camera at cell culture microscope EP50	OLYMPUS, Tokyo, Japan

Material and Methods

Cell counter EVE TM Plus	NanoEntek, South Korea
Cell culture microscope CK53	OLYMPUS, Tokyo, Japan
Centrifuge 1K15	Sigma/ Sigma-Aldrich, St. Louis, USA
Centrifuge 5810 R	Eppendorf, Hamburg, Germany
CO2 Incubator HERAccl vios 250i	Thermo Fisher Scientific, Waltham, USA
Flow Cytometer Gallios	Beckman Coulter, Brea, USA
Column oven	Shimadzu Deutschland GmbH, Duisburg, Germany
Degassing Unit	Shimadzu Deutschland GmbH, Duisburg, Germany
HLC Heating-ThermoMixer	DITABIS, Pforzheim, Germany
Incubator	Thermo Fisher Scientific, Waltham, USA
Mass spectrometer LCMS-8050	Shimadzu Deutschland GmbH, Duisburg, Germany
Mercury Burner at cell culture microscope	OLYMPUS, Tokyo, Japan
Microplate reader, CLARIOstar Plus	BMG Labtech, Ortenberg, Germany
Mini centrifuge	Biozym Scientific, Hessisch Oldendorf, Germany
Mini-Extruder	Avanti Polar Lipids, Alabaster, USA
Multipette E3	Eppendorf, Hamburg, Germany
Nanodrop One	Thermo Fisher Scientific, Waltham, USA
Nitrogen generator	CMC Instruments, Eschborn, Germany
PH meter, pH Level2	WTW Ivotlab/ Xylem Analytics, Weilheim, Germany

Material and Methods

Pipettes	Eppendorf, Hamburg, Germany
Power PAC 200	BioRad, Hercules, USA
Real-Time System CFX96™	BioRad, Hercules, USA
Rotary Pump with noise reduction cover	Shimadzu Deutschland GmbH, Duisburg, Germany
Scintillation Counter	Packard Instrument Company/ PerkinElmer, Waltham, USA
Solvent delivery Unit	Shimadzu Deutschland GmbH, Duisburg, Germany
System controller	Shimadzu Deutschland GmbH, Duisburg, Germany
Thermal Cycler C100™	BioRad, Hercules, USA
UHPLC autoinjector	Shimadzu Deutschland GmbH, Duisburg, Germany
Vet abc Plus	Scil, Viernheim, Germany
Western Blot Imaging System ChemiDoc™ XRS	BioRad, Hercules, USA
Western Blot System	BioRad, Hercules, USA
Camera at cell culture microscope EP50	OLYMPUS, Tokyo, Japan
Cell counter EVE TM Plus	NanoEntek, South Korea
Cell culture microscope CK53	OLYMPUS, Tokyo, Japan
Centrifuge 1K15	Sigma/ Sigma-Aldrich, St. Louis, USA
Centrifuge 5810 R	Eppendorf, Hamburg, Germany
CO2 Incubator HERAccl vios 250i	Thermo Fisher Scientific, Waltham, USA

Material and Methods

Flow Cytometer Gallios	Beckman Coulter, Brea, USA
Column oven	Shimadzu Deutschland GmbH, Duisburg, Germany
Degassing Unit	Shimadzu Deutschland GmbH, Duisburg, Germany
HLC Heating-ThermoMixer	DITABIS, Pforzheim, Germany
Incubator	Thermo Fisher Scientific, Waltham, USA
Mass spectrometer LCMS-8050	Shimadzu Deutschland GmbH, Duisburg, Germany
Mercury Burner at cell culture microscope	OLYMPUS, Tokyo, Japan
Microplate reader, CLARIOstar Plus	BMG Labtech, Ortenberg, Germany
Mini centrifuge	Biozym Scientific, Hessisch Oldendorf, Germany
Mini-Extruder	Avanti Polar Lipids, Alabaster, USA
Multipipette E3	Eppendorf, Hamburg, Germany
Nanodrop One	Thermo Fisher Scientific, Waltham, USA
Nitrogen generator	CMC Instruments, Eschborn, Germany
PH meter, pH Level2	WTW Ivolab/ Xylem Analytics, Weilheim, Germany
Pipettes	Eppendorf, Hamburg, Germany
Power PAC 200	BioRad, Hercules, USA
Real-Time System CFX96™	BioRad, Hercules, USA
Rotary Pump with noise reduction cover	Shimadzu Deutschland GmbH, Duisburg, Germany

Material and Methods

Scintillation Counter	Packard Instrument Company/ PerkinElmer, Waltham, USA
Solvent delivery Unit	Shimadzu Deutschland GmbH, Duisburg, Germany
System controller	Shimadzu Deutschland GmbH, Duisburg, Germany
Thermal Cycler C100™	BioRad, Hercules, USA
UHPLC autoinjector	Shimadzu Deutschland GmbH, Duisburg, Germany
Vet abc Plus	Scil, Viernheim, Germany
Western Blot Imaging System ChemiDoc™ XRS	BioRad, Hercules, USA
Western Blot System	BioRad, Hercules, USA
Camera at cell culture microscope EP50	OLYMPUS, Tokyo, Japan
Cell counter EVE TM Plus	NanoEntek, South Korea
Cell culture microscope CK53	OLYMPUS, Tokyo, Japan
Centrifuge 1K15	Sigma/ Sigma-Aldrich, St. Louis, USA
Centrifuge 5810 R	Eppendorf, Hamburg, Germany
CO2 Incubator HERAccl vios 250i	Thermo Fisher Scientific, Waltham, USA
Flow Cytometer Gallios	Beckman Coulter, Brea, USA
Column oven	Shimadzu Deutschland GmbH, Duisburg, Germany
Degassing Unit	Shimadzu Deutschland GmbH, Duisburg, Germany

Material and Methods

HLC Heating-ThermoMixer	DITABIS, Pforzheim, Germany
Incubator	Thermo Fisher Scientific, Waltham, USA
Mass spectrometer LCMS-8050	Shimadzu Deutschland GmbH, Duisburg, Germany
Mercury Burner at cell culture microscope	OLYMPUS, Tokyo, Japan
Microplate reader, CLARIOstar Plus	BMG Labtech, Ortenberg, Germany
Mini centrifuge	Biozym Scientific, Hessisch Oldendorf, Germany
Mini-Extruder	Avanti Polar Lipids, Alabaster, USA
Multipette E3	Eppendorf, Hamburg, Germany
Nanodrop One	Thermo Fisher Scientific, Waltham, USA
Nitrogen generator	CMC Instruments, Eschborn, Germany
PH meter, pH Level2	WTW Ivolab/ Xylem Analytics, Weilheim, Germany
Pipettes	Eppendorf, Hamburg, Germany
Power PAC 200	BioRad, Hercules, USA
Real-Time System CFX96™	BioRad, Hercules, USA
Rotary Pump with noise reduction cover	Shimadzu Deutschland GmbH, Duisburg, Germany
Scintillation Counter	Packard Instrument Company/ PerkinElmer, Waltham, USA
Solvent delivery Unit	Shimadzu Deutschland GmbH, Duisburg, Germany

Material and Methods

System controller	Shimadzu Deutschland GmbH, Duisburg, Germany
Thermal Cycler C100™	BioRad, Hercules, USA
UHPLC autoinjector	Shimadzu Deutschland GmbH, Duisburg, Germany
Vet abc Plus	Scil, Viernheim, Germany
Western Blot Imaging System ChemiDoc™ XRS	BioRad, Hercules, USA
Western Blot System	BioRad, Hercules, USA

7.1.2 Consumables

6-well plate for cell culture	Sarstedt, Nümbrecht, Germany
96-well plate for cell culture	Sarstedt, Nümbrecht, Germany
96-well plate for luminescent measurement, white, Optiplate™	PerkinElmer, Waltham, Germany
Pipette tips 1000 µl	Sarstedt, Nümbrecht, Germany
Pipette tips 1200 µl	Sarstedt, Nümbrecht, Germany
Pipette tips 20 µl	Sarstedt, Nümbrecht, Germany
Pipette tips 200 µl	Sarstedt, Nümbrecht, Germany
Polycarbonate filters 200 nm	Whatman, Maidstone, Germany
T75 Cell culture flask	Sarstedt, Nümbrecht, Germany
Tube 15 ml	Sarstedt, Nümbrecht, Germany
Tube 50 ml	Sarstedt, Nümbrecht, Germany
Reaction tube 1.5 ml	Sarstedt, Nümbrecht, Germany

Material and Methods

Reaction tube 2 ml	Sarstedt, Nümbrecht, Germany
MCE Membrane 0.22 µM	Merck Millipore, Burlington, USA
Re-usable Syringe Filter Holders	Sartorius, Göttingen, Germany
Polyvinylidene difluoride membrane (PVDF)	Merck Millipore, Burlington, USA

7.1.3 Chemicals & Reagents

Acrylamid (30%)	AppliChem, Darmstadt, Germany
Acrylamid 4K Solution (30%) Mix 37,5:1	AppliChem, Darmstadt, Germany
Amberlite XAD-2 beads	Sigma-Aldrich, St. Louis, USA
Ammonium molybdat tetrahydrat	Sigma-Aldrich, St. Louis, USA
Ammonium persulfate	Sigma-Aldrich, St. Louis, USA
Ascorbic acid (L-)	Sigma-Aldrich, St. Louis, USA
BSA fatty acid free (Bovine Serum Albumin Fraction V)	Serva, Hamburg, Germany
Coomassie Brilliant Blue R250	Merck, Darmstadt, Germany
Dimethylsulfoxid (DMSO)	Sigma-Aldrich, St. Louis, USA
Dinatriumhydrogenphosphate (Na_2HPO_4)	Merck, Darmstadt, Germany
Dipotassium phosphate (K_2HPO_4)	Sigma-Aldrich, St. Louis, USA
Disodium phosphate (Na_2HPO_4)	Sigma-Aldrich, St. Louis, USA
Dulbecco's Modified Eagle's Medium (DMEM)	Thermo Fisher Scientific, Waltham, USA
Ethanol (99%)	Sigma-Aldrich, St. Louis, USA

Material and Methods

Ethylenbis(oxyethylenitrilo)tetraessigsäure (EGTA)	Sigma-Aldrich, St. Louis, USA
Ethylenediaminetetraacetic acid (EDTA)	Sigma-Aldrich, St. Louis, USA
Fetal Bovine Serum (FCS)	Thermo Fisher Scientific, Waltham, USA
Forskolin	Sigma-Aldrich, St. Louis, USA d
FTY720 (Fingolimod)	Cayman Chemical, Ann Arbor, USA
FTY720-P	Cayman Chemical, Ann Arbor, USA
Fugene6	Promega, Madison, USA
Geneticin (G418)	Thermo Fisher Scientific, Waltham, USA
Glucose (D-)	Sigma-Aldrich, St. Louis, USA
Glucose, D-[3- ³ H]	American Radiolabeled Chemicals, St. Louis, USA
Glycine	Sigma-Aldrich, St. Louis, USA
HALT Protease inhibitor	Thermo Fisher Scientific, Waltham, USA
HALT Protease-phosphatase inhibitor	Thermo Fisher Scientific, Waltham, USA
HEPES	Sigma-Aldrich, St. Louis, USA
Hydrogen peroxide (H ₂ O ₂)	Sigma-Aldrich, St. Louis, USA
IgG1, κ	Biolegend, San Diego, USA
Imidazole	AppliChem. Darmstadt, Germany
iQ™ SYBERGreen	BioRad, Hercules, USA
L-α-phosphatidic acid, chicken egg (Egg PA)	Avanti Polar Lipids, Alabaster, USA
L-α-phosphatidylcholine, chicken egg (Egg PC)	Avanti Polar Lipids, Alabaster, USA
Magnesium sulfate (MgSo ₄)	Sigma-Aldrich, St. Louis, USA

Material and Methods

Methanol	Carl Roth, Karlsruhe, Germany
Milk powder	Sigma-Aldrich, St. Louis, USA
Monopotassium phosphate (KH ₂ PO ₄)	Sigma-Aldrich, St. Louis, USA
NP-40	Sigma-Aldrich, St. Louis, USA
Okadaic acid	Sigma-Aldrich, St. Louis, USA
OptiMem	Thermo Fisher Scientific, Waltham, USA
Penicillin-Streptomycin	Thermo Fisher Scientific, Waltham, USA
Perchloric acid	Sigma-Aldrich, St. Louis, USA
Phosphate-buffered saline (PBS)	AppliChem, Darmstadt, Germany
Phloretin	Sigma-Aldrich, St. Louis, USA
Potassium bicarbonate (KHCO ₃)	Merck, Darmstadt, Germany
Potassium Chloride (KCL)	Sigma-Aldrich, St. Louis, USA
Recombinant glucose transporter 4 #MBS2086793	MyBioSource, San Diego, USA
Sodium chloride (NaCl)	Carl Roth, Karlsruhe, Germany
Sodium dodecylsulfate polyacrylamide (SDS)	Sigma-Aldrich, St. Louis, USA
Sphingomab LT1002	Lpath Inc., San Diego, USA
Sphingosine 1-Phosphate, D-erythro	Enzo Life Sciences GmbH, Lörrach, Germany
Sphingosine, D-erythro	Enzo Life Sciences GmbH, Lörrach, Germany
Taurine	Sigma-Aldrich, St. Louis, USA
Tetramethylethylenediamine (TEMED)	Sigma-Aldrich, St. Louis, USA
Tris base	AppliChem, Darmstadt, Germany
Tris(hydroxymethyl)aminomethane (Tris)	Carl Roth, Karlsruhe, Germany

Material and Methods

Tris-HCl	AppliChem, Darmstadt, Germany
Triton X-100	Sigma-Aldrich, St. Louis, USA
Trypan blue (0,4% Solution)	Sigma-Aldrich, St. Louis, USA
Tween 20	Sigma-Aldrich, St. Louis, USA
β -Mercaptoethanol	Sigma-Aldrich, St. Louis, USA
Acrylamid (30%)	AppliChem, Darmstadt, Germany
Acrylamid 4K Solution (30%) Mix 37,5:1	AppliChem, Darmstadt, Germany
Amberlite XAD-2 beads	Sigma-Aldrich, St. Louis, USA
Ammonium molybdat tetrahydrat	Sigma-Aldrich, St. Louis, USA
Ammonium persulfate	Sigma-Aldrich, St. Louis, USA
Ascorbic acid (L-)	Sigma-Aldrich, St. Louis, USA
BSA fatty acid free (Bovine Serum Albumin Fraction V)	Serva, Hamburg, Germany
Coomassie Brilliant Blue R250	Merck, Darmstadt, Germany
Dimethylsulfoxid (DMSO)	Sigma-Aldrich, St. Louis, USA
Dinatriumhydrogenphosphate (Na_2HPO_4)	Merck, Darmstadt, Germany
Dipotassium phosphate (K_2HPO_4)	Sigma-Aldrich, St. Louis, USA
Disodium phosphate (Na_2HPO_4)	Sigma-Aldrich, St. Louis, USA
Dulbecco's Modified Eagle's Medium (DMEM)	Thermo Fisher Scientific, Waltham, USA
Ethanol (99%)	Sigma-Aldrich, St. Louis, USA
Ethylenbis(oxyethylenitrilo)tetraessigsäure (EGTA)	Sigma-Aldrich, St. Louis, USA
Ethylenediaminetetraacetic acid (EDTA)	Sigma-Aldrich, St. Louis, USA

Material and Methods

Fetal Bovine Serum (FCS)	Thermo Fisher Scientific, Waltham, USA
Forskolin	Sigma-Aldrich, St. Louis, USA d
FTY720 (Fingolimod)	Cayman Chemical, Ann Arbor, USA
FTY720-P	Cayman Chemical, Ann Arbor, USA
Fugene6	Promega, Madison, USA
Geneticin (G418)	Thermo Fisher Scientific, Waltham, USA
Glucose (D-)	Sigma-Aldrich, St. Louis, USA
Glucose, D-[3- ³ H]	American Radiolabeled Chemicals, St. Louis, USA
Glycine	Sigma-Aldrich, St. Louis, USA
HALT Protease inhibitor	Thermo Fisher Scientific, Waltham, USA
HALT Protease-phosphatase inhibitor	Thermo Fisher Scientific, Waltham, USA
HEPES	Sigma-Aldrich, St. Louis, USA
Hydrogen peroxide (H ₂ O ₂)	Sigma-Aldrich, St. Louis, USA
IgG1, κ	Biolegend, San Diego, USA
Imidazole	AppliChem. Darmstadt, Germany
iQ™ SYBERGreen	BioRad, Hercules, USA
L-α-phosphatidic acid, chicken egg (Egg PA)	Avanti Polar Lipids, Alabaster, USA
L-α-phosphatidylcholine, chicken egg (Egg PC)	Avanti Polar Lipids, Alabaster, USA
Magnesium sulfate (MgSO ₄)	Sigma-Aldrich, St. Louis, USA
Methanol	Carl Roth, Karlsruhe, Germany
Milk powder	Sigma-Aldrich, St. Louis, USA
Monopotassium phosphate (KH ₂ PO ₄)	Sigma-Aldrich, St. Louis, USA

Material and Methods

NP-40	Sigma-Aldrich, St. Louis, USA
Okadaic acid	Sigma-Aldrich, St. Louis, USA
OptiMem	Thermo Fisher Scientific, Waltham, USA
Penicillin-Streptomycin	Thermo Fisher Scientific, Waltham, USA
Perchloric acid	Sigma-Aldrich, St. Louis, USA
Phosphate-buffered saline (PBS)	AppliChem, Darmstadt, Germany
Phloretin	Sigma-Aldrich, St. Louis, USA
Potassium bicarbonate (KHCO ₃)	Merck, Darmstadt, Germany
Potassium Chloride (KCL)	Sigma-Aldrich, St. Louis, USA
Recombinant glucose transporter 4 #MBS2086793	MyBioSource, San Diego, USA
Sodium chloride (NaCl)	Carl Roth, Karlsruhe, Germany
Sodium dodecylsulfate polyacrylamide (SDS)	Sigma-Aldrich, St. Louis, USA
Sphingomab LT1002	Lpath Inc., San Diego, USA
Sphingosine 1-Phosphate, D-erythro	Enzo Life Sciences GmbH, Lörrach, Germany
Sphingosine, D-erythro	Enzo Life Sciences GmbH, Lörrach, Germany
Taurine	Sigma-Aldrich, St. Louis, USA
Tetramethylethylenediamine (TEMED)	Sigma-Aldrich, St. Louis, USA
Tris base	AppliChem, Darmstadt, Germany
Tris(hydroxymethyl)aminomethane (Tris)	Carl Roth, Karlsruhe, Germany
Tris-HCl	AppliChem, Darmstadt, Germany
Triton X-100	Sigma-Aldrich, St. Louis, USA
Trypan blue (0,4% Solution)	Sigma-Aldrich, St. Louis, USA

Material and Methods

Tween 20 Sigma-Aldrich, St. Louis, USA

β -Mercaptoethanol Sigma-Aldrich, St. Louis, USA

7.1.4 Commercial Kits

Glucose Uptake-Glo™ Assay Promega, Madison, USA

PP2A Immunoprecipitation Phosphatase Assay Merck Millipore, Burlington, USA

Kit

Mouse Glycated Hemoglobin A1c (Hba1c) ELISA MyBioSource San Diego, USA

Kit

Pierce™ BCA Protein Assay Kit Thermo Fisher Scientific, Waltham, USA

RevertAid RT Reverse Transcription Kit Thermo Fisher Scientific, Waltham, USA

7.1.5 Laboratory animal diet

Normal cow diet (12% fat, 18% protein, 70% carbohydrates) Altromin Spezialfutter GmbH & Co. KG, Lage, Germany

Normal chow diet with low vitamin B6 Altromin Spezialfutter GmbH & Co. KG Lage, Germany

High fat diet (35% fat) Altromin Spezialfutter GmbH & Co. KG Lage, Germany

Normal cow diet (12% fat, 18% protein, 70% carbohydrates) Altromin Spezialfutter GmbH & Co. KG, Lage, Germany

Normal chow diet with low vitamin B6 Altromin Spezialfutter GmbH & Co. KG Lage, Germany

Material and Methods

7.1.6 Cell culture media

Table 1: Media and supplements for cell cultivation.

Celltype	Cell culture medium	Supplements
HEK293-wt	DMEM	10% FCS 1% penicillin-streptomycin
HEK293-Mfsd2b	DMEM	10% FCS 1% penicillin-streptomycin 300 µg/ ml G418
HEK293-SphK1-wt	DMEM	10% FCS 1% penicillin-streptomycin 500 µg/ ml Zeocin
HEK293-SphK1-Mfsd2b	DMEM	10% FCS 1% penicillin-streptomycin 300 µg/ ml G418 500µg /ml Zeocin

7.1.7 Antibodies for Western blot

Glut4 (1F8) Mouse mAb #2213	Cell Signaling Technology, Danvers, USA
Recombinant Anti-Stomatin antibody [EPR10421]	Abcam, Cambridge, UK
GAPDH	HyTest, Turku, Finland
Peroxidase labelled Anti-Mouse IgG (H+L)	Vector, Burlingame, USA
Peroxidase labelled Anti-Rabbit IgG (H+L)	Vector, Burlingame, USA

7.1.8 Antibodies/ Proteins for flow cytometry

IgG Fc antibody (biotinylated goat anti-human)	eBioscience, ThermoFisher Scientific, Waltham, USA
anti-GLUT4 PE (clone IF8)	Santa Cruz Biotechnology, Heidelberg, Germany

Material and Methods

LM048 (anti GLUT4 external domain) Joseph Rucker, Integral Molecular, Philadelphia, PA 19104

HRBDEGFP protein (anti GLUT1 external domain) Dr. Vincent Petit, METAFORA biosystems, Paris, France

7.1.9 Primers for quantitative Real-Time PCR

Table 2: Primers for different genes used for RT qPCR.

Primer	Gene/ Origin of the gene	5'-3' sequence
<i>Sphk1</i> _forward	<i>Sphk1</i> / mouse	AGAACCACGCTAGGGAATTG
<i>Sphk1</i> _reverse		GGCCTCTCCATCAAACCATTA
SPHK1_ <i>forward</i>	SPHK1/ human	GGCTGCTGTCACCCATGAA
SPHK1_ <i>reverse</i>		TCACTCTCTAGGTCCACATCAG
<i>Mfsd2b</i> _forward	<i>Mfsd2b</i> / mouse	AGGCCCTGGCTACGTTCTT
<i>Mfsd2b</i> _reverse		GTGGGCACTGGACACAATGA
MFSD2B_ <i>forward</i>	MFSD2B/ human	ACAAAGGTGTGCTATGGCATT
MFSD2B_ <i>reverse</i>		GGGATCTGTGCTATATCAAGCAG
GAPDH_ <i>reverse</i>	GAPDH/ human	AATCCCATCACCATCTTCCAG
GAPDH_ <i>reverse</i>		AAATGAGCCCCAGCCTTC

7.2 Methods

7.2.1 Human samples

Human blood was donated by healthy volunteers as well as control and diabetic patients. The study was in accordance with the Declaration of Helsinki and was approved by the University of Duesseldorf Ethics Committee (vote no° 4658).

7.2.2 Mouse models

All mouse experiments were approved by the LANUV (LANUV Recklinghausen, Germany) as stated by the European Convention of the Protection of Vertebrate Animals used for Experimental and other Scientific Purposes (Az 84-02.04.2017.A097, 84-02.04.2017.A087 and 81-02.04.2021.A048). Mice were kept and bred in the animal facility of the Heinrich-Heine university Düsseldorf. Sphk1^{-/-} mice (B6J.129S6(B6N)-Sphk1^{tm1Rpl}/J) were kindly provided by R. Proia (National Institutes of Health, Bethesda, USA). Mfsd2b^{+/+} and Mfsd2b^{-/-} (C57BL/6N-Mfsd2b^{tm1a(KOMP)Wtsi}/Wtsi) were purchased from the MMRRC at UC Davis. The Sgpl vav-cre mice were generated by crossing Sgpl flox/flox mice (A. Billich, Novartis) with Commnd10Tg(vav1-iCre)A2Kio/J vav Cre transgenic mice. 4-deoxypyridoxine (DOP) (Sigma, St. Louis, USA), a pharmacological inhibitor of S1P lyase, was administrated to wild type (C57BL/6J) mice via drinking water at 3 mg/l (0.5 mg per kg body weight per day) for three weeks. Simultaneously, with DOP treatment, mice received a normal chow diet with low vitamin B6 (Altromin Spezialfutter GmbH & Co. KG, Lage, Germany). Diet-induced obesity was induced by feeding a diet with 60% energy from fat (35% fat, 5.228 kcal/kg, Altromin Spezialfutter GmbH & Co. KG, Lage, Germany) for 12 or 8 weeks, as indicated.

7.2.3 Culturing of HEK293-Mfsd2b cells

HEK293 cells overexpressing mouse Mfsd2b (Vektor ORF MFSD2B; Origene, Rockville, USA) (HEK293-Mfsd2b) and control HEK293 cells (HEK293-wt) were cultured in Dulbecco's Modified Eagle's Medium (DMEM, Gibco; Thermo Fisher Scientific, Waltham, USA) supplemented with 10% Fetal Bovine Serum (FCS), 1% penicillin-streptomycin and

additionally 300 µg/ml G418 for Mfsd2b selection, at 37 °C in an incubator with 5% CO₂ and 95% humidity. Transfected HEK293 cells were kindly provided by Prof. Dr. Markus Gräler from University Hospital Jena, Germany.

7.2.4 Transient transfection of HEK293 cells with SphK1

HEK293-wt and Hek293-Mfsd2b cells were transfected with an *EGFP-C1-Sphk1* plasmid construct (Fig.2), which is based on a pBMN-I-GFP vector plasmid, by the technician Kerstin Petch. Enhanced green fluorescent protein (EGFP) is coupled to SphK1 expression, so that GFP is also expressed if transfection and SphK1 expression are successful. To transfect cells, 75 000 cells per well were seeded in a 6 well plate in DMEM (Gibco; Thermo Fisher Scientific, Waltham, USA) supplemented with 10% FCS, 1% penicillin-streptomycin. On the following day 150 µl of pre warmed OptiMem medium per well (Gibco; Thermo Fisher Scientific, Waltham, USA) were mixed with 6 µl of transfection reagent Fugene6 (Promega, Madison, USA). After 5 min at room temperature (RT) 2 µg of plasmid was added and the mix was incubated for 15 min at RT. Next, the OptiMem-Fugene6-DNA- mix was added drop by drop to the according well and the plate was mixed with circular, horizontal movements. After incubation for 24 h in the incubator (37°C, 5% CO₂, 95% humidity) the medium was changed for HEK293-wt cells to DMEM (+ 10% FCS, 1% penicillin-streptomycin) and for Hek293-mfsd2b cells to the same medium with additionally with 300 µg/ml G418. Cells are checked for successful transfection by imaging the GFP signal via microscope (Olympus, Tokyo, Japan) 48 h after transfection. After successful transfection HEK293-SphK1-wt and HEK293-SphK1-Mfsd2b cells were transferred into a 96 well pate (20 000 cells/well) and thus prepared for the glucose uptake experiment.

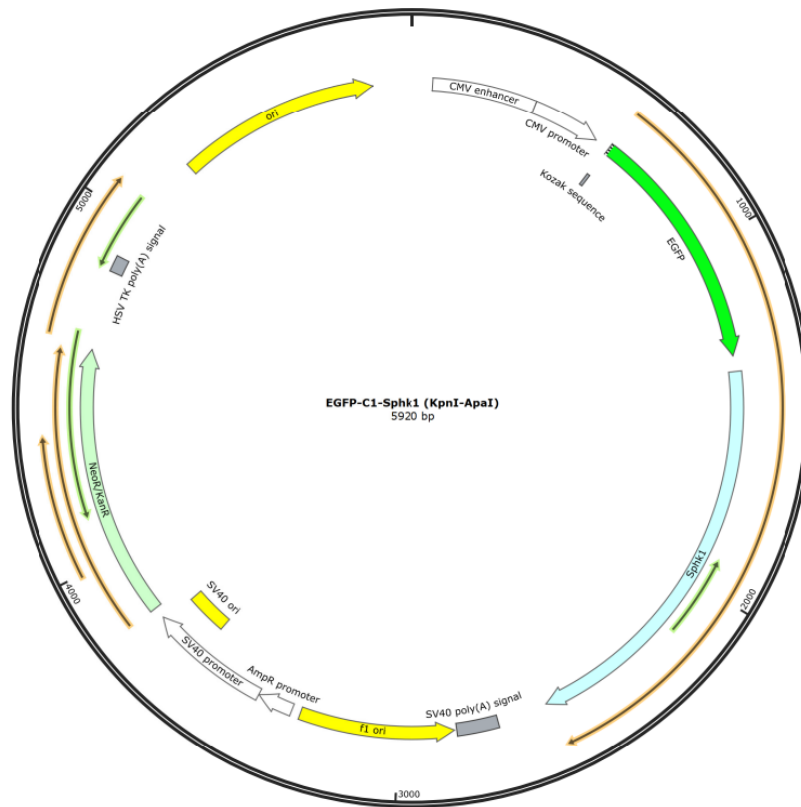


Figure 6: Plasmid construct of EGFP-C1-Sphk1 plasmid.

7.2.5 Stable transfection of HEK293 cells with Sphk1

The following steps were carried out by Dr. Shahrooz Ghaderi. The transfected cells were then used for further experiments.

Bacterial strains and plasmid preparation.

DH5 α strain of *Escherichia coli* was used as a competent cell (Invitrogen; Thermo Fisher Scientific, Waltham, USA) for transfection. *E. coli* bearing the desired plasmid were cultured in lysogeny broth (LB) media for 16 h at 37°C in a shaking incubator. After harvesting the cells, plasmid DNA was extracted by mini-prep plasmid extraction kit (Macherey-Nagel, Düren, Germany).

Cloning

To amplify mouse SphK1, cloning primers including *Bam*HI and *Xho*I restriction sites were used. After cutting the insert, it was inserted/ligated cloned into the pCDNA4-zeo mammalian expression vector.

Material and Methods

Transfection

For transfecting the pCDNA4-zeo and pCDNA-sphk1 into the HEK cells FuGENE (Promega, Madison, USA), has been used according to the manufacture protocol.

Selection

One day after transfection, successfully transfected HEK cells have been selected with 500 µg/ml Zeocin (Invitrogen, Thermo Fisher scientific, Germany). After three weeks single clones have been expanded. To confirm the SphK1 expression in HEK293 cells qRT-PCR were performed.

7.2.6 RBC isolation and preparation

RBCs were isolated from whole mouse and human blood by separation from plasma based on centrifugation at 1500 x g for 10 min at 4 °C. Afterwards, cells were washed twice with PBS. The number of RBCs was determined a scil Vet abc Plus blood counting system (Scil animal care company GmbH, Viernheim, Germany).

7.2.7 Sphingolipid loading

RBCs were isolated and prepared as described before. 100×10^6 cells/ml were incubated with 1 µM sphingosine (D-erythro, Enzo Life Sciences GmbH, Lörrach, Germany), 1 µM FTY720 (Cayman Chemical, Ann Arbor, USA) or 1 µM FTY720-P (Cayman Chemical, Ann Arbor, USA) for 30 min at 37°C in tyrode buffer (113 mM NaCl, 4.7 mM KCl, 0.6 mM KH₂PO₄, 0.6 mM Na₂HPO₄, 1.2 mM MgSO₄, 12 mM NaHCO₃, 10 mM KHCO₃, 10 mM HEPES, 30 mM taurine, pH 7.0) under continuously gentle shaking (Thermoshaker, Haep Labor Consult, Bovenden, Germany). The corresponding amount of Ethanol (EtOH) (0.1%) served as solvent control for Sph and FTY720 incubation, whereas DMSO (0.1%) served as control for FTY720-P. After incubation, RBCs were washed once with tyrode buffer (300 x g, 10 min) and the RBC pellet was dissolved in 1 ml MeOH to determine Sphingolipid level of loaded and unloaded RBCs by LC-MS/MS measurements. 10 µl C17 Sph/ C17 S1P standard was added and RBC-MeOH mixes were stored over night at -80 °C before tubes were centrifuged 5 min at maximum speed (21460 x g) at 4°C. Supernatants were transferred in

1.5 ml glass tubes and measured by LC-MS/MS as described below. C17 Sph/ C17 S1P is not occurring naturally in the cell and can thus be used as a standard for later calculations of the S1P quantity. The PP2A inhibitor okadaic acid (Sigma-Aldrich, St. Louis, USA) was applied in a concentration of 2 nM 15 min before sphingosine incubation.

7.2.8 Efflux assay

To perform an efflux assay, S1P-loaded and unloaded RBCs were incubated with 1 mM D-glucose and with or without 1% BSA (fatty-acid free) for 20 min at 37 °C under continuously soft shaking. Alternatively, RBCs were incubated with 800 pmol/l of the specific S1P antibody Sphingomab LT1002 (Lpath Inc., San Diego, USA) or 800 pmol/l of the isotype control IgG1, κ (Biolegend, San Diego, USA). To separate RBCs from supernatant, RBCs were centrifuged by 300 x g for 10 min. supernatants were transferred in new tubes and RBC pellets were precipitated with 1 ml MeOH. 10 μ l C17 Sph (0.3 pmol/ μ l)/ C17 S1P (0.1 pmol/ μ l) standard was added to RBCs and supernatant. Both were stored over night at -80 °C before tubes were centrifuged for 5 min at maximum speed (21460 x g) at 4°C. Supernatants were transferred to 1.5 ml glass tubes and measured by LC-MS/MS as described below.

7.2.9 LC-MS/MS measurement

The detection of sphingolipids was performed using positive electrospray ionization with a LCMS-8050 Triple Quadrupol mass spectrometer (Shimadzu Deutschland GmbH, Duisburg, Germany). The ion source conditions and gas settings are as follows: Nebulizer: 3 l/min, Interface Temperature: 300 °C, Desolvation Temperature: 526 °C, Heat Block Temperature: 400 °C and Drying Gas Flow: 10 l/min. Gradient separation of lipids (10 μ l injection) was performed with a Nexera X2 UHPLC system (Shimadzu Deutschland GmbH, Duisburg, Germany) and 60 x 2.0 mm MultoHigh 100 RP18 column (CS Chromatographie Service, Langerwehe, Germany) with 3 μ m particle size at 40 °C. HPLC is performed with 10% MeOH as eluent A and 90% formic acid (1% v/v in H₂O) as eluent B. The flow rate is 0.4 ml/min and the gradient settings are shown in Table 3: Mobile phase gradient settings..

Metabolome primary data were analysed and further processed with LabSolutions 5.99 (Shimadzu Deutschland GmbH, Duisburg, Germany). The measurements and analysis of the data were performed by Dr. Philipp Wollnitzke.

Table 3: Mobile phase gradient settings.

Time [min]	A conc.	B conc.	B.curve
0	10	90	-2
3	100	0	0
12	100	0	0
12.01	10	0	0

7.2.10 Glucose uptake

Glucose uptake was investigated in RBCs as well as HEK293 cells by using a luciferase based 2-deoxyglucose assay (2DG) (Promega, Madison, USA). The operation principle of the kit is shown in Figure 7. Briefly, cells were stimulated and quiesced in a zero glucose media. Afterwards, cells were incubated with 2-deoxyglucose (1 mM) for 20 min at 37 °C in an incubator with 5% CO₂ and 95% humidity. To stop glucose uptake cells were lysed and neutralized before a custom lucigenic reaction mixture was added. This ensures that 2-deoxyglucose 6-phosphate (2DG6P), which was phosphorylated by the cells, oxidizes to 6-phosphodeoxygluconate and simultaneously reduces NADP⁺ to NADPH. A reductase uses NADPH to convert proluciferin to luciferin, which is used by a luciferase to produce a luminescent signal. This is proportional to the concentration of phosphorylated 2DG6P and thus proportional to the glucose uptake. The luminescent signal was detected in a white 96 well plate 90 min after editing the detection reagent via microplate reader CLARIOstar Plus (BMG LABTECH GmbH, Offenburg, Germany).

Material and Methods

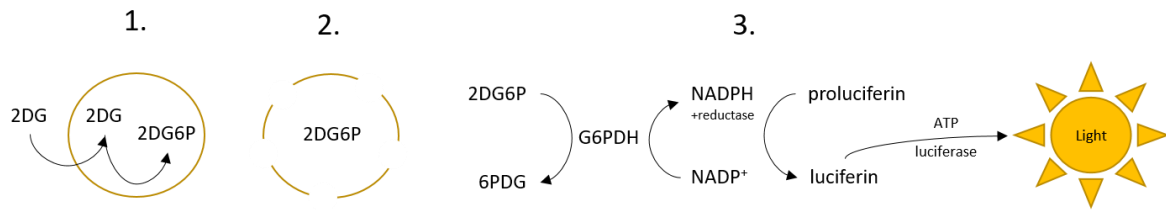


Figure 7: Principle of Glucose uptake-glow assay Kit (Promega, Madison, USA).

1. Addition of 2-deoxyglucose (2DG) to the cells. Phosphorylation to 2-deoxyglucose-6-phosphate (2DG6P).
2. Ends of reaction by addition of Stop and Neutralization buffer. Cell lysis and elimination of NADPH. 3. Detection of phosphorylated 2DG6P by addition of 2DG6P detection reagent leads to measurement of luminescent light. Figure modified from Glucose Uptake-Glo™ Assay manual (Promega, Madison, USA).

Glucose uptake assay with RBCs

To investigate glucose uptake in erythrocytes, RBCs were isolated, washed and loaded with S1P as described before. Subsequently 50 μ l of RBC suspension (100×10^6 / ml) were transferred in each well of a white 96 well plate. This way, each well contained 5 million RBCs in 50 μ l and received 1 mM 2DG for 20 min, incubated at 37 °C and 5% CO₂. In the corresponding wells, 1 μ l of a 50% BSA (fatty-acid free) solution was added immediately after the 2DG addition, so that they contained 1% BSA. BSA serves as S1P acceptor. Instead of 1% BSA, 800 pmol Sphingomab was also used. The identical concentration of IgGk served as a control. Simultaneously, to 2DG, a defined concentration of 2DG-6-phosphate (2DG6P) was added to wells containing the RBC suspension. This served as standard series for later calculation. The wells of the standard series contained the same amount of RBCs as those of the measurement, since the quenching of the luminescent signal by haemoglobin is taken into account. The standard series included 0, 5, 10 and 15 μ M 2DG6P. To stop the glucose uptake, cells were lysed with 25 μ l stop buffer and short shaking at room temperature. Afterwards 25 μ l neutralisation buffer and 100 μ l of detection buffer were added to the cells and incubated 90 min at room temperature before the luminescent signal was measured via microplate reader CLARIOstar Plus (BMG LABTECH GmbH, Offenburg, Germany)

Material and Methods

Glucose uptake assay with HEK293 cells

HEK293 cells (20 000/ well) were seeded in a 96 well plate 24 h before starting the assay. For the glucose uptake assay, cells were washed and quiesced in glucose free, phenol red free DMEM (Gibco; Thermo Fisher Scientific, Waltham, USA) for 1 h. Afterwards cells were incubated with 1 μ M sphingosine for 1 h at 37 °C in an incubator with 5% CO₂ and 95% humidity. The corresponding amount of EtOH served as solvent control. Subsequently, cells were washed with glucose free, phenol red free medium and all approaches were incubated with 50 μ l of this medium containing 1 mM 2DG for 20 min (37°C, 5% CO₂). The respective wells received additional 1% BSA. To stop glucose uptake, cells were lysed with 25 μ l stop buffer and continuously shaken for 1 h at room temperature. Afterwards, 25 μ l neutralisation buffer and 100 μ l of detection buffer, which contains luciferase reagents, NADP⁺, G6PDH, reductase and reductase substrate were added to the cells and incubated for 90 min at room temperature. To measure the luminescent signal, 150 μ l of the total reaction solution was transferred in a white 96-well plate. The same procedure was performed with wells that contained the standard series (0-20 μ M 2DG6P). Afterwards, the plate was measured by microplate reader CLARIOstar Plus (BMG LABTECH GmbH, Offenburg, Germany).

7.2.11 PP2A activity

PP2A was measured with the PP2A Immunoprecipitation Phosphatase Assay Kit (Merck Millipore, Burlington, USA). Before measuring the phosphatase activity of RBC samples with the kit, all required buffers, water and samples were tested for phosphate contamination. To do so, the malachite green phosphate detection solution is prepared by mixing supplied solution A and B. For the assay RBCs were isolated and loaded with S1P like described before, but instead of tyrode buffer TBS buffer (200 mM Tris, 1500 mM NaCl, pH 7.4) was used. Cells were lysed by mixing in 200 μ l cold buffer containing 20 mM imidazole, 2 mM Ethylenediaminetetraacetic acid (EDTA), 2 mM ethylene glycol-bis(β -aminoethyl ether)-N,N,N',N'-tetraacetic acid (EGTA) and total protease inhibitor cocktail (Thermo Fisher Scientific, Waltham, USA). Cell lysates were centrifuged at 200 x g for 5 min at 4°C. The supernatants were used for protein determination and to detect phosphatase activity. Per preparation 500 μ g protein were used and 4 μ l of Anti-PP2A C subunit clone 1D6 (1 μ g/ μ l)

Material and Methods

was added. Afterwards 30 μ l Protein A agarose slurry beads were added and filled up to 500 μ l with provided pNPP Ser/Thr Assay Buffer. The mix was incubated for 1.5 h at 4 °C with constant shaking to carry out an immunoprecipitation (ip). Subsequently, the beads were washed 3 times with 700 μ l TBS, followed by one wash with 500 μ l Ser/Thr Assay Buffer. 60 μ l of 1 mM Threonine phosphopeptide together with 20 μ l of Ser/Thr Assay Buffer were added and incubated for 10 min at 30 °C in a shaking incubator. The more active PP2A is isolated by ip, the more phosphate is cleaved from the added phosphopeptide. Afterwards the tubes were centrifuged briefly and 25 μ l were transferred in a ½ volume microplate. 100 μ l of Malachite Green Phosphate Detection Solution, which was prepared like described before, was added. The Malachite Green detects the amount of free phosphate by a color change from yellow to green. The mix was incubated at RT for 15 min until a color change was observed. The plate was measured at 650 nm by the microplate reader CLARIOstar Plus (BMG LABTECH GmbH, Offenburg, Germany). To investigating the activity of the PP2A holoenzyme, PP2A was isolated from murine C57Bl6 RBCs by immunoprecipitation followed by incubation of the beads with the substances to be tested for 30 min at 37 °C with. C6 ceramide (Cayman Chemical, Ann Arbor, USA) served as positive control [210]. In the case of testing the human recombinant PP2A catalytic subunit (Cayman Chemical, Ann Arbor, USA) the commercially purchased enzyme was incubated with 0.58 mU in 100 μ l with all substances for 10 min at 30 °C.

7.2.12 GLUT activity

To investigating the impact of different S1P concentrations in the plasma membrane on GLUT activity, liposomes were used as a model for the plasma membrane. Liposomes can be constructed with known lipid composition and by integrating a GLUT transporter, the influence of the different membrane composition on glucose uptake can be investigated. L- α -phosphatidylcholine from chicken egg (Egg PC) serves as main component and liposomes consisting of 0.1% S1P (+99.9% Egg PC), 1% S1P (+99% Egg PC) and 15% S1P (+75% Egg PC) are compared with the control liposomes consisting of 100% Egg PC and no S1P. Liposomes consisting of 15% L- α -phosphatidic acid from chicken egg (Egg PA) and 75% Egg PC serves as positive control for enhanced glucose uptake [163].

Material and Methods

Liposome reconstitution

The lipids (Egg PC, Egg PA and S1P) are dissolved in chloroform, mixed in 13 x 100 mm glass tubes and dried under light stream of nitrogen. For that, glass tubes are slowly rotated under the influx of nitrogen so that the solvent evaporates and a thin lipid layer was formed in the tube. It is important to use glass tubes because the lipids have a very high affinity to plastic. Afterwards, lipids were dried under 10 min continuously nitrogen stream. The dried lipid film was resuspended in 1 ml buffer containing 100 mM NaCl and 20 mM HEPES (pH 7.4-7.6), mixed and shaken 1 h at room temperature. To form large unilamellar vesicles, liposomes were freeze and thawed 5 times in liquid nitrogen and water (RT). Then they were extruded 13 times through 200 nm polycarbonate filters (Whatman, Maidstone, UK) using a mini-extruder (Avanti Polar Lipids, Alabaster, USA). To determine the concentration of prepared liposomes a phosphate assay was performed. To insert purified GLUT4 in the liposomes, the procedure was performed as described by Hresko et al. 2016 [163]. Liposomes were first destabilized by 0.5% Triton X-100 for 10 min at RT and then rotated with recombinant GLUT4 protein (MyBioSource San Diego, USA) at a lipid to protein ratio of 100:1 for 45 min at 4 °C. Amberlite XAD-2 beads (Sigma-Aldrich, St. Louise, USA) were added to remove detergent at a wet weight of 15-16 mg of beads per mg of Triton X-100. Fresh beads were added after 1 h, at the next day and additionally after two hours. The beads were removed by centrifugation at 10 000 x g for 5 min. Afterwards, liposomes are collected by ultracentrifugation at 4 °C for 1 h at 267 000 x g and resuspended in buffer containing 50 mM potassium phosphate (34.8 mM K₂HPO₄, 15.2 mM KH₂PO₄), 130 mM KCl (pH 7.4) and complete protease inhibitor (Thermo Fisher Scientific, Waltham, USA). If liposomes were not immediately used for glucose uptake experiment, they were flash-frozen with liquid nitrogen and stored at -80°C.

Phosphate assay (quantification of phospholipids)

To quantify liposomes after extrusion a phosphate assay was performed. A 40 mM phosphate (Pi) stock solution was prepared using disodiumhydrogenphosphate which was sequential 10-fold diluted to obtain working solutions of 4 mM and 0.4 mM Pi. Thus, a standard series of 0 to 80 mmol Pi was prepared in 13 x 100 mm glass tubes in a total volume of 50 µl. Samples (10µl) were added to H₂O (40µl). 300 µl perchloric acid was added

Material and Methods

to all standard and sample tubes and heated for 1 h at 145 °C in a heating block. Marbles on the tubes prevented evaporation. After 1 h tubes were removed from heat and 1 ml of H₂O was added, tubes were mixed. Samples were cooled down to room temperature and 400 µl of 12 mg/ml fresh ammonium molybdate tetrahydrate and 400 µl fresh 50 mg/ml ascorbic acid were added to the tubes. After mixing, tubes were heated 10 min at 100 °C and 200 µl standard and liposome samples was measured in a clear 96 well plate (SARSTEDT AG & Co. KG, Nümbrecht, Germany) at 797 nm absorbance in a microplate reader CLARIOstar Plus (BMG LABTECH GmbH, Offenburg, Germany).

Liposome [³H] glucose uptake

Frozen liposomes were thawed at RT and afterwards freeze and thawed for five cycles in liquid nitrogen and water (RT) followed by extrusion through 200 nm polycarbonate filter (Whatman, Maidstone, UK) using a mini-extruder (Avanti Polar Lipids, Alabaster, USA). Glucose uptake assay was performed in a total volume of 1000 µl with 100 µl liposomes. Uptake was started by adding 1 µl of D-[³H] glucose (1 mCi/ml) and cold D-glucose (200 µM). After 2 min incubation at room temperature transport was stopped with 4 ml of ice-cold quenching buffer (50 mM potassium phosphate, pH 7.4; 130 mM KCL, pH 7.4 and 100 µM phloretin). Liposomes were filtered through a 0.22 µm MCE Membrane (Merck Millipore, Burlington, USA). Membranes were washed twice with 5 ml quenching buffer, transferred in 20 ml scintillation vials and 10 ml scintillation fluid was added. Vials were mixed and ³H was measured by scintillation counter (Packard Instrument Company/PerkinElmer, Waltham, USA). Liposomes without GLUT4 were used to determine nonspecific transport. The experiments were conducted in accordance with the guidelines set forth by the Institute of Molecular Medicine I under the supervision of Dr. Christoph Peter.

7.2.13 RBC ghost preparation

For RBC ghost preparation RBCs were isolated and washed as described before (6.2.6). RBC ghosts are largely intact RBC membranes from which the haemoglobin has been flushed. After treatment of 1000 x 10⁶ RBCs, carried out as described in 7.2.7, 2 ml of ghost preparation buffer (5 mM Tris-HCL pH 7.4, 1 mM EDTA, 1 mM EGTA) was mixed with fresh

Material and Methods

HALT protease/ phosphatase inhibitor (Thermo Fisher Scientific, Waltham, USA) and added to the cells.. The cell suspension was mixed extensively and incubated on ice for 30 min. Afterwards, tubes were centrifuged for 25 min at 17 500 x g at 4°C. After centrifugation, the supernatant was removed and the whole procedure was repeated four times. RBC ghosts remain as a colourless pellet. The pellet was dissolved in 50 µl RIPA buffer (150 mM NaCl, 1% Nonidet P-40, 0.5% sodium deoxycholate, 0.1% SDS, 50 mM Tris pH 7.4) and the protein concentration was determined.

7.2.14 Lipid raft isolation

For lipid raft isolation RBCs were isolated and washed as described before (7.2.6). Treatment was carried out as described in 7.2.7 and cells were washed twice with cold PBS. Afterwards RBCs were incubated for 30 min at 4°C in 500 µl HEPES buffer (10 mM sodium HEPES, 150 mM NaCl, 5 mM EDTA, 0,5 mM PMSF) which contains 1% Triton X-100. After incubation, RBCs were centrifuged for 30 min at 12 000 x g at 4 °C. The red coloured supernatant contains haemoglobin and the soluble parts of the cell membrane. The pellet contains the insoluble membrane fragments, called lipid rafts. These were washed twice with 1 ml HEPES buffer without Triton X-100 and centrifuged at 13 000 x g for 10 min at 4°C. Lipid rafts were resuspended in 20 µl lipid raft lysis buffer (150 mM NaCl, Tris–HCl pH 7.4, 1 mM EDTA, 1 mM EGTA, 1% Triton X-100 and 0.5% NP-40). Lipid rafts lysis mix was incubated for at least 30 min on ice and then sonicated two times for 1 min. Afterwards, protein concentration was determined with Pierce™ BCA Protein Assay Kit (Thermo Fisher Scientific, Waltham, USA) and used for Western blot analysis as described below.

7.2.15 Western blot analysis

Protein determination

The protein concentration of isolated lipid rafts and RBC ghosts was determined by using the Thermo Scientific™ Pierce™ BCA Protein Assay Kit (Thermo Fisher Scientific, Waltham, USA). For this purpose, a protein standard series (0 to 2 mg/ml) was prepared by a dilution series of BSA (Bovine Serum Albumin Fraction V). Standard series and sample (2.5 µl) were

Material and Methods

pipetted in a clear 96-well microplate. Detection reagent consisting of solution A and solution B (50:1 ratio) was added to each well (200 μ l). After incubation for 30 min at 37°C the optical density (OD) at wavelength of 562 nm was measured by CLARIOstar Plus (BMG LABTECH GmbH, Offenburg, Germany).

Protein separation with sodium dodecyl sulfate–polyacrylamide gel electrophoresis (SDS-Page)

Samples were prepared by mixing 70 μ g protein with H₂O and 1x Laemmli buffer (Thermo Fisher Scientific, Waltham, USA) in a total volume of 60 μ l. For protein separation, a 12% separation gel with 4% overlay collection gel was used. The pipetting schemes for SDS-PAGE gels are shown in Table 4. The gels were loaded with protein mix. Gels run in fresh prepared SDS buffer (25 mM Tris-Base, 190 mM glycine, 0,1% SDS pH 8.3) at 130 V for 90 min. As ladder 5 μ l of Cozy Hi™ (HighQu, Kraichtal, Germany) was used.

Table 4: Pipetting scheme for 12%/4% SDS-PAGE gels, 1.5 mm.

Component	12% separating gel	4% collecting gel
Acrylamide	9.8 ml	1.32 ml
dH ₂ O	8.4 ml	5.7 ml
1.5 M Tris-HCl (pH 8.8)	6.2 ml	
0.5 M Tris-HCl (pH 6.8)		2.6 ml
10% SDS	500 μ l	240 μ l
8% Ammoniumpersulphat	156 μ l	64 μ l
TEMED	26 μ l	10 μ l

Western blot

After separation of proteins by SDS-Page, the proteins were transferred to a polyvinylidene difluoride (PVDF) membrane, using an electric field in the Mini-Trans-Blot Cell System (BioRad, Hercules, USA). The PVDF membrane was activated in methanol for 1-2 min and together with the gel, filter papers and sponges placed in the holder. Ice-cold transfer buffer (25 mM Tris-Base, 190 mM glycine, 20% MeOH) was added to the blotting system. The wet transfer was performed at 30 V for 960 min. Afterwards the membrane was washed three times in T-PBS (PBS + 1% Tween-20). To prevent non-specific binding of antibodies, the membrane was incubated in 5% milk/T-PBS at RT for 1 h. Primary antibodies were diluted 1:1000 in 0.5% milk/T-PBS and incubated at 4°C overnight. A list of the used

antibodies can be seen in 7.1.7. On the next day the membrane was washed three times in T-PBS and the membrane was incubated with secondary antibody (1:5000 in 0.5% BSA in T-PBS) for 1 h at RT. After washing the membrane three times, 1 ml enhanced chemiluminescence solution (ECL) was added to the membrane and the signal was detected by ChemiDoc™ XRS+ Imaging System (BioRad, Hercules, USA). ECL consists of 1 ml Solution A (0.1 Tris-HCL pH 8.6, 1.4 mM luminol), 100 µl Solution B (DMSO, 7.9 mM coumaric acid) and 0.3 µl H₂O₂ (30%). With western blot analyses the protein amount of GLUT4 is checked. Additionally, the protein amount of stomatin is checked, because it has been localized to lipid rafts [217].

7.2.16 Quantitative Real-Time PCR

RNA isolation

Quantitative Real-Time PCR (q-RT-PCR) was performed to determine the extent to which the transfected Hek293 cells express Mfsd2b and Sphk1. For this purpose, RNA was first isolated from the cells using the innuPREP RNA Mini Kit (Analytic Jena, Jena, Germany). HEK293 cells (5 Mio.) were lysed in 400 µl supplied lysis buffer. Afterwards, cell lysate was added to Spin Filter D and centrifuged at 10 000 x g for 2 min to remove genomic DNA from the sample. Filtrate was mixed with 400 µl of 70% EtOH and added to Spin Filter R. This was centrifuged again at 10 000 x g for 2 min to bind RNA to the filter. After two washing steps, the first with 500 µl HS Buffer and the second with 700 µl LS Buffer (10 000 x g for 2 min), the RNA was eluted from Spin Filter R with 50 µl of RNase-free water. The RNA concentration was determined with a NanoDrop (Thermo Fisher Scientific, Waltham, USA).

cDNA synthesis

The RevertAid™ First Strand cDNA Synthesis Kit (Thermo Fisher Scientific, Waltham, USA) was used to obtain cDNA from RNA by reverse transcription. The cDNA synthesis was carried out according to the protocol of the manufacturer with an RNA concentration of 50 ng/µl per preparation.

Quantitative Real-Time PCR

Quantitative Real-Time PCR is based on polymerase chain reaction. An enzymatic amplification of a DNA sequence takes place using two specific primers running in opposite

Material and Methods

directions and allows the quantification of this by the detection of a fluorescence signal. The fluorescent dye iQ™ SYBRGreen (BioRad, Hercules, USA) in the reaction intercalates into the newly formed DNA during DNA amplification, resulting in an increase in the fluorescence signal proportional to the amount of DNA over the progressive cycles. The fluorescence signal is detected by an optical sensor at the end of each cycle. The actual quantification is done using the threshold cycle (CT), which is reached when the fluorescence signal of the sample exceeds the background fluorescence. From the CT values, the Δ CT method can be used to calculate the X-fold expression of the target gene compared to an internal control gene. For this purpose, the CT of the gene of interest is divided through the CT of the housekeeping gene glyceraldehyde 3-phosphate dehydrogenase (GAPDH). The X-fold expression of the target gene can be calculated from the Δ CT values using the formula $2^{-\Delta CT}$. An overview of the used primers is listed in Table 2. For qPCR 1 μ l cDNA was used. The qPCR-master mix was composed as followed:

cDNA	1 μ l
5' Primer	0.5 μ l
3' Primer	0.5 μ l
H2O	8 μ l
<u>iQ™ SYBR® Green Supermix</u>	<u>10 μl</u>
Total volume	20 μ l

This master mix was transferred to one well of a 96-well PCR plate and the plate was sealed with an optical clear film. The quantitative Real-Time PCR was performed in the C100™ ThermalCycler/CFX96™ Real-Time System (BioRad, Hercules, USA). The PCR protocol used is listed in Table 5. Each sample in this work was prepared in duplicate. A mean value was calculated from the duplicate and used as the total CT value of the sample and for calculations of Δ CT. The results are given as relative gene expression in $2^{-\Delta CT}$, where the relative expression refers to the respective expression of the housekeeper gene Glyceraldehyde-3-phosphate dehydrogenase (GAPDH).

Table 5: Protocol for quantitative Real-Time PCR.

Step	Temperature (°C)	Time (min: sec)	Number of cycles
Denaturation	95	03:00	1
Denaturation	95	00:10	40
Hybridization	55	00:10	
Elongation	72	00:30	
Fluorescence detection			
Denaturation	95	00:10	1

7.2.17 GLUT4 surface measurement

Preparation and validation

Surface Glut4 expression in mouse RBCs was measured by flow cytometry detecting a specialized antibody that recognizes an extracellular domain of the transporter (LM048), as published by Tucker et al. in 2018 [218]. On-site validation was performed using the L6-GLUT4myc rat myoblast cell line (Kerafast, Boston, USA), which over-expresses GLUT4. Briefly, 450.000 L6 cells were kept in phenol- and glucose free DMEM medium supplemented with 1% normal goat serum (NGS) for 3 h at 37°C, 5% CO₂ in a humidified atmosphere and incubated with LM048 for additional 20 min at 37°C. Fixation was performed in a final concentration a 3.5% perfluoroalkoxy polymers (PFA), for 10 min on ice. After a washing-step (400 x g, 5 min), L6 cells were incubated with a biotinylated goat anti-human IgG Fc secondary antibody (1:100, eBioscience, ThermoFisher Scientific, Waltham, USA) for 1h at 4°C in the same medium, followed by streptavidin PE (1:1000, BD Biosciences, Heidelberg, Germany) for 30 min at 4°C. To perform a negative control, cells were cere incubated with secondary antibody alone as well as anti-GLUT4 PE (1:200, clone IF8, Santa Cruz Biotechnology, Heidelberg, Germany) that recognizes an intracellular epitope of GLUT4. Intracellular staining was also performed with fixed/washed L6 cells after treatment. Cell permeabilization was achieved by incubation in 0.1% Triton/PBS for 5 min at RT. Cells were then blocked in PBS with 1 % BSA and FBS for 1h at RT and stained.

Measurement

For GLUT4 measurement on RBCs, cells were isolated and washed like described before (7.2.6) followed by S1P loading via incubating 100 Mio RBCs with 1 μ M sphingosine in Tyrode buffer at 37°C for 30 min with gentle shaking, as described with more detail in 7.2.7. After loading the cells, 10 x 10⁶ RBCs were fixed in 2 % final PFA for 24 h at room temperature, spun down (500 x g, 6 min) and resuspended in 1 ml PBS at RT. 2.5 x 10⁶ RBCs were washed in phenol- and glucose free DMEM medium, supplemented with 1% NGS and stained with LM048 at 37°C in the same medium for 20 min. After washing, RBCs were incubated with a biotinylated goat anti-human IgG Fc secondary antibody followed by streptavidin PE as described above. Fluorescence was detected by a Gallios Flow Cytometer (Beckman Coulter, Brea, USA). The measurements and analysis of the data were performed by Dr. Karin von Wnuck-Lipinski.

7.2.18 GLUT1 surface measurement

Surface Glut1 expression in human RBCs was measured using the receptor-binding domain of a recombinant envelope glycoprotein from human T lymphotropic virus (HTLV) fused to EGFP (H2-EGFP) kindly provided by Naomi Taylor, Institute of Molecular Genetics of Montpellier, France as described [219, 220]. Briefly, RBCs were incubated with H2-EGFP in PBS containing 0.33 mg/ml BSA and 1 mM EDTA at 37°C for 20 min. Afterwards, RBCs are washed twice with PBS and resuspended in 400 μ l FACS buffer (NaCl 140 mM, H₂Na₂O₆P 13 mM, EDTA 1.075 mM, KCL 5.5 mM, NaH₂PO₄·H₂O 1.6 mM, NaF 75.55 mM). GFP signal was detected by flow cytometry on a Gallios Flow Cytometer (Beckman Coulter, Brea, USA). The measurements and analyses were carried out by Dr Karin von Wnuck Lipinski.

7.2.19 Hba1c measurement

Mouse glycated hemoglobin A1c (HbA1c) was measured with an ELISA Kit (MyBioSource San Diego, USA). The kit was carried out according to the manufacturer's instructions. Briefly, RBCs were isolated and washed as described before. Afterwards, isolated RBCs

Material and Methods

were 1000-fold diluted in Sample diluent. A standard series is used for later calculations. 50 µl of standard and sample was used per well and incubated for 60 min at 37 °C together with 50 µl supplied HRP-conjugate in the ELISA plate. After five wash steps 90 µl of 3,3',5,5'-Tetramethylbenzidine (TMB) substrate was added to each well and the plate was incubated 20 min at 37 °C in the dark. Afterwards, reaction was stopped with 50 µl stop solution and the OD was measured at 450 nm as well as 540 nm after 5 min. The reading at 540 nm was subtracted from the readings at 450 nm.

7.2.20 Lipid peroxidation measurement

The lipid peroxidation of RBCs was determined by extracting and measuring malondialdehydes (MDAs) from fresh RBC as described by Kanias, T. et al. in their publication of *Determination of lipid peroxidation in desiccated red blood cells*, published in 2007. Briefly, freshly isolated RBC from mice in which lipid peroxidation is to be measured, were mixed with Trichloroacetic acid (TCA) (28% w/v) in a 2:1 ratio, vortexed and incubated for 10 min at RT. After centrifugation (16,100 g, 10 min, 18°C), the MDA extracts (supernatants) were collected. Extracts were mixed in a 4:1 ratio with either thiobarbituric acid (TBA) (1%, dissolved in 0.05 mol/L NaOH) or 0.05 mol/L NaOH as blank. MDA standards were prepared and treated as all samples. RBC extracts, sample blank, and MDA standards were boiled in a water bath for 15 min and immediately cooled on ice for 10 min. Afterwards 100 µl were transferred into a 96-well plate. The Thiobarbituric acid reactive substances (TBARS) were quantified with microplate reader (BMG LABTECH GmbH, Offenburg, Germany) at 453 nm and 532 nm. For calculations concentrations were determined from the MDA standard curve after correcting standard and samples with measurements of 453 nm $[(532 - \text{blank } 532) - 0,2 \times (453 - \text{blank } 453)]$.

7.2.21 Statistics

All results in this thesis are shown as mean \pm standard deviation (SD). The statistical analysis was performed using a paired or unpaired T-test, a paired one-way ANOVA with subsequent Tukey-test or a paired two-way ANOVA with subsequent Tukey-test. The tests

Material and Methods

used are indicated below the figures. All statistical analysis was performed with GraphPad Prism 9.0. Difference between two groups were considered significant at a P value >0.05 . Significances are indicated by * or # = $p < 0.05$, ** or ## = $p < 0.01$, *** or ### = $p < 0.001$. **** or #### = $p < 0,0001$. Statistical analysis with two-way ANOVA is analyzed paired with matched values in a sub-column.

8 Results

8.1 Glucose uptake in erythrocytes determined by dynamic regulation of intracellular S1P levels

In considering to what extent intracellular S1P affects glucose uptake in RBCs, we first investigated the correlation between intracellular S1P levels and 2-deoxyglucose (2DG) uptake in murine RBC under normal conditions. Indeed, a negatively correlation of these two factors could be observed with a correlation coefficient of 0.6337 (Fig. 8A). To investigate whether there was a causal relationship between intracellular S1P and glucose uptake, sphingosine treatment was used as an established method to increase intracellular S1P in RBCs [104]. Therefore, the cells were incubated with the S1P precursor sphingosine for 30 min. Serum albumin was used as an extracellular S1P acceptor to subsequently unload the previously loaded RBCs [104]. In this way, the S1P content of erythrocytes can be regulated in both directions, *ex vivo*. It could be shown that incubating RBCs with 1 μ M sphingosine leads to about 15 times higher S1P levels compared to vehicle (EtOH) loaded control RBCs (Fig. 8B) measured by LC-MS/MS. This higher S1P levels were accompanied by a 34% reduction in glucose uptake measured by the incorporation of 2-deoxyglucose (2DG) (Fig. 8D). Unloading S1P-loaded RBC by 1% albumin reduced the intracellular S1P concentration by 40% and, due to efficient efflux, increased the S1P concentration in the supernatant (Fig. 8C). This S1P unloading completely restored RBC glucose uptake to initial levels (Fig 8D). Albumin by itself had no influence on the internal S1P level, S1P efflux or glucose uptake rate (Fig 8B – D). Interestingly, sphingosine incubation led to 10 times less intracellular sphingosine accumulation than S1P due to the highly efficient conversion of sphingosine to S1P (Fig. 8E). Along with this, it can be shown that that the low intracellular sphingosine levels result in no significant efflux through albumin (Fig. 8F). To ensure that the effect of restored glucose uptake driven by BSA in sphingosine-incubated RBCs was solely due to the extraction of S1P from erythrocytes, the loaded RBC were incubated with the S1P-neutralizing antibody Sphingomab (LT1002) which efficiently removes S1P from RBCs, by driving its efflux [221]. It could be observed that Sphingomab extracted 8.8 pmol S1P per 10^6 sphingosine-loaded RBC compared to an isotype-matched control IgG that had

Results

no extracting effect at all (Fig. 8G). Accordingly, Spingomab restored glucose uptake of sphingosine-treated RBC to normal levels (Fig. 8H).

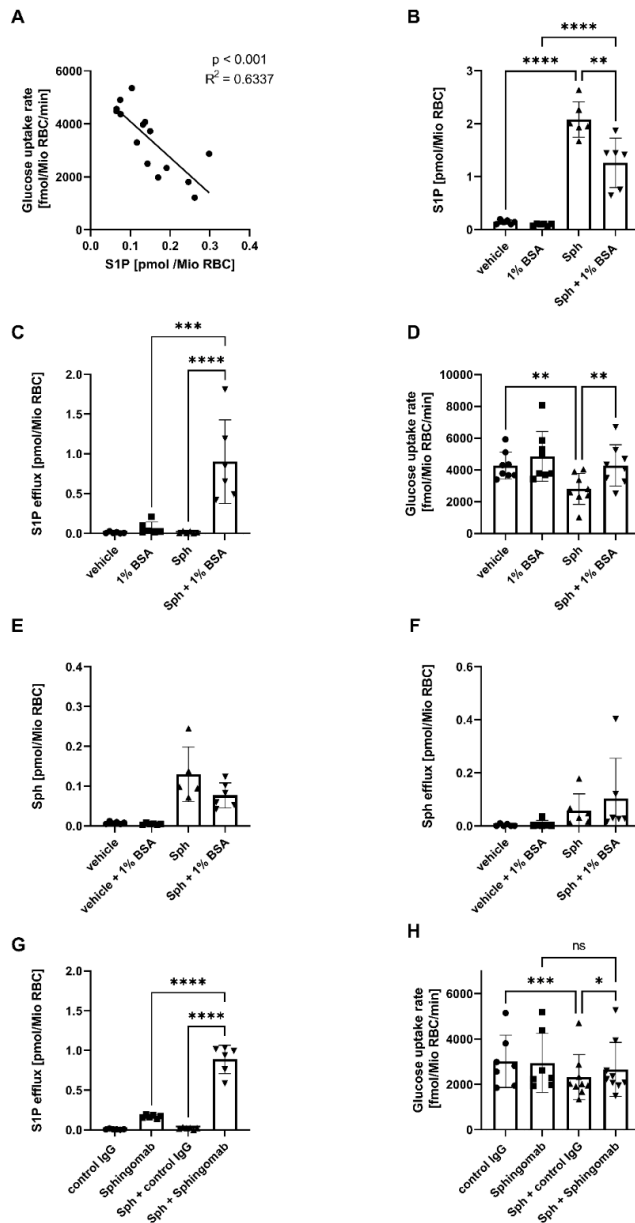


Figure 8: S1P loading of RBCs by sphingosine leads to lower glucose uptake. S1P-unloading with BSA or a S1P neutralizing antibody restores glucose uptake.

A) Correlation between glucose uptake rate and intracellular S1P concentration in freshly isolated RBC from C57Bl6 (n=15) as calculated by two-tailed Pearson correlation coefficient ($p=0.004$). B) Intracellular S1P levels in RBC and C) S1P efflux from RBCs after incubation with 1 μ M sphingosine (Sph) or EtOH (vehicle) for 30 min followed by incubation in the absence or presence of 1% BSA for 20 min (n=6 each). D) Glucose uptake rate in RBCs loaded or not with Sph and incubated with or without 1% BSA (n=8). E) Intracellular Sph levels in RBC and F) Sph efflux from RBCs after incubation with 1 μ M Sph or EtOH (vehicle) for 30 min followed by

Results

incubation in the absence or presence of 1% BSA for 20 min (n=6 each). G) S1P efflux from RBCs after incubation with vehicle or 1 μ M Sph (n=6) followed by 800 pmol/ml control IgG1 or Sphingomab (n=7) H) Glucose uptake rate in Sph-loaded RBC in the presence of Sphingomab or control IgG1 (n=7/9). B-H: Data are presented as mean \pm sd and tested with paired one-way ANOVA followed by a Tukey's multiple comparison test; ns= not significant; P**<0.01; P***<0.001; P****<0.0001. Parts of the results of this figure have been published in Thomas et al., 2023 [222].

Incorporating sphingosine during the incubation process is a widely practiced technique to enrich red blood cells (RBCs) with S1P. This method demonstrates its efficacy as incubating RBCs with 1 μ M sphingosine notably elevates S1P levels within the cells. Conversely, there is no observable alteration in S1P levels when RBCs are incubated with 1 μ M S1P alone (Figure 9B). Calculated for a single RBC, incubation with sphingosine leads to accumulation of 100 μ M S1P in whereas incubation with S1P accumulates barley 10 μ M. Consistent with this finding, incubation with 1 μ M S1P leads to no change in glucose uptake (Figure 9C). Increasing S1P concentrations beyond 6 μ M during RBC incubation result in hemolysis, as evidenced by the optical density of the supernatant. However, incubating RBCs with the for experiments in this thesis used concentration of 1 μ M sphingosine does not induce hemolysis (Figure 9A).

To investigate the dependency of RBC glucose uptake on the glucose transporter GLUT, the GLUT inhibitor cytochalasin B was used. This led to an inhibition of glucose uptake of more than 90%. As proof of concept, the incubation with sphingosine showed no further change after GLUT inhibition (Fig 9D).

Results

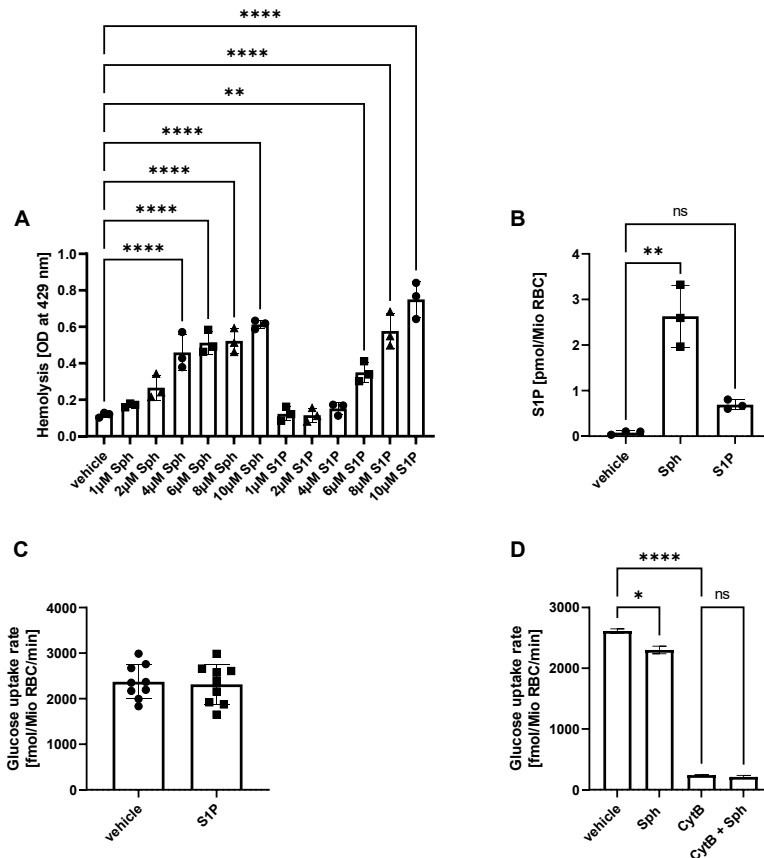


Figure 9: Effect of S1P and sphingosine on RBC integrity.

A) Hemolysis in murine RBCs supernatants after incubation with Sph and S1P in 1, 2, 4, 6 and 8 μM (30 min for 37°C) as measured by optical density of haemoglobin at the wavelength of 429 nm ($n=3$ each). B) Intracellular S1P levels in RBC after incubation with 1 μM Sph, 1 μM S1P and vehicle (MeOH, 0,1 %) for 30 min at 37°C ($n=3$ each). C) Glucose uptake rate in RBCs after incubation with 1 μM S1P and vehicle (MeOH, 0,1 %) for 30 min at 37°C ($n=8$ each). D) Glucose uptake rate in RBCs after incubation with Sph (1 μM) and vehicle (EtOH) with and without addition of GLUT inhibitor Cytocalasin B (CytB, 100 μM) ($n=2$ each). Data are presented as mean \pm sd and tested with one-way ANOVA (A,B,D) and two-tailed paired t-test (C); ns= not significant; $P^* < 0.05$; $p^{**} < 0.01$; $P^{****} < 0.0001$.

To investigate the potential correlation between elevated *in vivo* S1P levels in RBCs and reduced glucose uptake, similar to findings observed in *in vitro* S1P-enriched RBCs, RBCs from mice exhibiting inhibited S1P lyase (Sgpl) activity were examined. For these experiments RBCs were isolated from mice with pharmacologically inhibited S1P lyase due to 4-deoxypyridoxine (DOP) treatment and from mice with lower lyase expression due to genetic deletion. The fact, that DOP treatment leads to reduced Sgpl activity and thus to an increase in S1P levels in RBCs, has already been shown [45] and was confirmed by the results of this study. RBCs isolated from DOP treated mice had two times higher S1P

Results

concentrations compared to untreated RBCs (Fig. 10A). In line with the data shown with *in vitro* loaded cells, these RBC exhibited a 20% reduction in glucose uptake (Fig. 10C). Incubation of RBCs from DOP-treated mice with serum albumin reduced the intracellular S1P concentration by more than 70% and resulted in an efficient S1P efflux into the supernatants (Fig.10B). As previously demonstrated with *in vitro* loaded RBCs, the unloading of S1P resulted in a restoration of glucose uptake (Fig. 10C). In RBCs isolated from control mice, 1% serum albumin leads to no significant changes in intracellular S1P levels or efflux which is also reflected in an unchanged glucose uptake (Fig. 10 A-C).

As a second model for increased intracellular S1P levels, RBCs of $Sgpl^{vav-cre+}$ mice were used. In these mice a Cre recombinase is expressed under a hematopoietic specific promotor *vav*. This results in loss of *Sgpl* in this specific cell types and therefore in accumulation of S1P in different organs and cells. Mice that do not express this Cre recombinase (Cre-) serve as controls. It could be shown that the genetic loss of *Sgpl* results in a 1.8-fold increase in RBC S1P levels (Fig. 10D). As already shown in DOP-treated mice, albumin reduced intracellular S1P concentrations by 23% accompanied by S1P efflux into the supernatants (Fig. 10E). The glucose uptake rate is comparable to that observed in DOP treated animals. It was reduced by 26% in RBCs of $Sgpl^{vav-cre+}$ compared to $Sgpl^{vavCre-}$ and was recovered by S1P unloading effected by 1% BSA (Fig.10E-F). Thus, S1P negatively affects glucose uptake in mouse red blood cells, as demonstrated by *in vitro* S1P loading, *in vivo* pharmacological modulation of intracellular S1P levels, and stable genetic elevation of S1P levels.

Results

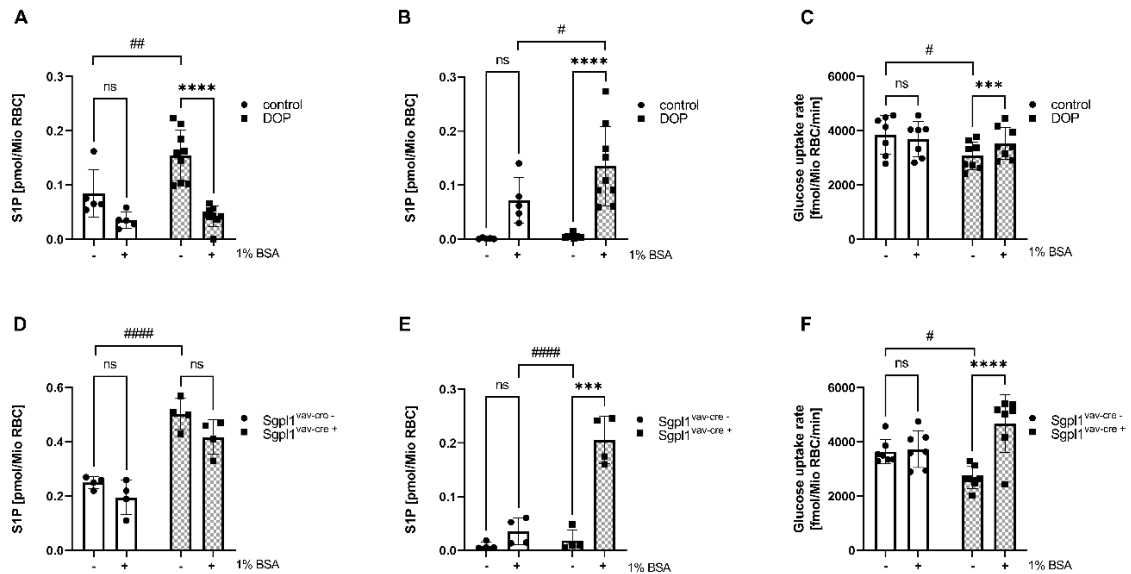


Figure 10: Elevated intracellular S1P decreased RBC glucose uptake in mice RBCs *in vivo*.

A) Intracellular S1P levels and B) corresponding S1P efflux to BSA in RBCs isolated from mice treated with or not 3 mg/l 4-deoxypyridoxine (DOP) for 3 weeks (n=5). C) Glucose uptake rate of the same RBCs with and without S1P unloading by BSA (n=7). D) Intracellular S1P levels and E) corresponding S1P efflux in RBCs from *Sgpl1^{vav-cre-}* and *Sgpl1^{vav-cre+}* mice (n=7). F) Glucose uptake of RBCs from same mice as in E) in the presence and absence of 1% BSA for 30 min (n=7 each). Data are presented as mean±sd and tested with stack matched two-way ANOVA followed by a Tukey's multiple comparison test (# for comparing DOP vs. control or *Sgpl1^{vav-cre+}* vs. *Sgpl1^{vav-cre-}*; * for comparing treatment with or without 1% BSA); ns= not significant; P#<0.05; P##<0.01 P###<0.0001; P****<0.0001; P***<0.001; P*****<0.0001. Results of this figure have been published in Thomas et al., 2023 [222].

To test if the opposite – a genetically generated low S1P content of RBC – stimulates glucose uptake, we employed mice lacking sphingosine kinase 1 (SphK1). SphK1 is the only sphingosine kinase present in the RBC and a lack of it is related to low S1P levels in blood [223]. Indeed, this could be observed for isolated RBCs, as *SphK1^{-/-}* RBC exhibited 13-fold lower S1P levels compared to control RBCs (Fig. 11A). This affects glucose uptake, which showed an increase of 34% in basal conditions (Fig. 11C). As might have been expected for RBCs lacking the only sphingosine kinase they possess, it was not possible to load them with S1P by incubation with sphingosine (Fig. 11A) and there certainly was no S1P efflux after albumin incubation (Fig. 11B). At the same time, however, an accumulation of sphingosine can be observed in this Sph incubated *SphK1^{-/-}* RBCs if it cannot be phosphorylated to S1P (Fig. 11D). This accumulated sphingosine the RBCs can be pulled out by albumin, which is reflected in an increased sphingosine efflux (Fig. 11E). *SphK1^{-/-}* RBCs

Results

can neither be loaded nor unloaded with S1P and so there is no effect on their glucose uptake (Figure 11C). It is important to note that the increased sphingosine levels observed in sphingosine loaded SphK1^{-/-} RBCs have no effect on glucose uptake, whereas the altered S1P levels cause clear differences in the glucose uptake of the cell.

In summary, modulating the S1P concentrations in RBC by interfering with precursor uptake, S1P synthesis and S1P efflux dynamically regulated glucose uptake.

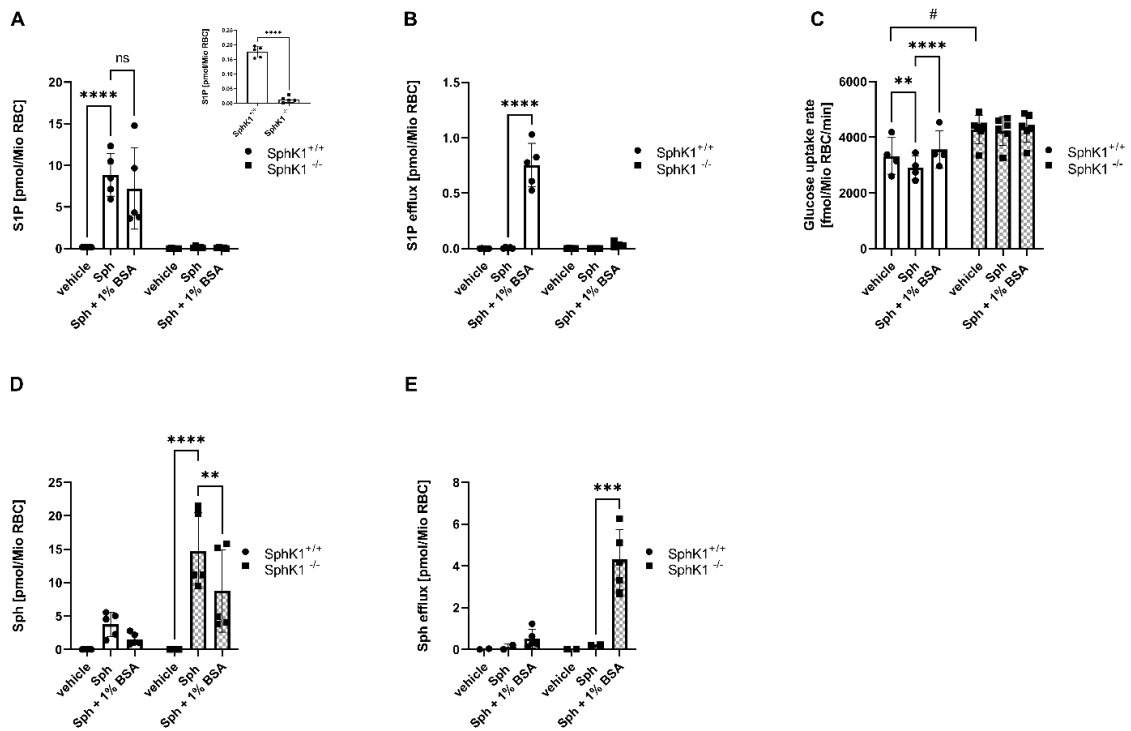


Figure 11: Low intracellular S1P increases glucose uptake in murine RBCs *in vivo*.

A) Intracellular S1P levels and B) corresponding S1P efflux in RBCs from SphK1^{+/+} and SphK1^{-/-} mice incubated with vehicle or 1 μM Sph followed by incubation without or with 1% BSA for 30 min; inset shows basal intracellular S1P level of SphK1^{+/+} and SphK1^{-/-} mice (n=5 each). C) Glucose uptake in RBCs from SphK1^{+/+} and SphK1^{-/-} mice treated as in A/B) (n=4/6). D) Intracellular sphingosine levels and E) corresponding sphingosine efflux in RBCs treated as in A/B). Data are presented as mean±sd and tested with stack matched two-way ANOVA followed by a Tukey's multiple comparison test (# for comparing SphK1^{+/+} vs. SphK1^{-/-}; * for comparing treatments); ns= not significant; P#<0.05; P**<0.01; P***<0.001; P****<0.0001. Results of this figure have been published in Thomas et al., 2023 [222].

8.2 The S1P exporter Mfsd2b impacts the extent of RBC glucose uptake

Mfsd2b is the main S1P transporter in RBCs which was recently discovered [104, 105]. The S1P unloading of RBCs by albumin is attributable to S1P export via this transporter [104]. In addition, RBCs isolated from mice lacking the Mfsd2b protein are known to have greatly increased S1P levels [104]. To test whether Mfsd2b is involved in the regulation of glucose uptake, the same experiments as described above, were performed with RBCs isolated from Mfsd2b^{-/-} mice, lacking Mfsd2b protein. RBCs of Mfsd2b^{+/+} served as controls. The results demonstrate that isolated RBCs from Mfsd2b^{-/-} mice had 40-fold higher S1P levels (Fig. 12A) together with a 20% decreased glucose uptake rate (Fig. 12C). It is remarkable that both Mfsd2b^{-/-} RBCs as well as control RBCs could be loaded with S1P by incubating them with sphingosine (Fig 12A). This results in approximately a 30% further reduction in glucose uptake in both scenarios, as illustrated in Figure 12C. However, S1P unloading was virtually absent in Mfsd2b^{-/-} RBCs resulting in high intracellular S1P levels, with no efflux observed and consequently no restoration of glucose uptake (Fig. 12B). In contrast, RBCs expressing Mfsd2b (Mfsd2b^{+/+}) show significantly increased S1P efflux along with increased glucose uptake, as it was the case in previously shown experiments with wild type RBCs. The S1P efflux via Mfsd2b is therefore crucial for the restored glucose uptake rate in RBCs.

Results

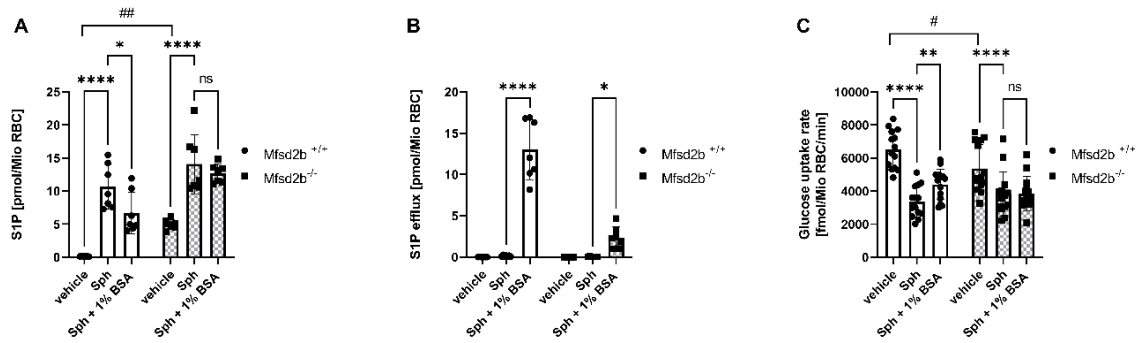


Figure 12: Mfsd2b activity controls glucose uptake in RBCs by modulating intracellular S1P levels.

A) Intracellular S1P levels and B) corresponding S1P efflux in RBCs from Mfsd2b^{+/+} and Mfsd2b^{-/-} mice (n=7 each). C) Glucose uptake in RBCs from Mfsd2b^{+/+} and Mfsd2b^{-/-} treated as in A) (n=14 each). Data are presented as mean±sd and tested with stack matched two-way ANOVA followed by a Tukey's multiple comparison test (# for comparing Mfsd2b^{+/+} vs. Mfsd2b^{-/-}; * for comparing treatments); ns= not significant; P#<0.05; P##<0.01 P###<0.0001; P*<0.05; P**<0.01; P***<0.001; P****<0.0001. Results of this figure have been published in Thomas et al., 2023 [222].

To further investigate how glucose uptake is affected by Mfsd2b, cells overexpressing Mfsd2b were co transfected with *Sphk1*. For this purpose, HEK293 cells stably expressing Mfsd2b and their controls were transfected with *Sphk1*. HEK293 cells are a specific immortalized cell line from human embryonic kidney, the *Mfsd2b* and *Sphk1* are of murine origin. Transfection with SphK1 is essential since HEK293 cells exhibit minimal endogenous expression of sphingosine kinase (Fig. 13D). Consequently, direct loading with S1P through sphingosine incubation would not be feasible. After successful transfection with *SphK1*, both the Mfsd2b-expressing cells as well as the controls were able to be loaded with S1P (Fig. 13A), which increased glucose uptake rate in both cell lines. Unloading by albumin and an associated increased S1P efflux could only be shown in the HEK293-SpkK1-Mfsd2b cells (Fig. 13B), which is reflected by an 2.5-fold increase in glucose uptake (Fig. 13C). In control cells, without Mfsd2b expression no significant S1P efflux (Fig. 13B) as well as no influence on glucose uptake trigger by 1% BSA could be observed. Accordingly, the same regulatory S1P/Mfsd2b-dependent mechanism of glucose uptake as observed in RBCs is present in nucleated cells.

Results

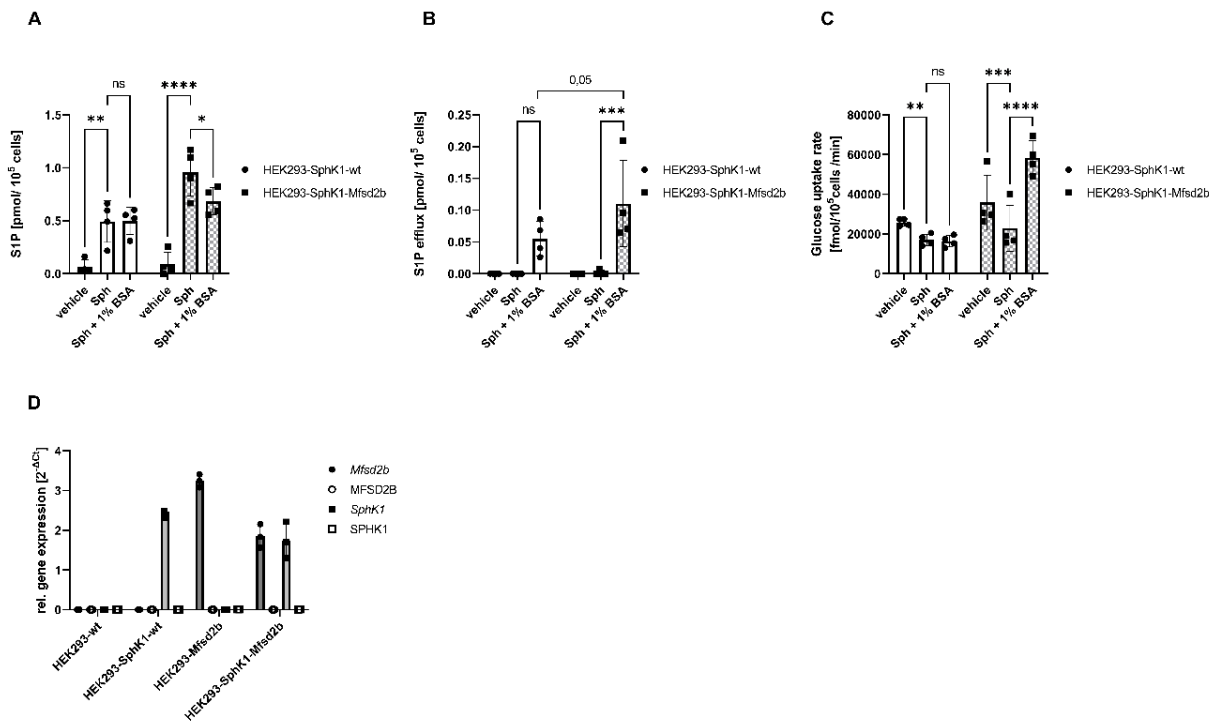


Figure 13: Mfsd2b activity controls glucose uptake in stable transfected HEK293 cells.

A) Intracellular S1P levels and B) corresponding S1P efflux in HEK293-SphK1-wt and SphK1-Mfsd2b cells treated for 1 h with vehicle (EtOH) or 1 μ M Sph followed by incubation with 1% BSA for 30 min (n=4 each). C) Glucose uptake rate in same cells and treatments as in A/B) (n=4 each). D) Relative gene expression of murine *Sphk1* and *Mfsd2b* in HEK293 cells stably overexpressing *Sphk1*, *Mfsd2b* or both by RT/real-time PCR. Human SPHK1 and MFSD2B expression was also quantified to assess basal levels in the Hek293 cell line and all transfectants. Data are normalised to GAPDH and shown as $2^{-\Delta C_t}$ (n=3). Data are presented as mean \pm sd and tested with stack matched two-way ANOVA (A-C) (# for comparing Mfsd2b^{+/+} vs. Mfsd2b^{-/-}; * for comparing treatments); ns= not significant; P* < 0.05; P** < 0.01; P*** < 0.001; P**** < 0.0001.

In addition to the stability-transfected HEK293-SphK1-Mfsd2b cells, the same initial cells expressing Mfs2b were transient –transfected with *SphK1*. In this case SphK1 was coupled to an EGFP, which enables a verification of transfection using a fluorescence microscope. The transient transfected HEK293 cells expressing additionally Mfsd2b (HEK293-SphK1(tr.)-Mfsd2b) showed the same behavior in glucose uptake as the stably transfected cells. After sphingosine incubation, their glucose uptake decreased and was subsequently rescued by albumin (Fig. 14A). Successful transfection could be determined by relative gene expression of murine *SphK1* in both HEK293 cell lines (Fig. 14B) as well as by fluorescent detection of EGFP coupled SphK1 (Figure 14C). Transfection without plasmid shows no GFP signal,

Results

whereas transfection with the empty *EGFP* plasmid gives a strong GFP signal which was completely distributed over the cell cytosol. Cells that were transfected with *EGFP-Sphk1* plasmid shows locally GFP signal within the cell (Fig. 14C), which can be related to the membrane-associated localization of SphK1 [223].

The use of the second *Mfsd2b* transfected cell model confirms the observations made earlier and underlines the central role of the S1P transporter *Mfsd2b* in role of restoring glucose uptake.

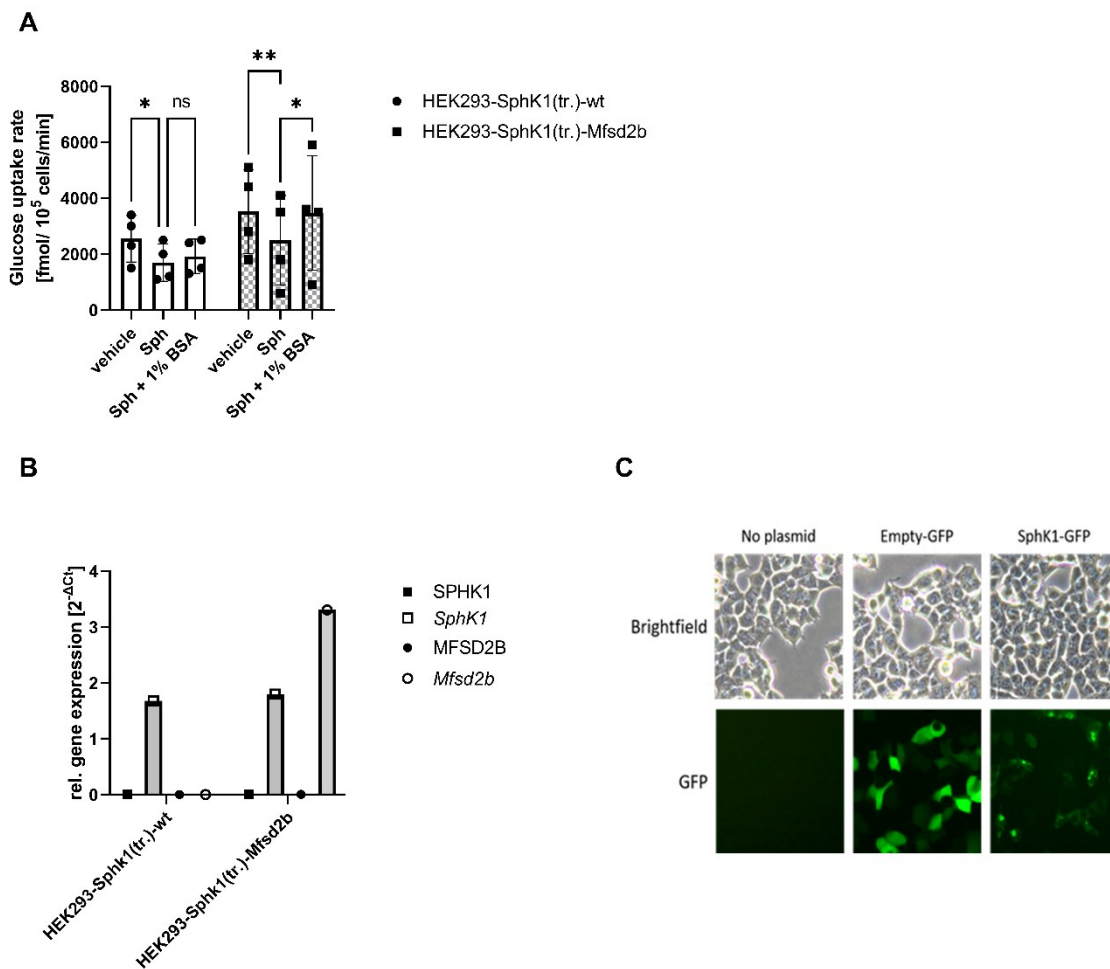


Figure 14: Mfsd2b activity controls glucose uptake in transiently transfected HEK293 cells.

A) Glucose uptake rate in HEK293-SphK1(tr.)-wt and SphK1(tr.)-Mfsd2b cells in which SphK1 is temporally expressed, treated with vehicle (EtOH) or 1 μ M Sph for 1 h followed by incubation with 1% BSA for 30 min (n=4). Data are presented as mean \pm sd and tested with stack matched two-way ANOVA (* for comparing treatments); ns= not significant; P* $<$ 0.05; P** $<$ 0.01. B) Relative gene expression of murine *Sphk1* and *Mfsd2b* in HEK293 cells overexpressing *Sphk1*, or *Sphk1* together with *Mfsd2b* by RT/real-time PCR. Human SPHK1 and MFSD2B expression was also quantified to assess basal levels in the transfectants. Data are normalised

Results

to GAPDH and shown as $2^{-\Delta Ct}$ (n=1). C) Brightfield and GFP imaging (72 h after transfection) of transiently transfected HEK293-wt cells with no plasmid, empty-EGFP plasmid or the Sphk1-EGFP plasmid.

8.3 FTY720-P decreases glucose uptake

FTY720 is used as an approved prodrug for relapsing multiple sclerosis with its phosphorylated form FTY720-P acting as a structural analogue of S1P *in vivo* [224, 225]. To investigate whether FTY720 or FTY720-P influence glucose uptake in RBCs, the cells were incubated with these substances and intracellular levels and efflux as well as glucose uptake was measured. Incubation of RBC with 1 μ M FTY720 resulted in its accumulation inside the cells without any conversion into FTY720-P (Fig. 15A). This observation is not surprising considering that FTY720 is phosphorylated via SphK2 and not SphK1, the only sphingosine kinase expressed in RBCs. The lack of SphK2 in RBCs is thus confirmed by these results. Incubation of RBCs with 1 μ M FTY720-P led to its accumulation in RBCs (Fig. 15D) albeit 30-fold less compared to the FTY720 accumulation observed after FTY720 incubation, which is caused by the polar nature of the phosphorylated form. Incubation with albumin decreased FTY720 level in RBCs incubated with it as well as FTY720-P levels in RBCs where it was accumulated (Fig. 15A, D). This is reflected in the corresponding efflux data. Albumin leads to increased FTY720 levels in combination with previous FTY720 loading (Fig. 15B) as well as to increased efflux of the phosphorylated form after incubating with it (Fig. 15E). Influencing intracellular FTY720 level in RBCs was possible by loading with FTY720 or unloading it by albumin. Nevertheless, glucose uptake was not influenced by loading or unloading of FTY720 (Fig. 15C). The intracellular levels of FTY720-P in RBCs could be affected by loading and unloading processes. Interestingly, this modulation also impacts glucose uptake: loading with FTY720-P reduced glucose uptake but unloading it restored glucose uptake back to its baseline level (Fig. 15F). To check whether the FTY720 and FTY720-P efflux is Mfsd2b dependent, the efflux in the corresponding knock outs was examined. Efflux of both FTY720 and the phosphorylated form could be observed in Mfsd2b^{-/-} RBCs in the same extent than in Mfsd2b^{+/+} RBCs (Fig. 15G, H), which therefore rules out transport via Mfsd2b.

In conclusion, the effect of S1P on RBC glucose uptake is confirmed by the S1P analogue FTY720-P. The loading with FTY720-P shows the same effect as S1P, but also the unloading

Results

of the cell, even though it could not be shown via which transporter the unloading takes place.

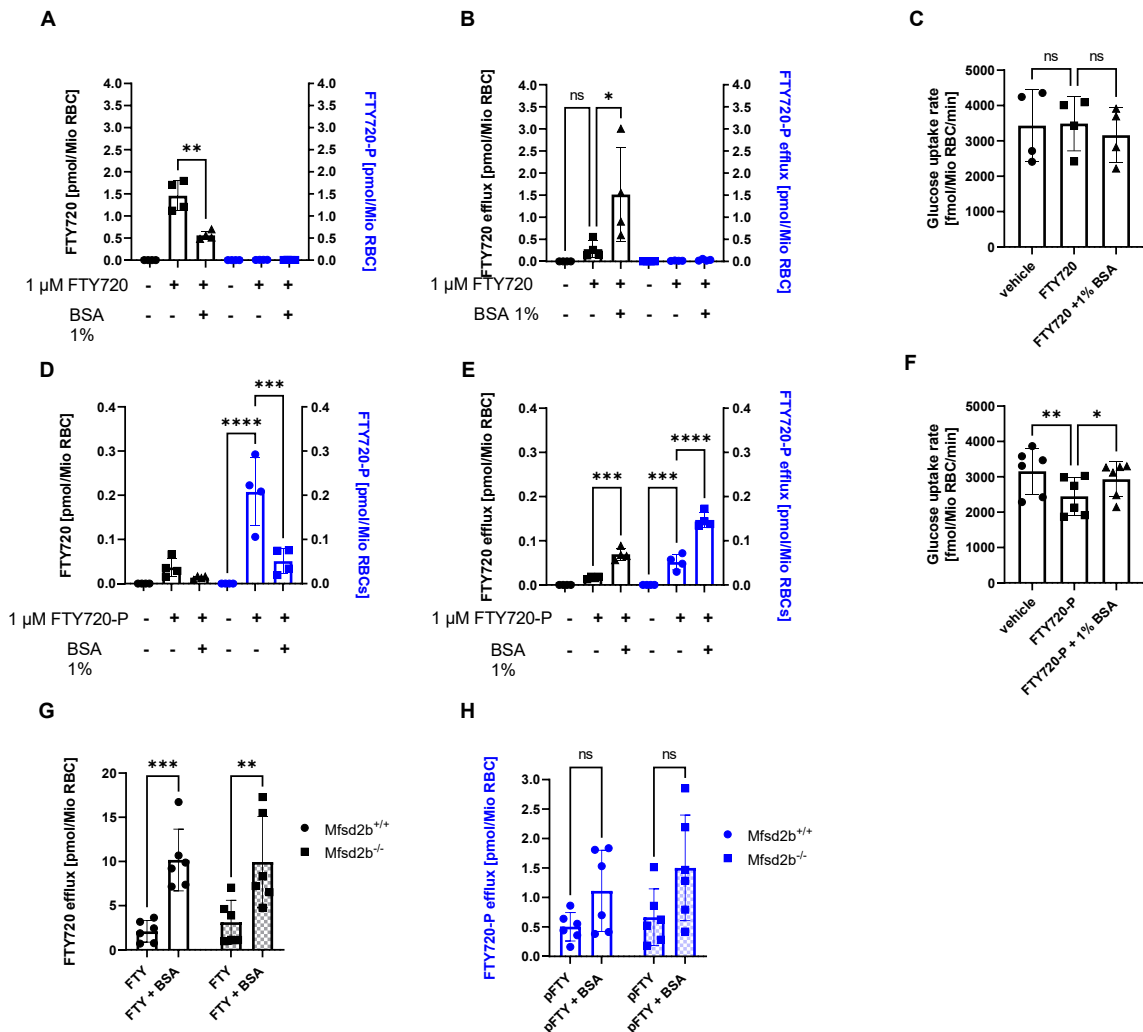


Figure 15: FTY720 and FTY720-P transport in RBC occurs independently of Mfsd2b with FTY720-P but not FTY720 suppressing glucose uptake.

A-D) Intracellular FTY720 (black colour) and FTY720-P (blue colour) levels and corresponding FTY720 and FTY720-P efflux after loading with A/B) 1 μM FTY720 and D/E) 1 μM FTY720-P followed by incubation with or without 1% BSA for 20 min (n=4 each). C) Glucose uptake of RBCs treated with FTY720 and F) FTY720-P, respectively, with and without addition of 1% BSA (n=4 each). Vehicle was EtOH for FTY720 and DMSO (0,1%) for FTY720-P. G) Efflux of FTY720-loaded RBCs and H) FTY720-P-loaded RBC to 1% BSA in RBC from Mfsd2b^{+/+} and Mfsd2b^{-/-} mice. Data are presented as mean±sd and tested with stack matched one-way ANOVA followed by a Tukey's multiple comparison test; ns= not significant; p* $<$ 0.05; P** $<$ 0.01; P*** $<$ 0.001; P**** $<$ 0.0001. Results of this figure have been published in Thomas et al., 2023 [222].

8.4 S1P reduces the amount of GLUT on the surface of RBCs

To investigate the mechanism underlying the observation that the level of S1P in a RBC determines its glucose uptake, a system was used which allows to measure glucose uptake by GLUT4 in a highly simplified membrane model. The uptake of 3H-labelled glucose was tracked in liposomes containing purified glucose transporter GLUT4 embedded in different lipid compositions with the aim, to find out whether different amounts of S1P in the membrane, or rather in the liposome, have an influence on glucose uptake. The glucose uptake in liposomes consisting of 100% egg phosphatidylcholine (PC) was compared with those containing different amounts of S1P. Liposomes with 75% egg PC and 15% egg phosphatidic acid (PA) (mol/mol) serve as positive control. As shown by Hresko et al. [163] liposomes containing anionic phospholipids, such as PA, have a higher glucose uptake via GLUT transporters than those without. In contrast to PA, S1P incorporated into liposomes (0,1%, 1% and 15%) shows no effect on glucose uptake (Fig. 16), indicating that S1P membrane content does not influence glucose uptake.

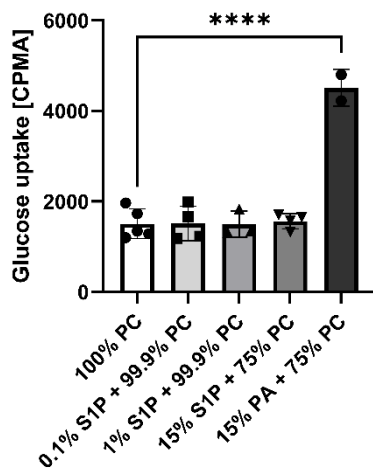


Figure 16: S1P content of liposomes has no influence on glucose uptake in GLUT4 reconstituted liposomes.

Uptake of 1 μCi D-[^3H] glucose into GLUT4-containing PC liposomes in presence of none (n=5), 0.1% (n=4), 1% (n=3) or 15% (n=4) (mol/mol) S1P. Liposomes containing 15% (mol/mol) PA serve as positive control; (n=2). Data is presented as mean \pm sd and tested with one-way ANOVA followed by a Tukey's multiple comparison test; P****<0.0001.

In the following, the amount and localization of GLUT4 protein on the RBC membrane, after sphingosine incubation, was determined. In adipocytes it could be shown, that glucose uptake depends on localization of the glucose transporter on the cell membrane [165]. The localization determines the activity of GLUT transporter and is dependent on the availability of extracellular glucose. GLUT is thereby more active, when it is present in

Results

certain areas of the membrane, the so-called lipid rafts. In this case, an increased glucose uptake could be observed [165]. The amount of protein on the membrane after sphingosine loading was determined by Western blot analysis of isolated erythrocyte ghosts. No difference between S1P loaded and unloaded RBCs were found using this method (Fig. 17A). Lipid rafts are membrane fractions that are insoluble in Triton-X-100, allowing them to be isolated using this substance. A western blot analysis of isolated lipid rafts indicated a smaller impact of GLUT4 on total protein amount, compared to the ghosts. Furthermore, no difference was observed between the GLUT4 protein levels on sphingosine incubated RBCs and controls (Fig. 17B). Given that stomatin has been identified within lipid rafts [217], it was anticipated that a higher proportion of stomatin would be present in the insoluble fraction, serving as a control for the isolation of lipid rafts.

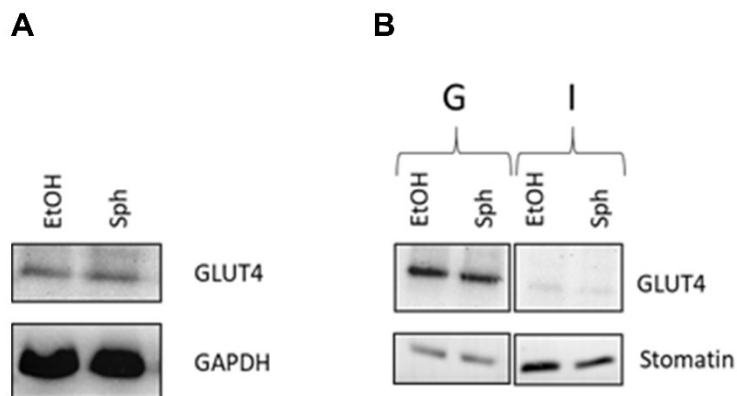


Figure 17: S1P has no influence on GLUT4 protein distribution on lipid rafts of RBCs.

A) GLUT4 amount of RBC ghosts, isolated from C57Bl6 RBCs, treated previously with 1 μ M Sph or EtOH, tested with western blot analysis. Glyceraldehyde 3-phosphate dehydrogenase (GAPDH) served as loading control
B) GLUT4 amount of RBC ghosts (G) and Triton X-100- insoluble fractions (I) from C57Bl6 RBCs which are treated with EtOH or Sph (1 μ M). Stomatin is detected as a control for insoluble fractions.

Given the inability to demonstrate an impact of S1P concentration on glucose transporter activity within the membrane, and the apparent lack of influence on the localization of GLUT in specific membrane regions following sphingosine incubation, we raised the question of whether protein detection via western blotting might not be specific to surface proteins.

Results

To enhance the sensitivity of detecting GLUT4 on the surface of erythrocytes, the globally unique available antibody targeting an extracellular domain of GLUT4 was utilized [218]. Using flow cytometry, the amount of fluorescence-labelled GLUT4 antibody on a given amount of S1P-loaded and unloaded erythrocytes could be determined. The amount of fluorescent signal correlates with the amount of bound GLUT4 antibody and thus with the amount of GLUT4 on the cell surface of the erythrocyte membrane, leading to the observation that erythrocytes incubated with sphingosine had less GLUT4 on their surface than the control group (Fig. 18 A, B).

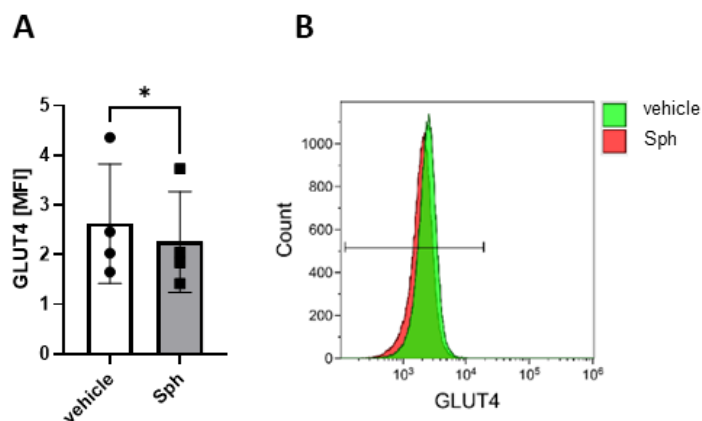


Figure 18: S1P regulates cell surface GLUT4 on mouse RBCs

A) Quantification of GLUT4 MFI fluorescence from mouse RBCs treated with 1 μ M Sph or vehicle (n=4).

B) Representative flow cytometry histograms of surface GLUT4 after incubation with 1 μ M Sph or vehicle for 30 min, as measured by fluorescents of an antibody that recognizes an extracellular domain of the GLUT4 transporter (LM048). Data are presented as mean \pm sd and tested with paired two-tailed t-test (A). $P^* < 0.05$. Results of this figure have been published in Thomas et al., 2023 [222].

8.5 S1P regulates glucose uptake through modulation of PP2A activity

It is known that GLUTs are not firmly anchored to the membrane but are in a constant state of flux between extracellularly accessible and intracellularly present. Numerous studies in tumor cell lines have shown that synthetic sphingolipids including FTY720 and C2-ceramide [211] block nutrient access by reducing the cell surface levels of nutrient transporters such as SLC2A1, SLC16A1, SLC16A3, SLC1A5 and SLC7A5 [171]. The underlying mechanism has

Results

been identified as disruption of membrane trafficking of the transporters by activation of the serine and threonine protein phosphatase 2A (PP2A) [171, 211, 226]. Although murine RBCs lack SLC2A1 (also known as GLUT1) they abundantly express GLUT4 (SLC2A4) [139]. For this reason, we investigated whether loading RBCs with S1P leads to activation of PP2A. And indeed, it could be shown, that incubation with 1 μ M sphingosine clearly increased PP2A activity (Fig. 19A). To test the relationship between PP2A activity and decreased glucose uptake after sphingosine incubation, glucose uptake was examined after inhibiting PP2A activation. The decrease of glucose uptake by S1P loading was abolished by the PP2A inhibitor okadaic acid (Fig. 19B). To determine how PP2A activity varies in RBCs that exhibit altered S1P levels *in vivo*, the previously studied RBCs from SphK1^{-/-} and Mfsd2b^{-/-} mice were investigated for PP2A activity, respectively. In line with a role of endogenous S1P in regulating PP2A in RBCs, PP2A activity was reduced in SphK1^{-/-} RBC which have low intracellular S1P and increased in Mfsd2b^{-/-} RBC with high S1P levels (Fig. 19C, D). After this correlation could be confirmed several times, it should be investigated whether S1P leads to a direct PP2A activation or whether a corresponding signaling pathway is interposed. Therefore, the effect of S1P on the activity of the native PP2A holoenzyme complex was examined *in vitro* by adding sphingolipids to PP2A immunoprecipitated from native mouse RBCs. Incubation with 1 μ M S1P resulted in a 2-fold activation of PP2A, whereas 1 μ M sphingosine had no effect (Fig. 19E). Furthermore, 1 μ M FTY720-P but not 1 μ M FTY720 activated PP2A (not shown). Finally, addition of 1 μ M C6 ceramide did not activate PP2A although it did so at higher concentrations (15 μ M) as published [210].

PP2A can be activated in several ways. One of them is the direct complexation and activation of the catalytic unit of the enzyme, also called PP2AC [210, 227, 228]. To test whether this is the case for PP2A activation through sphingolipids, experiments with a human PP2AC recombinant enzyme were performed. Identical to the results with the holoenzyme from RBC, 1 μ M S1P, and 15 μ M C6 ceramide activated PP2AC but not 1 μ M sphingosine, C6 ceramide, respectively (Fig. 15F). These data directly demonstrate that S1P is a highly potent PP2A activator and acts in this case directly via the activation of the catalytic unit.

Results

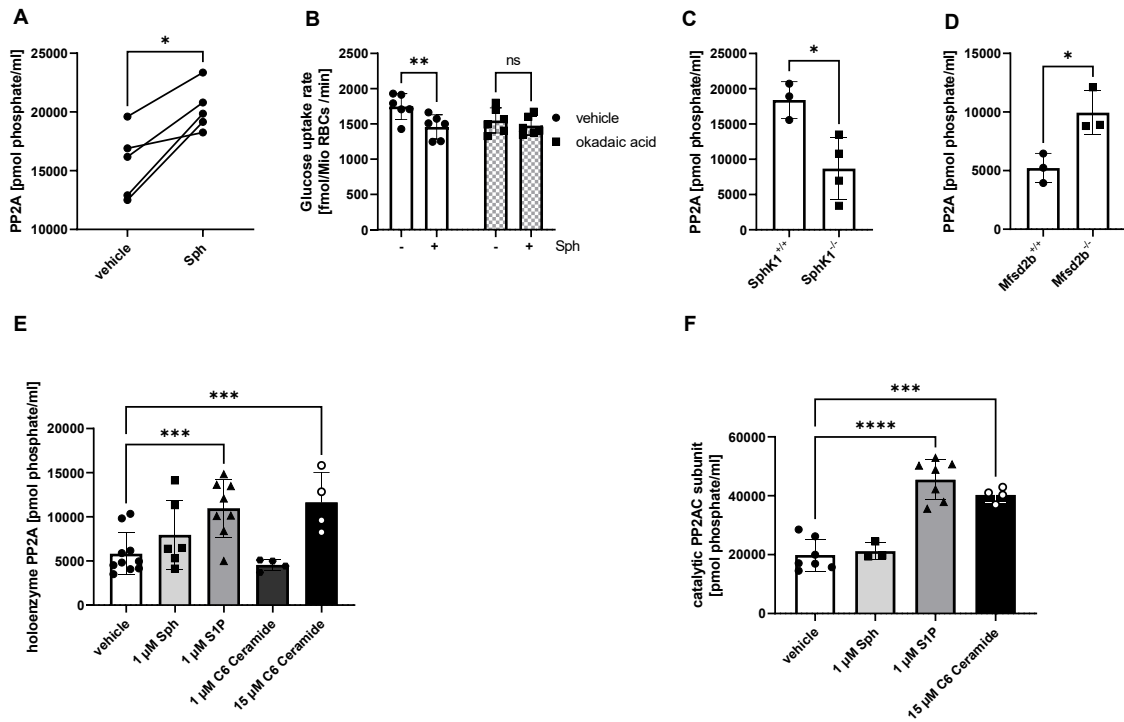


Figure 19: S1P regulates glucose uptake by activating PP2A *in vitro* and *in vivo*.

A) PP2A activity measured after immunoprecipitation from RBCs incubated with vehicle and 1 μM Sph (n=5 each) for 30 min. B) Glucose uptake in sphingosine-loaded RBCs in the absence or presence of 2 nM of the PP2A inhibitor okadaic acid (n=6 each). C) PP2A activity measured in RBCs from SphK1^{+/+} and SphK1^{-/-}, and D) in RBC from Mfsd2b^{+/+} and Mfsd2b^{-/-} mice (n=3-4 each). E) PP2A activity of the holoenzyme immunoprecipitated from C57Bl6 RBC lysates and incubated consecutively with Sph, S1P, and C6 ceramide in the indicated concentrations. F) PP2A activity of human recombinant PP2AC catalytic subunit in the presence of the same substances as in E); (n=3-10). Data are presented as mean±sd and tested with paired two-tailed t-test (A), unpaired t-test (C+D), two-way ANOVA (B) and one-way ANOVA (E+F); ns= not significant; p* < 0.05; P** < 0.01; P*** < 0.001; P**** < 0.0001. Parts of the results of this figure have been published in Thomas et al., 2023 [222].

8.6 S1P regulates cell surface GLUT1 expression, glucose uptake and PP2A activity in human RBCs

It was demonstrated that S1P governs glucose uptake in erythrocytes isolated from mice, attributable to the regulated localization of GLUT4 driven by PP2A activation. The subsequent investigation aimed to assess whether S1P similarly affects the localization of GLUT1 and whether these findings are applicable to human erythrocytes.

It was observed that human RBCs could be S1P-loaded by sphingosine in a manner comparable to murine RBCs and S1P-unloaded by albumin, respectively (Fig 20A, B). As well, human RBCs show the same response to S1P loading in terms of glucose uptake as mouse RBCs, which means a decreased glucose uptake rate after sphingosine incubation which increases after unloading with albumin (Fig. 20C). Finally, sphingosine incubation increased PP2A activity by 33% (Fig. 20D). In addition to the experiments that have already been performed with mouse RBCs, the use of human RBCs allowed to directly measure the abundance of their main glucose transporter GLUT1 on the cell surface in response to sphingosine, something that was not possible for GLUT4 in murine RBCs since the absence of reliable tools. However, in the case of GLUT1, there is an elegant assay using as GLUT1 ligand the receptor-binding domain of a recombinant envelope glycoprotein from human T-lymphotrophic virus (HTLV) which is fused to the enhanced green fluorescent protein (EGFP) coding sequence ($H_{RBD}EGFP$), as shown previously [177]. By using this system, the observation that sphingosine incubation decreased the presence of GLUT1 on the RBC cell surface by almost 50% was made (Fig. 20E, F).

In summary, the same observations were made in human erythrocytes as in murine RBCs. S1P regulates glucose uptake via the PP2A activity, leading to a reduced amount of GLUT on the membrane surface of erythrocytes, which can be attributed to internalization of the transporter.

Results

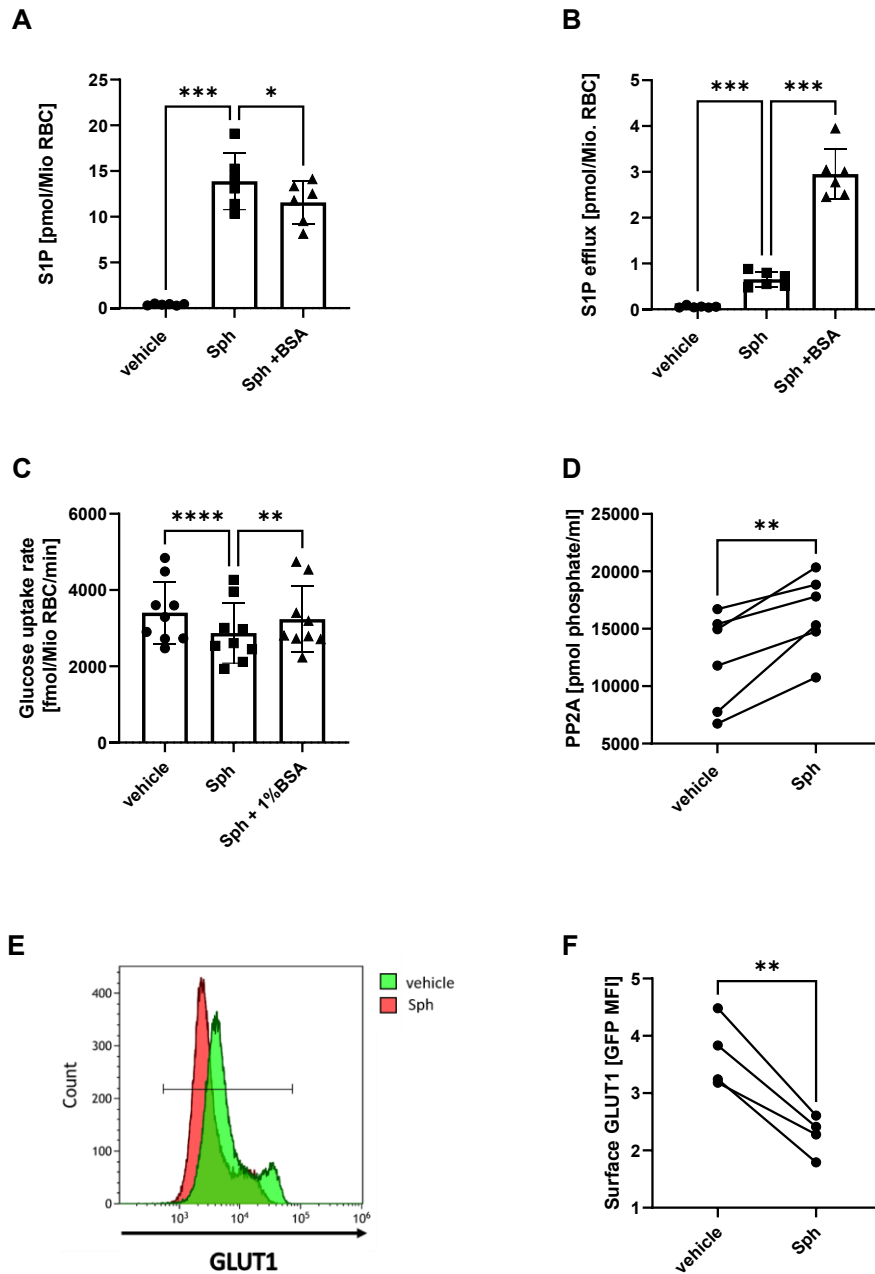


Figure 20: S1P regulates human RBC glucose uptake, PP2A activity and cell surface GLUT1.

A) Intracellular S1P levels and B) corresponding S1P efflux in human RBCs after incubation with 1 μ M Sph for 30 min followed by exposure or not to 1% BSA for 30 min (n=6 each). C) Glucose uptake rate in human RBCs treated as in A) (n=9). D) PP2A activity of human RBCs treated with 1 μ M Sph or vehicle (n=6 each). E) Representative flow cytometry histograms of surface GLUT1 as measured by H_{RBD}EGFP after incubation with 1 μ M Sph or vehicle for 30 min. F) quantification of GLUT1 MFI fluorescence from human RBCs treated with 1 μ M Sph or vehicle (n=4). Data are presented as mean \pm sd and tested with paired one-way ANOVA followed by a Tukey's multiple comparison test (A+B+C); paired two-tailed t-test (D + F). P* $<$ 0.05; P** $<$ 0.01; P*** $<$ 0.001; P**** $<$ 0.0001. This figure and the containing results of have been published in Thomas et al., 2023 [222].

8.7 RBCs from chronically hyperglycemic mice have higher S1P levels and increased Sphk1 and PP2A activities

It is current understanding that in RBCs, glucose is transported passively by GLUTs along concentration gradients [155, 156]. Thus, the concentration of extracellular glucose determines the rate of glucose entry into RBCs which, in the case of the hyperglycemia, e.g. associated with diabetes mellitus, leads to hemoglobin glycation (HbA1c) that is clinically used to monitor long-term glycemic state. To understand whether the mechanism of S1P-regulated glucose uptake may be affected by disease, its performance was tested in an environment with chronically elevated glucose levels. For this, a murine model of high caloric diet-induced obesity (DIO) was used. These animals are hyperglycemic and insulin-resistant as reflected by elevated fasting glucose levels and the substantial increase in HbA1c concentrations (Fig. 21A, B). RBCs from DIO mice were isolated and tested for S1P level, PP2A activity and glucose uptake. Interestingly, RBCs from hyperglycemic environments show 40% increased S1P levels compared to their controls (Fig. 21C). This can be explained by an almost 100% increased sphingosine kinase activity, which could be assessed by the conversion of C17-sphingosine to C17-S1P by LC-MS/MS measurement (Fig. 21F). Consistent with the elevated S1P level, PP2A is 52% more active in DIO-RBCs compare to controls (Fig. 21D). Only in the determination of the glucose uptake rate no difference between the hyperglycemia and control RBCs could be observed (Fig. 21E).

Results

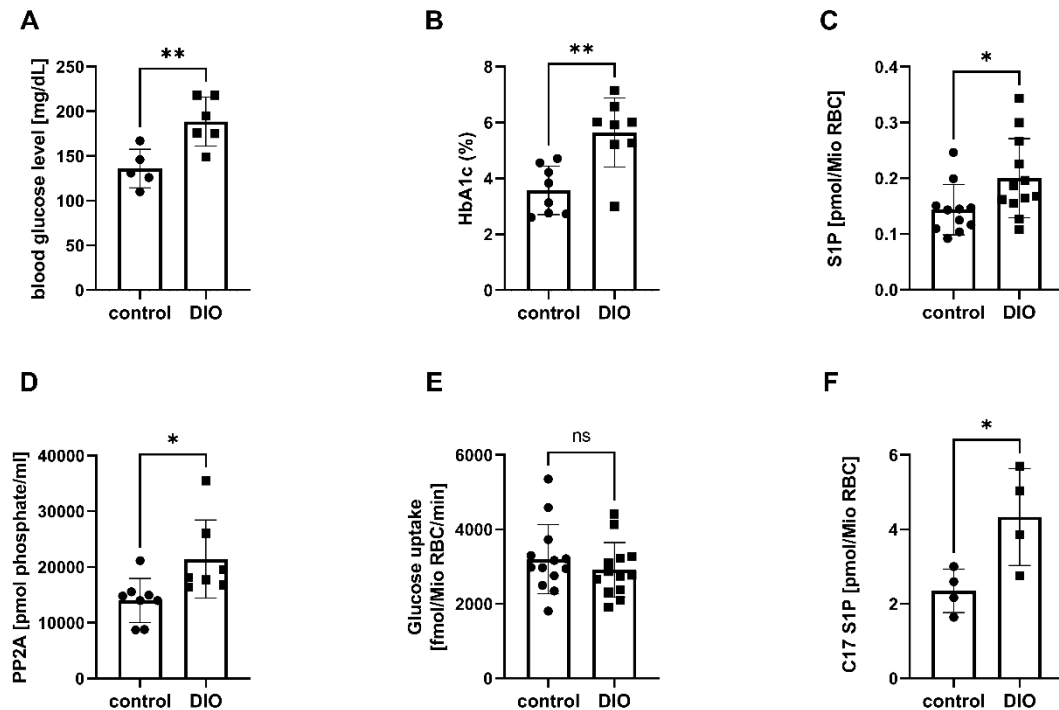


Figure 21: RBC from chronically hyperglycemic mice have higher S1P levels and increased PP2A activity.

A) Fasting blood glucose levels and B) HbA1c of age matched male mice fed standard chow or high caloric diet (DIO) for 12 weeks (n=5-8 each). C) intracellular S1P concentrations (n=11/12), D) PP2A activity (n=8/7), and B) glucose uptake rate (n=13 each) in RBCs of control and DIO mice. F) Sphk activity in RBCs of control and DIO mice as measured by LC-MS/MS based on the conversion of C17-sphingosine to C17-S1P during a 30 min incubation with 1 μ M C17-Sph (n=4). Data are presented as mean \pm sd and tested with two-tailed unpaired t-test; ns= not significant; $P^* < 0.05$; $P^{**} < 0.01$. Results of this figure have been published in Thomas et al., 2023 [222].

8.8 Patients with diabetes mellitus type 2 exhibit high S1P and increased PP2A activity in RBCs

Given the elevated S1P levels observed in erythrocytes of hyperglycemic mice, leading to the regulation of PP2A activity, the subsequent logical progression was to assess the validity of these observations in human patients diagnosed with type 2 diabetes mellitus (T2DM), through a case-control study. In T2DM, β -cell function is insufficient relative to the level of insulin sensitivity, resulting in the presence of insulin resistance, ultimately leading to chronic hyperglycemia. Consequently, insulin resistance ensues, culminating in long-term hyperglycemia.

Results

The patients with T2DM examined in this study exhibited an average HbA1c level of 8.9 mg/dl, in contrast to the control group's average of 5.2 mg/dl (Fig. 22A). Similar to the murine model, human diabetic RBCs showed 34% increased S1P levels (Fig. 22B) and a 2-fold increased PP2A activity (Fig. 22C). The glucose uptake of the RBCs also behaved as observed in the DIO mouse model and did not differ in the RBCs of T2DM patients compared to those of the healthy control patients (Fig. 22D). However, by investigating the human RBCs, which as mentioned above use GLUT1 for glucose transport, it was possible to investigate GLUT1 on the surface of RBCs in T2DM patients and controls by using the H_{RBD}EGFP. It could be shown that cell surface GLUT1 was decreased by 26% in diabetic RBCs compared to controls (Fig. 22E). In addition, it could be demonstrated that RBC S1P concentrations correlated positively with the activity of PP2A in these RBCs isolated from T2DM patients while the healthy controls did not show this correlation (Fig. 22F).

Results

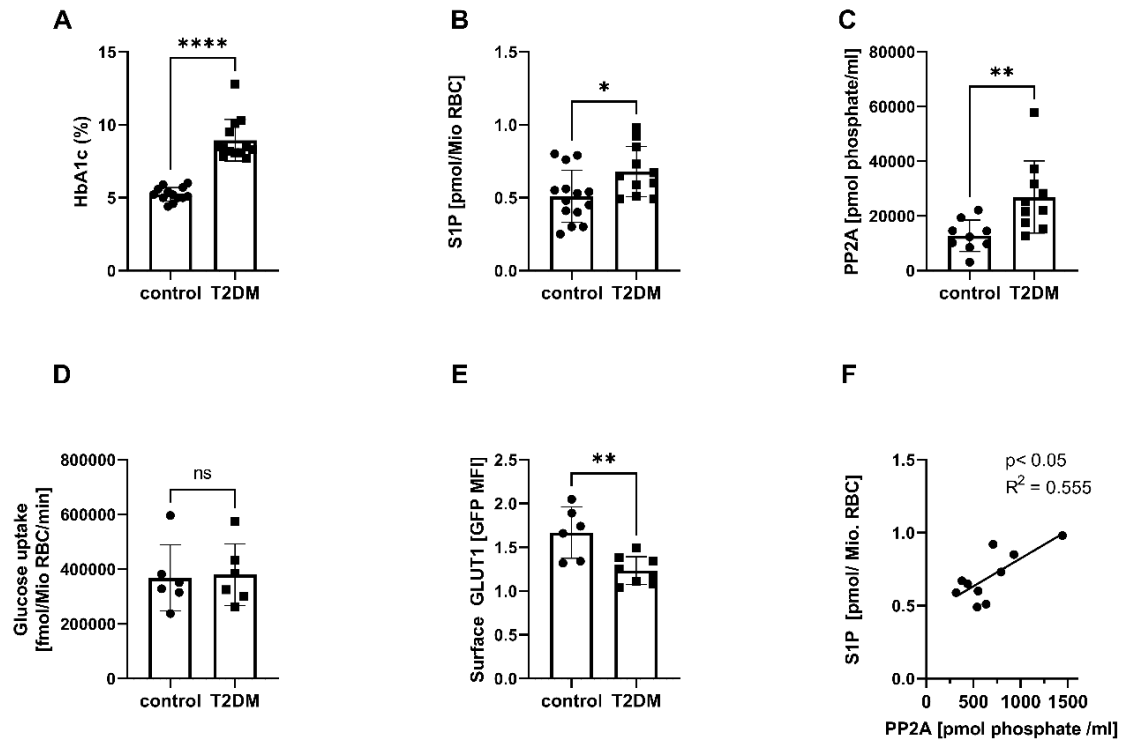


Figure 22: RBC from patients with diabetes mellitus type 2 have higher S1P levels and increased PP2A activity.

A) HbA1c levels of human patients with and without T2DM (n=13 each). B) intracellular S1P concentrations (n=13 each) and C) PP2A activity (n=10/9) in RBCs from the same human subjects. D) Glucose uptake rate (n=6 each) in RBCs and E) cell surface GLUT1 (n=8/6) on RBCs from patients with and without T2DM (randomly selected from above groups). F) Correlation between intracellular S1P and PP2A activity in RBCs from the T2DM patients group. Data are presented as mean±sd and tested with two-tailed unpaired t-test (A-E) and two-tailed Pearson correlation coefficients (F); ns=not significant; $P < 0.05$; $P^{**} < 0.01$; $P^{****} < 0.0001$. Results of this figure have been published in Thomas et al., 2023 [222].

8.9 Lack of Mfsd2b prevents the pathological HbA1c increase in chronic hyperglycemia

Up to this point, it has been shown that hyperglycemia leads to increased S1P levels in RBCs and thus to activation of PP2A, which in turn leads to lower levels of GLUT transporters on the surface of the RBCs. To test if an increase of intracellular S1P may causally prevent the pathological hemoglobin glycosylation occurring in diabetes, *Mfsd2b*^{-/-} mice, with naturally high S1P level in their RBCs, were fed a high caloric diet (DIO diet) for 8 weeks. As a control, *Mfsd2b*^{+/+} mice were fed the same diet for the same time and examined simultaneously. First, the glucose tolerance of these animals was investigated and both genotypes

Results

developed a highly pathological glucose tolerance as a result of the DIO diet, indicating a diabetic phenotype (Fig. 23A). By analyzing the area under the glucose tolerance curves obtained, the change in blood glucose levels of each group showed differences between the DIO-fed mice of both genotypes, whereas the different genotypes on the same diet showed no differences in their area under the curve (Fig. 23B). But HbA1c levels differed dramatically. The *Mfsd2b*^{+/+} mice developed the expected 9-fold increase in HbA1c, whereas the *Mfsd2b*^{-/-} mice showed virtually no increase (Fig. 23C). This indicates that high intracellular S1P protects them from pathological hemoglobin glycation in diabetes, which is highly supported by the observation that *Mfsd2b*^{-/-} mice have less lipid peroxidation in their RBCs due to DIO diet compare to the *Mfsd2b*^{+/+} mice. DIO led to an increase in Thiobarbituric Acid Reactive Substances (TBARS), which are formed as a by-product of lipid peroxidation, in *Mfsd2b*^{+/+} RBC but to a much lesser extent in *Mfsd2b*^{-/-} RBC (Fig. 23D). This suggests that high intracellular S1P in RBC protected against the chronic effects of intracellular hyperglycemia such as lipid peroxidation by limiting glucose inflow.

Results

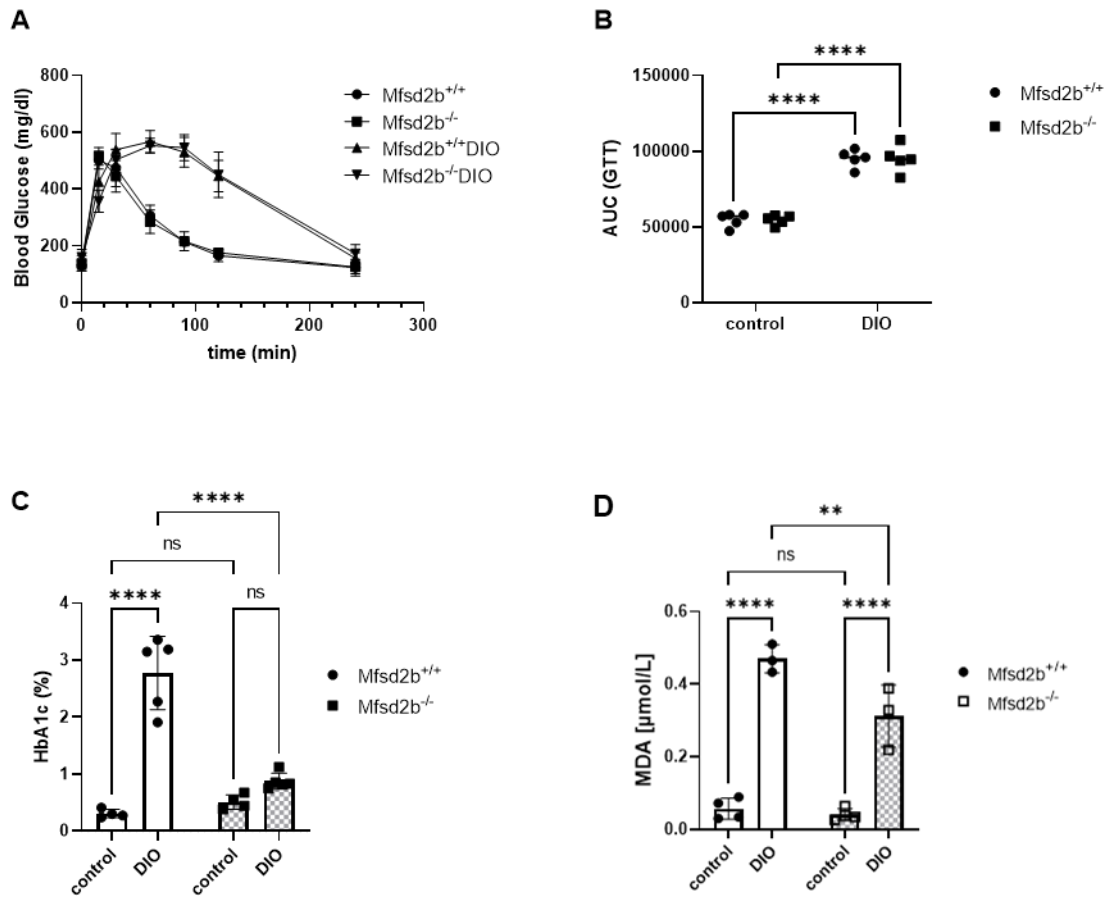


Figure 23: RBC from chronically hyperglycemic Mfsd2b^{-/-} mice have no changes in HbA1c level.

A) Change in blood glucose level over time, B) related area under the curve and C) HbA1c level of Mfsd2b^{+/+} and Mfsd2b^{-/-} mice with and without DIO for 8 weeks (n=5 each). D) TBARS levels (n=4/3) in the same mice as determined by MDA measurements. Data are presented as mean±sd and tested with one-way ANOVA (A) and unpaired two-way ANOVA, followed by Tuckey's; ns= not significant; ns=not significant; P****<0.0001. Results of this figure have been published in Thomas et al., 2023 [222].

9 Discussion

9.1 S1P regulates glucose uptake in human and mice RBCs under normoxic conditions

In this thesis, it was investigated how S1P influences the glucose uptake in RBCs under normoxic conditions and how this is reflected in the clinical picture of diabetes mellitus. This is the first report of intracellular S1P regulating glucose uptake in cells and it reveals an underlying mechanism of this effect. Although this study is mainly concentrated on RBCs, this may very well be the case for other tissues particularly where insulin-independent GLUT activity is physiologically important such as the brain. In order to investigate the influence of S1P on the glucose uptake of RBCs, first of all a system that allowed to regulate the S1P level in the cell *in vitro* was used. Freshly isolated RBCs are able to be loaded with S1P by sphingosine incubation [104, 105, 148]. An increase in intracellular S1P levels could be confirmed by LC-MS/MS measurements. Sphingosine is non-polar and can pass through the membrane better than its polar phosphorylated form. Inside the cell, sphingosine is phosphorylated to S1P by sphingosine kinase 1[229]. Incubation with sphingosine therefore led to more efficient loading with S1P than direct incubation with the phosphorylated form, as shown by this study. Furthermore, it was shown that glucose uptake decreased upon *in vitro* S1P loading in isolated mice and human RBCs, respectively. The same effect could be investigated in mouse RBCs with elevated S1P levels *in vivo*. This RBCs were isolated from mice with inhibited Sgpl1 activity due to a DOP treatment [45] or a tissue specific Sgpl1 knock out. In past studies, inhibiting Sgpl1 has been shown to result in increased S1P levels in RBCs [148, 230], which was confirmed by the results of this study. Since elevated S1P levels have a negative effect on glucose uptake, the question how glucose uptake develops in RBCs with lowered S1P levels arose. It was observed by other research groups, that unloading a RBC from S1P is possible when a S1P acceptor is provided extracellularly to previously loaded RBCs [104]. In this case a measurable S1P efflux was indicated by elevated S1P levels in the extracellular medium. The S1P acceptor in this study was albumin (BSA) and it could be shown that incubating RBCs with it not only increase S1P efflux, but also improved glucose uptake. This observation was independent of the fact

Discussion

whether human or mouse RBCs were previously loaded *in vitro* or had increased S1P levels *in vivo*.

The fact that the regulation of glucose uptake by intracellular S1P applies to both mice and humans is of great importance, not only with regard to possible therapeutic applications. Glucose is mainly transported through glucose transporters, of which a different form is expressed on RBCs of mice and humans. In mature mouse RBCs GLUT4 is the main GLUT transporter whereas in human RBCs GLUT1 is most abundant [139]. Both seems to be affected by S1P.

After unloading of S1P by albumin showed a positive effect on the glucose uptake in mice and human RBCs, it needed to be investigated which influence lowered S1P levels have *in vivo*. Therefore, RBCs of SphK1^{-/-} mice were used. Experiments by the group of Timothy Hla showed lower S1P levels in the blood of SphK1^{-/-} mice compared to wildtype mice [141]. In this study, decreased S1P levels were specifically detected in the RBCs. These RBCs served as a suitable model to test how lower S1P levels in the RBCs *in vivo* affect its glucose uptake. Interestingly, the same effect as after unloading the RBC with albumin could be observed. The reduced S1P levels led to an improved glucose uptake. It is known that SphK1 is present in the cytosol while SphK2 is localized in the nucleus. Since RBCs lose their nucleus during maturation, only SphK1 is expected in this cell type [151, 152]. This could be confirmed by LC-MS/MS measurements, as incubation of SphK1^{-/-} RBCs with sphingosine did not increase S1P levels whereas it was the case in wild type RBCs. If no sphingosine kinase is present, the incorporated sphingosine cannot be phosphorylated to S1P and it accumulates intracellularly. Interestingly incubation with sphingosine had no effect on glucose uptake in these animals, proving that elevated S1P levels regulating glucose uptake and not the unphosphorylated sphingosine. In respect of all these results, a relation between S1P levels and glucose uptake in RBCs was shown in mouse and human.

9.2 Glucose update rescue happens via the export of S1P through the transporter Mfsd2b

The Mfsd2b transporter protein, which was recently discovered as a S1P transporter, is mainly found in RBCs [104]. If it is not present, S1P cannot be exported from RBCs as usual

Discussion

which results in an S1P accumulation in the cell. Therefore, RBCs of *Mfsd2b*^{-/-} mice show highly increased S1P levels [104], which was confirmed in this study. These *in vivo* increased S1P levels led to decreased glucose uptake in RBCs which is in line with the previously made observations. RBCs lacking *Mfsd2b* could further be loaded with S1P by sphingosine incubation which led to a further decrease in glucose uptake rate. However, because RBCs lacking the transporter for S1P, unloading by extracellular albumin could not be observed as shown before [104]. What has not been shown yet is the effect lacking *Mfsd2b* has on the glucose uptake rate of RBCs. The inability to unload the *Mfsd2b*^{-/-} RBCs by a S1P acceptor resulted in failure to rescue glucose uptake.

To further investigate the role of *Mfsd2b* on glucose uptake, with regard to its role in nuclear cells, a glucose uptake assay was performed with cells overexpressing *Mfsd2b*. For this study, HEK293 cells expressing *Mfsd2b* were transfected, both transient and stable, for co-expression of SphK1. The emerging cell lines showed same results for its glucose uptake, indicating that their behavior in loading and unloading with S1P is not different. As shown in the gene expression data, HEK293 cells do not naturally express SphK1. To make loading with S1P possible and to get close to the conditions of the assays with RBCs, transfection with SphK1 was necessary. HEK293 cells with *Mfsd2b* and SphK1 co expression were also used for *Mfsd2b* studies by the research group of Long N. Nguyen [104]. Successful transfection and subsequent SphK1 expression were detected by qPCR. Furthermore, transient transfection of EGFP-coupled SphK1 allowed optical localization of the expressed protein in the cell after transfection. Glucose uptake experiments showed that in cells with and without additional *Mfsd2b* expression, loading with S1P by sphingosine incubation had a negative effect on glucose uptake. This is an important finding as it indicates that the observed regulation of glucose uptake by S1P does not appear to be unique to RBCs. However, the decreased glucose uptake rate in *Mfsd2b* overexpressing cells could be rescued by extracellular albumin. In contrast, glucose uptake remained suppressed after sphingosine incubation despite extracellular albumin administration in cells without *Mfsd2b* expression. In line with these observations no S1P efflux could be observed in HEK293 cells without *Mfsd2b* expression whereas an elevated efflux was detected in

loaded HEK293-Mfsd2b cells. Mfsd2b is the biggest contributor to S1P efflux and thus plays a crucial role in the regulation of glucose uptake.

9.3 Phosphorylated Fingolimod, like S1P, regulates glucose uptake in RBCs

This study demonstrated repeatedly that the intracellular S1P level is crucial for glucose uptake of RBCs. The question then arose as to whether this is also the case for an S1P analogue approved in a clinical context. FTY720, also known as Fingolimod, is an immunomodulating medication, mostly used for treating multiple sclerosis [231]. The phosphorylated form FTY720-P is a structural analogue to S1P but its phosphorylation takes place only through the SphK2 [224, 225], which is not present in RBCs [151, 152]. This is the reason why incubation with FTY720 led to accumulation of itself, but not to differences in FTY720-P levels. This shows a great advantage of the RBC to study the system of glucose uptake regulation. In contrast to other cells in which both kinases are present, the effect of FTY720 can be clearly distinguished from its phosphorylated form. Elevated FTY720 levels were found to have no effect on RBC glucose uptake, whereas elevated FTY720-P levels resulted in decreased glucose uptake, which was reversible when FTY720-P levels were reduced again.

9.4 The activity of GLUT protein is not regulated by S1P concentration in the plasma membrane

Since both S1P and its analogue FTY720-P regulate glucose uptake in RBCs, the question arose which mechanism is involved in that regulation. In murine RBCs, glucose is transported via GLUT4, in human RBCs via GLUT1. It has been shown that glucose uptake in both mouse and human RBCs can be regulated by S1P. In addition, it is known, that GLUT inhibitor cytochalasin B suppresses glucose uptake in RBCs from different species [232-234], which was confirmed by results of this study. It is therefore reasonable to assume that S1P influences the activity of GLUT.

Discussion

S1P is a phospholipid present in the plasma membrane. Experiments indicate that 10% of RBC S1P is located to its plasma membrane (data not shown) and past studies have shown that the phospholipid composition of the plasma membrane itself influences glucose uptake by effecting GLUT4 function [163]. Liposomes contained anionic phospholipids such as phosphatidic acid, phosphatidylserine and phosphatidylinositol stabilized and activated GLUT4, whereas liposomes which contained conical lipids such as phosphatidylethanolamine and diacylglycerol enhanced transporter activity without stabilizing protein structure [163]. Thus, modulation of GLUT activity by alterations in plasma membrane phospholipids under physiological and pathophysiological settings may be a novel and still underexplored metabolic regulatory mechanism, which could also be the case in regulation of glucose uptake by S1P. With regards to this, it was investigated whether the amount of S1P in the plasma membrane has an influence on glucose uptake. To test this, liposomes with known lipid compositions were prepared. In these liposomes purified GLUT4 was incorporated and glucose uptake was measured by using ^3H labeled glucose. In contrast to the anionic phospholipid phosphatidic acid (PA), the incorporation of 0.1%, 1% or 15% S1P (mol/mol) led to no effect on glucose uptake in liposomes. Therefore, it can be assumed that S1P in the plasma membrane has no direct effect on glucose uptake.

9.5 S1P leads to increased internalization of GLUT transporter at the cell surface of RBCs

If the activity of GLUT transporters is not affected by S1P in the membrane, it may be its localization that is altered by increased intracellular S1P. Indications for this are the observations that GLUT transporters, which are present at the cell surface, form clusters as working units and it is the clustered distribution of the transporter that is associated with activation [235]. GLUT1 as well as GLUT4 have been found biochemically in these detergent-resistant membranes (lipid rafts) [236, 237] and it is known that GLUT clusters are mostly regulated by lipid rafts and restricted in size by the cytoskeleton and glycosylation [235]. However, little is known about the regulation of the insulin-

Discussion

independent GLUT1 and GLUT4 activation and trafficking in RBCs. Most of the evidence stems from transformed cell lines, where GLUT1 has been shown to translocate from intracellular storage pools to the cell surface upon metabolic stress [165, 238]. Additionally, randomly distributed transporters are recruited to lipid rafts in response to glucose deprivation leading to an increase in glucose inflow [165, 238]. To determine whether altered GLUT activity is due to changed localisation of the transporter on the lipid rafts, these were isolated from mouse RBCs that had previously been loaded with S1P and accordingly showed lower glucose uptake in previous experiments. Both the complete plasma membrane of RBCs, the so-called ghosts, as well as the Triton X-100 insoluble lipid rafts were isolated. Depending on the S1P level of the RBCs, no difference in GLUT4 protein quantity could be detected, neither in the complete membrane nor in the isolated lipid rafts.

However, either the activity of the transporter or its amount at the surface must be regulated by S1P. When S1P does not affect the activity of Glut by altering the membrane composition, nor the localization of the transporter within the activating membrane zones, another mechanism must influence the activity or localization of the GLUT transporter.

It is known that GLUTs are not permanently available on the surface but in a cycle of internalization and supply. In insulin dependent glucose transport, insulin stimulates translocation of GLUT from an intracellular membrane compartment to the cell surface [239-241]. So far, little is known about the insulin-independent translocation of GLUT. However, by using specialized GLUT4 antibody [218] as well as an GLUT1 EGFP-tagged HTLV receptor-binding domain (H_{RBD}) fusion protein [242], which both specifically binds GLUT at the cell surface [218-220], it was possible to demonstrate that a similar mechanism appears to be at work in insulin-independent glucose uptake of RBCs. In S1P-loaded RBCs less GLUT4 respectively GLUT1 could be detected at the cell surface, active for glucose transport. These results, which were initially contradictory to the western blot, appear credible when one considers that the western blot is a much less sensitive method than flow cytometry. Furthermore, it is difficult to determine which parts of the erythrocyte membranes are contained in the isolated ghosts used for protein detection by western blotting. The main goal of ghost preparation is to wash hemoglobin out of the RBCs without

Discussion

severely disrupting the membrane. When GLUT is internalized, it is nevertheless membrane bound but no longer available at the cell surface for glucose transport. The detection of GLUT on the cell surface using specialized external domain binding proteins yields a much more meaningful result. It could be observed that not all surface GLUT was lost due to sphingosine incubation. However, less fluorescence was detected, which proves that due to increased S1P levels, less GLUT is available at the surface of the RBCs.

9.6 S1P activates PP2A, resulting in internalization of GLUT in mice and human RBCs

This raised the question of how S1P regulates GLUT on the cell surface. Various studies, indicate that different natural or synthetic sphingolipids reduce cell surface levels of nutrient transporters, which has been particularly studied in tumor research [169, 171, 211]. The underlying mechanism has been identified as disruption of membrane trafficking of the transporters by activation of PP2A [171, 211, 226]. Sphingolipids such as C6 ceramide have been shown to activate PP2A (and protein phosphatase-1) in a stereospecific manner requiring the amide group, the primary hydroxyl group and the secondary hydroxyl group of the sphingoid backbone [210]. Thereby, ceramide binds to the PP2A catalytic subunit and increases its activity [210]. To investigate if this is the case for S1P as well, PP2A activity was determined in RBCs with altered S1P levels *in vitro* as well as *in vivo*. Indeed, it was shown that increased intracellular S1P levels led to increased PP2A activity, both in sphingosine-loaded murine and human RBCs as well as RBCs of *Mfsd2b*^{-/-} mice. On the contrary, reduced S1P levels of *SphK1*^{-/-} RBCs are accompanied by decreased PP2A activity. A lack of effect on glucose uptake after sphingosine loading in combination with the PP2A inhibitor okadaic acid proved the relationship between S1P levels, PP2A activity and glucose uptake. Thus, this study not only showed that PP2A activation is responsible for decreased glucose uptake and that increased S1P levels lead to increased PP2A activity but also proved that this is due to the direct activation of the catalytic unit PP2AC without an intermediate pathway.

Discussion

As for FTY720-P, there is controversy whether it activates PP2A *per se* [213, 214] or whether activation is achieved after its de-phosphorylation. As a matter of fact, whether FTY720 is really active on PP2A only in its non-phosphorylated form is also controversial as endogenous phosphorylation by Sphk2 has never been completely excluded. In this study the issue was resolved by investigating PP2A activity in a biochemical assay with the holoenzyme and the catalytic subunit alone. Thereby only FTY720-P and not FTY720 activated PP2A at equimolar concentrations. This is consistent with the observation that FTY720 had no effect of glucose uptake in RBCs lacking SphK2 activity and hence wasn't phosphorylated, whereas FTY720-P was an effective regulator. Accordingly, both reduced glucose uptake due to increased intracellular S1P levels and increased FTY720-P levels can be explained by an activation of PP2A.

9.7 S1P has a protective effect on RBCs under hyperglycemic conditions

Hyperactivation of PP2A and desensitization of the insulin/Akt signaling pathway has been suggested as one pathophysiological principle in insulin-dependent tissues in diabetes [243-245]. According to present knowledge, there are no reports on S1P content or PP2A activity in RBCs in diabetes. Erythrocytes of diabetic patients are in a permanently hyperglycemic environment. The regulation of glucose uptake therefore seems particularly important for them as it was shown that permanently high intracellular glucose levels cause considerable damage to RBCs [187, 189, 192, 246]. To investigate the S1P level in diabetic RBCs, erythrocytes from a murine model of obesity-induced hyperglycemia and insulin resistance as well as RBCs from human T2DM patients were isolated and studied. Interestingly, elevated S1P levels were detected in both diabetic mouse and human RBCs, which is not published yet. Furthermore, increased S1P levels of the diabetic mice RBCs could be traced back to increased SphK1 activity by measuring the kinase activity. The regulation of S1P levels in the diabetic RBCs thus appears to be an active process and does not occur passively. As in the previous results, increased S1P levels in diabetic RBCs led to increased PP2A activity both in human T2DM and in the murine model which is indicated

Discussion

by a strong positive correlation between both. Even the examination of the cell surface GLUT1 showed lower presence of the transporter on human diabetic RBCs. Given the ability of S1P to activate PP2A and of PP2A to reduce cell surface GLUT, a causal relationship seems plausible in which increased intracellular S1P, in response to chronic hyperglycemia, stimulates PP2A in a counter-regulatory manner to limit glucose influx into the erythrocytes. In fact, this would protect RBCs against the many deleterious results of high intracellular glucose concentration such as lipid peroxidation, loss of activities of erythrocyte enzymes such as glutathione S-transferase and glutathione reductase, hemolysis and eryptosis [192, 247].

The observation that diabetic human and murine RBCs did not show altered glucose uptake despite their higher intracellular S1P levels can be linked to the long-term elevated extracellular glucose concentrations to which the RBCs are exposed in the organism. At the same time, elevated HbA1c levels show that diabetic red blood cells have increased glucose uptake in the long term. However, the protective effect of high S1P in RBCs under chronic hyperglycemia *in vivo* is clearly visible and causally proven from the observations that were made in RBCs of hyperglycemic *Mfsd2b*^{-/-} mice. RBCs from these mice are harboring genetically high S1P levels but surprisingly they were completely resistant to the dramatic HbA1c increase what was observed in RBCs of wild type DIO models. In addition, the erythrocytes of hyperglycemic *Mfsd2b*^{-/-} mice were shown to have less lipid peroxidation than those of animals expressing *Mfsd2b* normally. These observations confirm the hypothesis that S1P has a protective effect on RBCs under hyperglycemic conditions.

10 Summary and outlook

The aim of this study was to investigate the relationship between intracellular S1P and glucose uptake in red blood cells. It is the first study that examines this under normoxic conditions and reveals the mechanism behind this regulation as well as establishes a medically relevant reference. It could be shown that increased S1P levels led to a decreased glucose uptake rate, whereas the opposite could be observed with decreased S1P levels. Therefore, it was shown that glucose uptake in RBCs is dependent on its intracellular S1P level. The S1P level in RBCs can be changed rapidly, leading to an immediate adjustment of the glucose uptake rate. It could be proven, that the altered glucose uptake by S1P is due to a loss of glucose transporter at the cell surface. Intracellular S1P leads to activation of PP2A by direct complexing with the catalytic subunit, which in turn leads to internalization of the surface transporter. Initial experiments with HEK293 cells showed that the regulation of glucose uptake by S1P is not restricted to RBCs since S1P was also able to influence the glucose uptake of these nucleated cells. For future studies, it would be interesting to find out in which types of cells this mechanism applies and in which it might not. Especially cells in which insulin-independent glucose uptake takes place should be considered for examination. Red blood cells provided a relatively simple experimental model, as their S1P levels are easy to influence and both their S1P influx and efflux can be monitored well. The results of this study provide insight into the relationship between S1P and glucose uptake, which gives deep insights into the general insulin-independent regulation of GLUT.

Sphingolipid metabolism is dysregulated in many metabolic diseases and its interventional correction often positively affects the associated disease suggesting causal interrelationships as e.g. has been shown for ceramides [14, 248]. The questions thus remain how RBC S1P concentration are regulated in disease and whether this is a contributing or a counter-acting factor. Data of this study strongly suggest that the latter is the case because one of the strongest findings demonstrate a protection against a diabetic phenotype thanks to increased S1P levels. However, an important question that arises from this, is how this protective mechanism is activated. One explanation may lie in the study on hypoxia leading to increased S1P synthesis, where SphK1 was shown to be activated by hypoxia-related increase in adenosine signaling through the adenosine receptor 2B (A2B)

[154, 249]. In this study it was observed that SphK1 activity is increased in diabetic RBCs but it was not possible to stimulate SphK1 by acute hyperglycemia neither *in vitro* nor *in vivo* (data not shown). However, A2B signaling is well known to be increased in diabetes with particularly the A2B receptor having major roles in insulin secretion and glucose homeostasis thus serving as a target for new drugs for diabetes treatment [250, 251]. It is thus conceivable that increased A2B signaling may increase in diabetic RBCs and is responsible for the increased SphK1 activity there. This should be the focus of future studies.

Another point to investigate is the activity of Mfsd2b in diabetic RBCs and if the observed increased S1P levels are also Mfsd2b dependent. It is interesting to note that S1P export capacity of Mfsd2b is less efficient at basic pH [105], and diabetic RBC are known to have higher pH levels [252].

In summary, the novel S1P/PP2A/GLUT module that was identified in this study dynamically regulates glucose uptake in RBCs in response to metabolic cues from the environment by controlling S1P production and efflux. This module may also be functional in other tissues in parallel to insulin-dependent glucose transport and surely deserves future consideration. Finally, the idea of intracellular S1P fluctuations affecting PP2A in perhaps other cell types makes it a mechanism possibly relevant to a variety of human diseases.

11 Graphical abstract

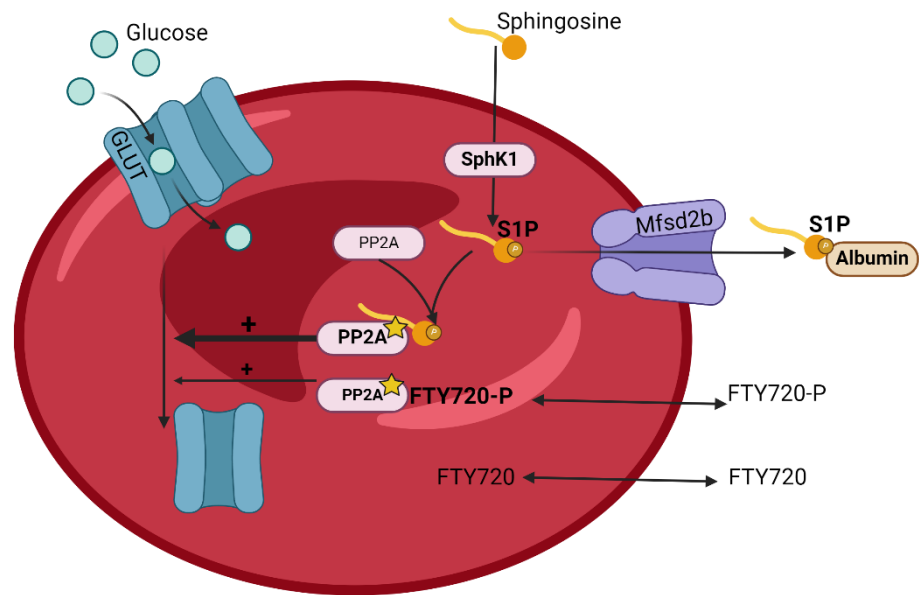


Figure 24 Illustrative description of the uncovered role of S1P in regulation of glucose uptake in red blood cells.

Sphingosine is passively absorbed by the RBC where it gets phosphorylated by SphK1 to S1P. S1P efflux is possible via Mfsd2b with the help of an extracellular acceptor such as albumin (BSA). In the cell, S1P complexes in with the catalytic subunit unit of PP2A, leading to its activation (indicated with a star), which in turn results in the internalization of GLUT (GLUT4 in mouse and GLUT1 in human RBCs). The result is a reduced glucose uptake rate. FTY720-P also complexes with PP2A and thus leads to the internalization of GLUT, unlike FTY720. Both FTY270 and FTY720-P are not transported via Mfsd2b.

12 References

1. Thudichum, J.L.W. and D.L. Drabkin, *A treatise on the chemical constitution of the brain*. 1962, Hamden, Conn.: Archon Books.
2. Hannun, Y.A., *Functions of ceramide in coordinating cellular responses to stress*. *Science*, 1996. **274**(5294): p. 1855-9.
3. Hannun, Y.A. and R.M. Bell, *Regulation of protein kinase C by sphingosine and lysosphingolipids*. *Clin Chim Acta*, 1989. **185**(3): p. 333-45.
4. Hannun, Y.A., et al., *Sphingosine inhibition of protein kinase C activity and of phorbol dibutyrate binding in vitro and in human platelets*. *J Biol Chem*, 1986. **261**(27): p. 12604-9.
5. Hannun, Y.A. and L.M. Obeid, *Sphingolipids and their metabolism in physiology and disease*. *Nat Rev Mol Cell Biol*, 2018. **19**(3): p. 175-191.
6. Okazaki, T., R.M. Bell, and Y.A. Hannun, *Sphingomyelin turnover induced by vitamin D3 in HL-60 cells. Role in cell differentiation*. *J Biol Chem*, 1989. **264**(32): p. 19076-80.
7. Mamode Cassim, A., et al., *Sphingolipids in plants: a guidebook on their function in membrane architecture, cellular processes, and environmental or developmental responses*. *FEBS Lett*, 2020. **594**(22): p. 3719-3738.
8. Zhu, X.M., et al., *The biological functions of sphingolipids in plant pathogenic fungi*. *PLoS Pathog*, 2023. **19**(11): p. e1011733.
9. Santos, F.C., et al., *Sphingolipid-enriched domains in fungi*. *FEBS Lett*, 2020. **594**(22): p. 3698-3718.
10. Galadari, S., et al., *Tumor suppressive functions of ceramide: evidence and mechanisms*. *Apoptosis*, 2015. **20**(5): p. 689-711.
11. Maceyka, M., et al., *Sphingosine-1-phosphate signaling and its role in disease*. *Trends Cell Biol*, 2012. **22**(1): p. 50-60.
12. Weske, S., et al., *Targeting sphingosine-1-phosphate lyase as an anabolic therapy for bone loss*. *Nat Med*, 2018. **24**(5): p. 667-678.
13. Keul, P., et al., *Potent anti-inflammatory properties of HDL in vascular smooth muscle cells mediated by HDL-S1P and their impairment in coronary artery disease due to lower HDL-S1P: a new aspect of HDL dysfunction and its therapy*. *FASEB J*, 2019. **33**(1): p. 1482-1495.
14. Cartier, A. and T. Hla, *Sphingosine 1-phosphate: Lipid signaling in pathology and therapy*. *Science*, 2019. **366**(6463).
15. Paul, B., M. Lewinska, and J.B. Andersen, *Lipid alterations in chronic liver disease and liver cancer*. *JHEP Rep*, 2022. **4**(6): p. 100479.
16. Czubowicz, K., et al., *The Role of Ceramide and Sphingosine-1-Phosphate in Alzheimer's Disease and Other Neurodegenerative Disorders*. *Mol Neurobiol*, 2019. **56**(8): p. 5436-5455.
17. Schuchman, E.H. and R.J. Desnick, *Types A and B Niemann-Pick disease*. *Mol Genet Metab*, 2017. **120**(1-2): p. 27-33.
18. Nelson, D.L., et al., *Lehninger principles of biochemistry*. 2008, New York: W.H. Freeman.
19. Coant, N., et al., *Ceramidases, roles in sphingolipid metabolism and in health and disease*. *Adv Biol Regul*, 2017. **63**: p. 122-131.
20. Wigger, D., et al., *Monitoring the Sphingolipid de novo Synthesis by Stable-Isotope Labeling and Liquid Chromatography-Mass Spectrometry*. *Frontiers in Cell and Developmental Biology*, 2019. **7**.
21. Bajjalieh, S.M., T.F. Martin, and E. Floor, *Synaptic vesicle ceramide kinase. A calcium-stimulated lipid kinase that co-purifies with brain synaptic vesicles*. *J Biol Chem*, 1989. **264**(24): p. 14354-60.
22. Jeckel, D., et al., *Glucosylceramide is synthesized at the cytosolic surface of various Golgi subfractions*. *J Cell Biol*, 1992. **117**(2): p. 259-67.

References

23. Mehra, V.C., et al., *Ceramide-activated phosphatase mediates fatty acid-induced endothelial VEGF resistance and impaired angiogenesis*. *Am J Pathol*, 2014. **184**(5): p. 1562-76.
24. Apostolidis, S.A., et al., *Phosphatase PP2A is requisite for the function of regulatory T cells*. *Nat Immunol*, 2016. **17**(5): p. 556-64.
25. Jain, A., et al., *Diverting CERT-mediated ceramide transport to mitochondria triggers Bax-dependent apoptosis*. *J Cell Sci*, 2017. **130**(2): p. 360-371.
26. Futerman, A.H. and Y.A. Hannun, *The complex life of simple sphingolipids*. *EMBO Rep*, 2004. **5**(8): p. 777-82.
27. El Bawab, S., et al., *Molecular cloning and characterization of a human mitochondrial ceramidase*. *J Biol Chem*, 2000. **275**(28): p. 21508-13.
28. Bernardo, K., et al., *Purification, characterization, and biosynthesis of human acid ceramidase*. *J Biol Chem*, 1995. **270**(19): p. 11098-102.
29. Spiegel, S. and S. Milstien, *Sphingosine-1-phosphate: an enigmatic signalling lipid*. *Nat Rev Mol Cell Biol*, 2003. **4**(5): p. 397-407.
30. Hannun, Y.A. and L.M. Obeid, *Principles of bioactive lipid signalling: lessons from sphingolipids*. *Nat Rev Mol Cell Biol*, 2008. **9**(2): p. 139-50.
31. Lucke, S. and B. Levkau, *Endothelial functions of sphingosine-1-phosphate*. *Cell Physiol Biochem*, 2010. **26**(1): p. 87-96.
32. Zhou, K. and T. Blom, *Trafficking and Functions of Bioactive Sphingolipids: Lessons from Cells and Model Membranes*. *Lipid Insights*, 2015. **8**(Suppl 1): p. 11-20.
33. Futerman, A.H., *Intracellular trafficking of sphingolipids: relationship to biosynthesis*. *Biochim Biophys Acta*, 2006. **1758**(12): p. 1885-92.
34. Narita, T., et al., *Long-chain bases of sphingolipids are transported into cells via the acyl-CoA synthetases*. *Sci Rep*, 2016. **6**: p. 25469.
35. Goto, H., M. Miyamoto, and A. Kihara, *Direct uptake of sphingosine-1-phosphate independent of phospholipid phosphatases*. *J Biol Chem*, 2021. **296**: p. 100605.
36. Stoffel, W., G. Sticht, and D. LeKim, *Metabolism of sphingosine bases. IX. Degradation in vitro of dihydrospingosine and dihydrospingosine phosphate to palmitaldehyde and ethanolamine phosphate*. *Hoppe-Seyler's Zeitschrift fur physiologische Chemie*, 1968. **349**(12): p. 1745-1748.
37. Proia, R.L. and T. Hla, *Emerging biology of sphingosine-1-phosphate: its role in pathogenesis and therapy*. *J Clin Invest*, 2015. **125**(4): p. 1379-87.
38. Troupiotis-Tsailaki, A., et al., *Ligand chain length drives activation of lipid G protein-coupled receptors*. *Scientific Reports*, 2017. **7**(1): p. 2020.
39. Payne, S.G., S. Milstien, and S. Spiegel, *Sphingosine-1-phosphate: dual messenger functions*. *FEBS Lett*, 2002. **531**(1): p. 54-7.
40. Pierce, K.L., R.T. Premont, and R.J. Lefkowitz, *Seven-transmembrane receptors*. *Nat Rev Mol Cell Biol*, 2002. **3**(9): p. 639-50.
41. Ishii, I., et al., *Lysophospholipid receptors: signaling and biology*. *Annu Rev Biochem*, 2004. **73**: p. 321-54.
42. Graler, M.H., G. Bernhardt, and M. Lipp, *EDG6, a novel G-protein-coupled receptor related to receptors for bioactive lysophospholipids, is specifically expressed in lymphoid tissue*. *Genomics*, 1998. **53**(2): p. 164-9.
43. Anliker, B. and J. Chun, *Cell surface receptors in lysophospholipid signaling*. *Semin Cell Dev Biol*, 2004. **15**(5): p. 457-65.
44. Rosen, H., G. Sanna, and C. Alfonso, *Egress: a receptor-regulated step in lymphocyte trafficking*. *Immunol Rev*, 2003. **195**: p. 160-77.
45. Schwab, S.R., et al., *Lymphocyte sequestration through S1P lyase inhibition and disruption of S1P gradients*. *Science*, 2005. **309**(5741): p. 1735-9.

References

46. Hla, T. and V. Brinkmann, *Sphingosine 1-phosphate (S1P): Physiology and the effects of S1P receptor modulation*. *Neurology*, 2011. **76**(8 Suppl 3): p. S3-8.
47. Schwab, S.R. and J.G. Cyster, *Finding a way out: lymphocyte egress from lymphoid organs*. *Nat Immunol*, 2007. **8**(12): p. 1295-301.
48. Spiegel, S. and S. Milstien, *The outs and the ins of sphingosine-1-phosphate in immunity*. *Nat Rev Immunol*, 2011. **11**(6): p. 403-15.
49. Sanchez, T., et al., *Induction of vascular permeability by the sphingosine-1-phosphate receptor-2 (S1P2R) and its downstream effectors ROCK and PTEN*. *Arterioscler Thromb Vasc Biol*, 2007. **27**(6): p. 1312-8.
50. Du, J., et al., *LPS and TNF-alpha induce expression of sphingosine-1-phosphate receptor-2 in human microvascular endothelial cells*. *Pathol Res Pract*, 2012. **208**(2): p. 82-8.
51. Imasawa, T., et al., *Blockade of sphingosine 1-phosphate receptor 2 signaling attenuates streptozotocin-induced apoptosis of pancreatic beta-cells*. *Biochem Biophys Res Commun*, 2010. **392**(2): p. 207-11.
52. Studer, E., et al., *Conjugated bile acids activate the sphingosine-1-phosphate receptor 2 in primary rodent hepatocytes*. *Hepatology*, 2012. **55**(1): p. 267-76.
53. Takashima, S., et al., *G12/13 and Gq mediate S1P2-induced inhibition of Rac and migration in vascular smooth muscle in a manner dependent on Rho but not Rho kinase*. *Cardiovasc Res*, 2008. **79**(4): p. 689-97.
54. Grabski, A.D., et al., *Sphingosine-1-phosphate receptor-2 regulates expression of smooth muscle alpha-actin after arterial injury*. *Arterioscler Thromb Vasc Biol*, 2009. **29**(10): p. 1644-50.
55. Loh, K.C., et al., *Sphingosine-1-phosphate enhances satellite cell activation in dystrophic muscles through a S1PR2/STAT3 signaling pathway*. *PLoS One*, 2012. **7**(5): p. e37218.
56. Kimura, A., et al., *Antagonism of sphingosine 1-phosphate receptor-2 enhances migration of neural progenitor cells toward an area of brain*. *Stroke*, 2008. **39**(12): p. 3411-7.
57. Liu, W., et al., *S1P2 receptor mediates sphingosine-1-phosphate-induced fibronectin expression via MAPK signaling pathway in mesangial cells under high glucose condition*. *Exp Cell Res*, 2012. **318**(8): p. 936-43.
58. Park, S.W., et al., *Inhibition of sphingosine 1-phosphate receptor 2 protects against renal ischemia-reperfusion injury*. *J Am Soc Nephrol*, 2012. **23**(2): p. 266-80.
59. Yamaguchi, H., et al., *Sphingosine-1-phosphate receptor subtype-specific positive and negative regulation of Rac and haematogenous metastasis of melanoma cells*. *Biochem J*, 2003. **374**(Pt 3): p. 715-22.
60. Arikawa, K., et al., *Ligand-dependent inhibition of B16 melanoma cell migration and invasion via endogenous S1P2 G protein-coupled receptor. Requirement of inhibition of cellular RAC activity*. *J Biol Chem*, 2003. **278**(35): p. 32841-51.
61. An, S., Y. Zheng, and T. Bleu, *Sphingosine 1-phosphate-induced cell proliferation, survival, and related signaling events mediated by G protein-coupled receptors Edg3 and Edg5*. *J Biol Chem*, 2000. **275**(1): p. 288-96.
62. Herr, D.R., et al., *Sphingosine 1-phosphate (S1P) signaling is required for maintenance of hair cells mainly via activation of S1P2*. *J Neurosci*, 2007. **27**(6): p. 1474-8.
63. Lorenz, J.N., et al., *Vascular dysfunction in S1P2 sphingosine 1-phosphate receptor knockout mice*. *Am J Physiol Regul Integr Comp Physiol*, 2007. **292**(1): p. R440-6.
64. Kono, M., et al., *Deafness and stria vascularis defects in S1P2 receptor-null mice*. *J Biol Chem*, 2007. **282**(14): p. 10690-6.
65. Bajwa, A., et al., *Dendritic cell sphingosine 1-phosphate receptor-3 regulates Th1-Th2 polarity in kidney ischemia-reperfusion injury*. *J Immunol*, 2012. **189**(5): p. 2584-96.
66. Nussbaum, C., et al., *Sphingosine-1-phosphate receptor 3 promotes leukocyte rolling by mobilizing endothelial P-selectin*. *Nat Commun*, 2015. **6**: p. 6416.

References

67. Guerrero, M., et al., *Probe Development Efforts for an Allosteric Agonist of the Sphingosine 1-phosphate Receptor 3 (S1P3)*, in *Probe Reports from the NIH Molecular Libraries Program*. 2010: Bethesda (MD).
68. Sun, X., et al., *Sphingosine-1-phosphate receptor-3 is a novel biomarker in acute lung injury*. *Am J Respir Cell Mol Biol*, 2012. **47**(5): p. 628-36.
69. Murakami, A., et al., *Sphingosine 1-phosphate (S1P) regulates vascular contraction via S1P3 receptor: investigation based on a new S1P3 receptor antagonist*. *Mol Pharmacol*, 2010. **77**(4): p. 704-13.
70. Hsu, A., et al., *Sphingosine-1-phosphate receptor-3 signaling up-regulates epidermal growth factor receptor and enhances epidermal growth factor receptor-mediated carcinogenic activities in cultured lung adenocarcinoma cells*. *Int J Oncol*, 2012. **40**(5): p. 1619-26.
71. Sukocheva, O., et al., *Estrogen transactivates EGFR via the sphingosine 1-phosphate receptor Edg-3: the role of sphingosine kinase-1*. *J Cell Biol*, 2006. **173**(2): p. 301-10.
72. Adada, M., et al., *Sphingosine-1-phosphate receptor 2*. *FEBS J*, 2013. **280**(24): p. 6354-66.
73. Mayol, K., et al., *Sequential desensitization of CXCR4 and S1P5 controls natural killer cell trafficking*. *Blood*, 2011. **118**(18): p. 4863-71.
74. van Doorn, R., et al., *Sphingosine 1-phosphate receptor 5 mediates the immune quiescence of the human brain endothelial barrier*. *J Neuroinflammation*, 2012. **9**: p. 133.
75. Chang, C.L., et al., *S1P(5) is required for sphingosine 1-phosphate-induced autophagy in human prostate cancer PC-3 cells*. *Am J Physiol Cell Physiol*, 2009. **297**(2): p. C451-8.
76. Hu, W.M., et al., *Effect of S1P5 on proliferation and migration of human esophageal cancer cells*. *World J Gastroenterol*, 2010. **16**(15): p. 1859-66.
77. Lanterman, M.M. and J.D. Saba, *Characterization of sphingosine kinase (SK) activity in Saccharomyces cerevisiae and isolation of SK-deficient mutants*. *Biochem J*, 1998. **332 (Pt 2)**: p. 525-31.
78. Kim, S., H. Fyrst, and J. Saba, *Accumulation of phosphorylated sphingoid long chain bases results in cell growth inhibition in Saccharomyces cerevisiae*. *Genetics*, 2000. **156**(4): p. 1519-29.
79. Zhang, X., et al., *Elevation of endogenous sphingolipid long-chain base phosphates kills Saccharomyces cerevisiae cells*. *Curr Genet*, 2001. **40**(4): p. 221-33.
80. Laviad, E.L., et al., *Characterization of ceramide synthase 2: tissue distribution, substrate specificity, and inhibition by sphingosine 1-phosphate*. *J Biol Chem*, 2008. **283**(9): p. 5677-84.
81. Gratshev, D., et al., *Sphingosine kinase as a regulator of calcium entry through autocrine sphingosine 1-phosphate signaling in thyroid FRTL-5 cells*. *Endocrinology*, 2009. **150**(11): p. 5125-34.
82. Pulli, I., et al., *Sphingolipid-mediated calcium signaling and its pathological effects*. *Biochim Biophys Acta Mol Cell Res*, 2018. **1865**(11 Pt B): p. 1668-1677.
83. Cummings, R.J., et al., *Phospholipase D activation by sphingosine 1-phosphate regulates interleukin-8 secretion in human bronchial epithelial cells*. *J Biol Chem*, 2002. **277**(33): p. 30227-35.
84. Desai, N.N., et al., *Sphingosine-1-phosphate, a metabolite of sphingosine, increases phosphatidic acid levels by phospholipase D activation*. *J Biol Chem*, 1992. **267**(32): p. 23122-8.
85. Kiss, Z., K.S. Crilly, and W.H. Anderson, *Extracellular sphingosine 1-phosphate stimulates formation of ethanolamine from phosphatidylethanolamine: modulation of sphingosine 1-phosphate-induced mitogenesis by ethanolamine*. *Biochem J*, 1997. **328 (Pt 2)**(Pt 2): p. 383-91.

References

86. Merrill, A.H., Jr. and V.L. Stevens, *Modulation of protein kinase C and diverse cell functions by sphingosine--a pharmacologically interesting compound linking sphingolipids and signal transduction*. *Biochim Biophys Acta*, 1989. **1010**(2): p. 131-9.
87. Olivera, A. and S. Spiegel, *Sphingosine-1-phosphate as second messenger in cell proliferation induced by PDGF and FCS mitogens*. *Nature*, 1993. **365**(6446): p. 557-60.
88. Olivera, A., et al., *Purification and characterization of rat kidney sphingosine kinase*. *J Biol Chem*, 1998. **273**(20): p. 12576-83.
89. Stoffel, W., D. LeKim, and G. Sticht, *Distribution and properties of dihydrosphingosine-1-phosphate aldolase (sphinganine-1-phosphate alkanal-lyase)*. *Hoppe Seylers Z Physiol Chem*, 1969. **350**(10): p. 1233-41.
90. Kunkel, G.T., et al., *Targeting the sphingosine-1-phosphate axis in cancer, inflammation and beyond*. *Nat Rev Drug Discov*, 2013. **12**(9): p. 688-702.
91. Adams, D.R., S. Pyne, and N.J. Pyne, *Sphingosine Kinases: Emerging Structure-Function Insights*. *Trends Biochem Sci*, 2016. **41**(5): p. 395-409.
92. Don, A.S. and H. Rosen, *A lipid binding domain in sphingosine kinase 2*. *Biochem Biophys Res Commun*, 2009. **380**(1): p. 87-92.
93. Spiegel, S., et al., *New insights into functions of the sphingosine-1-phosphate transporter SPNS2*. *J Lipid Res*, 2019. **60**(3): p. 484-489.
94. Nguyen, L.N., et al., *Mfsd2a is a transporter for the essential omega-3 fatty acid docosahexaenoic acid*. *Nature*, 2014. **509**(7501): p. 503-6.
95. Hediger, M.A., et al., *The ABCs of solute carriers: physiological, pathological and therapeutic implications of human membrane transport proteins* Introduction. *Pflugers Arch*, 2004. **447**(5): p. 465-8.
96. Pao, S.S., I.T. Paulsen, and M.H. Saier, Jr., *Major facilitator superfamily*. *Microbiol Mol Biol Rev*, 1998. **62**(1): p. 1-34.
97. Reddy, V.S., et al., *The major facilitator superfamily (MFS) revisited*. *FEBS J*, 2012. **279**(11): p. 2022-35.
98. Perland, E., et al., *The Novel Membrane-Bound Proteins MFSD1 and MFSD3 are Putative SLC Transporters Affected by Altered Nutrient Intake*. *J Mol Neurosci*, 2017. **61**(2): p. 199-214.
99. Perland, E., et al., *The Putative SLC Transporters Mfsd5 and Mfsd11 Are Abundantly Expressed in the Mouse Brain and Have a Potential Role in Energy Homeostasis*. *PLoS One*, 2016. **11**(6): p. e0156912.
100. Sreedharan, S., et al., *Long evolutionary conservation and considerable tissue specificity of several atypical solute carrier transporters*. *Gene*, 2011. **478**(1-2): p. 11-8.
101. Law, C.J., P.C. Maloney, and D.N. Wang, *Ins and outs of major facilitator superfamily antiporters*. *Annu Rev Microbiol*, 2008. **62**: p. 289-305.
102. Colas, C., P.M. Ung, and A. Schlessinger, *SLC Transporters: Structure, Function, and Drug Discovery*. *Medchemcomm*, 2016. **7**(6): p. 1069-1081.
103. Perland, E. and R. Fredriksson, *Classification Systems of Secondary Active Transporters*. *Trends Pharmacol Sci*, 2017. **38**(3): p. 305-315.
104. Vu, T.M., et al., *Mfsd2b is essential for the sphingosine-1-phosphate export in erythrocytes and platelets*. *Nature*, 2017. **550**(7677): p. 524-528.
105. Nguyen, T.Q., et al., *Erythrocytes efficiently utilize exogenous sphingosines for S1P synthesis and export via Mfsd2b*. *J Biol Chem*, 2021. **296**: p. 100201.
106. Sanchez, T. and T. Hla, *Structural and functional characteristics of S1P receptors*. *J Cell Biochem*, 2004. **92**(5): p. 913-22.
107. Brinkmann, V., et al., *The immune modulator FTY720 targets sphingosine 1-phosphate receptors*. *J Biol Chem*, 2002. **277**(24): p. 21453-7.

References

108. Brunkhorst, R., R. Vutukuri, and W. Pfeilschifter, *Fingolimod for the treatment of neurological diseases-state of play and future perspectives*. Front Cell Neurosci, 2014. **8**: p. 283.
109. Graler, M.H. and E.J. Goetzl, *The immunosuppressant FTY720 down-regulates sphingosine 1-phosphate G-protein-coupled receptors*. FASEB J, 2004. **18**(3): p. 551-3.
110. Pham, T.H., et al., *S1P1 receptor signaling overrides retention mediated by G alpha i-coupled receptors to promote T cell egress*. Immunity, 2008. **28**(1): p. 122-33.
111. Thangada, S., et al., *Cell-surface residence of sphingosine 1-phosphate receptor 1 on lymphocytes determines lymphocyte egress kinetics*. J Exp Med, 2010. **207**(7): p. 1475-83.
112. Allende, M.L., et al., *Expression of the sphingosine 1-phosphate receptor, S1P1, on T-cells controls thymic emigration*. J Biol Chem, 2004. **279**(15): p. 15396-401.
113. Kappos, L., et al., *Siponimod versus placebo in secondary progressive multiple sclerosis (EXPAND): a double-blind, randomised, phase 3 study*. Lancet, 2018. **391**(10127): p. 1263-1273.
114. Goodman, A.D., N. Anadani, and L. Gerwitz, *Siponimod in the treatment of multiple sclerosis*. Expert Opin Investig Drugs, 2019. **28**(12): p. 1051-1057.
115. Cao, L., et al., *Siponimod for multiple sclerosis*. Cochrane Database Syst Rev, 2021. **11**(11): p. CD013647.
116. Lamb, Y.N., *Ozanimod: First Approval*. Drugs, 2020. **80**(8): p. 841-848.
117. Cohen, J.A., et al., *Safety and efficacy of ozanimod versus interferon beta-1a in relapsing multiple sclerosis (RADIANCE): a multicentre, randomised, 24-month, phase 3 trial*. Lancet Neurol, 2019. **18**(11): p. 1021-1033.
118. Markham, A., *Ponesimod: First Approval*. Drugs, 2021. **81**(8): p. 957-962.
119. Ianniello, A. and C. Pozzilli, *Ponesimod to treat multiple sclerosis*. Drugs Today (Barc), 2021. **57**(12): p. 745-758.
120. Dickson, M.A., et al., *A phase I clinical trial of safinol in combination with cisplatin in advanced solid tumors*. Clin Cancer Res, 2011. **17**(8): p. 2484-92.
121. Buehrer, B.M. and R.M. Bell, *Inhibition of sphingosine kinase in vitro and in platelets. Implications for signal transduction pathways*. J Biol Chem, 1992. **267**(5): p. 3154-9.
122. Companioni, O., et al., *Targeting Sphingolipids for Cancer Therapy*. Front Oncol, 2021. **11**: p. 745092.
123. Antoon, J.W., et al., *Antiestrogenic effects of the novel sphingosine kinase-2 inhibitor ABC294640*. Endocrinology, 2010. **151**(11): p. 5124-35.
124. French, K.J., et al., *Pharmacology and antitumor activity of ABC294640, a selective inhibitor of sphingosine kinase-2*. J Pharmacol Exp Ther, 2010. **333**(1): p. 129-39.
125. Chumanevich, A.A., et al., *Suppression of colitis-driven colon cancer in mice by a novel small molecule inhibitor of sphingosine kinase*. Carcinogenesis, 2010. **31**(10): p. 1787-93.
126. Li, P.H., et al., *A sphingosine kinase-1 inhibitor, SKI-II, induces growth inhibition and apoptosis in human gastric cancer cells*. Asian Pac J Cancer Prev, 2014. **15**(23): p. 10381-5.
127. Antoon, J.W., et al., *Dual inhibition of sphingosine kinase isoforms ablates TNF-induced drug resistance*. Oncol Rep, 2012. **27**(6): p. 1779-86.
128. Leroux, M.E., et al., *Sphingolipids and the sphingosine kinase inhibitor, SKI II, induce BCL-2-independent apoptosis in human prostatic adenocarcinoma cells*. Prostate, 2007. **67**(15): p. 1699-717.
129. Noack, J., et al., *A sphingosine kinase inhibitor combined with temozolomide induces glioblastoma cell death through accumulation of dihydrosphingosine and dihydroceramide, endoplasmic reticulum stress and autophagy*. Cell Death Dis, 2014. **5**: p. e1425.
130. Watters, R.J., et al., *Targeting glucosylceramide synthase synergizes with C6-ceramide nanoliposomes to induce apoptosis in natural killer cell leukemia*. Leuk Lymphoma, 2013. **54**(6): p. 1288-96.

References

131. LeBlanc, F.R., et al., *Sphingosine kinase inhibitors decrease viability and induce cell death in natural killer-large granular lymphocyte leukemia*. *Cancer Biol Ther*, 2015. **16**(12): p. 1830-40.
132. Li, Y., et al., *Combined effects on leukemia cell growth by targeting sphingosine kinase 1 and sirtuin 1 signaling*. *Exp Ther Med*, 2020. **20**(6): p. 262.
133. French, K.J., et al., *Antitumor activity of sphingosine kinase inhibitors*. *J Pharmacol Exp Ther*, 2006. **318**(2): p. 596-603.
134. Purves, W.K., et al., *Biologie*. 2011.
135. Guizouarn, H. and B. Allegrini, *Erythroid glucose transport in health and disease*. *Pflügers Archiv - European Journal of Physiology*, 2020. **472**(9): p. 1371-1383.
136. Gottlieb, Y., et al., *Physiologically aged red blood cells undergo erythrophagocytosis in vivo but not in vitro*. *Haematologica*, 2012. **97**(7): p. 994-1002.
137. Wang, S., et al., *AMPKalpha1 deletion shortens erythrocyte life span in mice: role of oxidative stress*. *J Biol Chem*, 2010. **285**(26): p. 19976-85.
138. Lipowsky, R., E. Sackmann, and A.J. Hoff, *Structure and Dynamics of Membranes I. from Cells to Vesicles*. *Handbook of Biological Physics*, 1995. **1**.
139. Montel-Hagen, A., M. Sitbon, and N. Taylor, *Erythroid glucose transporters*. *Current Opinion in Hematology*, 2009. **16**(3): p. 165-172.
140. Pappu, R., et al., *Promotion of lymphocyte egress into blood and lymph by distinct sources of sphingosine-1-phosphate*. *Science*, 2007. **316**(5822): p. 295-8.
141. Venkataraman, K., et al., *Vascular endothelium as a contributor of plasma sphingosine 1-phosphate*. *Circ Res*, 2008. **102**(6): p. 669-76.
142. Zhang, B., et al., *Correlation of high density lipoprotein (HDL)-associated sphingosine 1-phosphate with serum levels of HDL-cholesterol and apolipoproteins*. *Atherosclerosis*, 2005. **178**(1): p. 199-205.
143. Yatomi, Y., et al., *Sphingosine 1-phosphate, a bioactive sphingolipid abundantly stored in platelets, is a normal constituent of human plasma and serum*. *J Biochem*, 1997. **121**(5): p. 969-73.
144. Okajima, F., *Plasma lipoproteins behave as carriers of extracellular sphingosine 1-phosphate: is this an atherogenic mediator or an anti-atherogenic mediator?* *Biochim Biophys Acta*, 2002. **1582**(1-3): p. 132-7.
145. Berdyshev, E.V., et al., *Quantitative analysis of sphingoid base-1-phosphates as bisacetylated derivatives by liquid chromatography-tandem mass spectrometry*. *Anal Biochem*, 2005. **339**(1): p. 129-36.
146. Kowalski, G.M., et al., *Plasma sphingosine-1-phosphate is elevated in obesity*. *PLoS One*, 2013. **8**(9): p. e72449.
147. Kharel, Y., et al., *Sphingosine kinase type 2 inhibition elevates circulating sphingosine 1-phosphate*. *Biochemical Journal*, 2012. **447**(1): p. 149-157.
148. Hänel, P., P. Andréani, and M.H. Gräler, *Erythrocytes store and release sphingosine 1-phosphate in blood*. *Faseb j*, 2007. **21**(4): p. 1202-9.
149. Levkau, B., *HDL-S1P: cardiovascular functions, disease-associated alterations, and therapeutic applications*. *Front Pharmacol*, 2015. **6**: p. 243.
150. Murata, N., et al., *Quantitative measurement of sphingosine 1-phosphate by radioreceptor-binding assay*. *Anal Biochem*, 2000. **282**(1): p. 115-20.
151. Pitson, S.M., et al., *Activation of sphingosine kinase 1 by ERK1/2-mediated phosphorylation*. *EMBO J*, 2003. **22**(20): p. 5491-500.
152. Igarashi, N., et al., *Sphingosine kinase 2 is a nuclear protein and inhibits DNA synthesis*. *J Biol Chem*, 2003. **278**(47): p. 46832-9.
153. Ito, K., et al., *Lack of sphingosine 1-phosphate-degrading enzymes in erythrocytes*. *Biochem Biophys Res Commun*, 2007. **357**(1): p. 212-7.

References

154. Sun, K., et al., *Sphingosine-1-phosphate promotes erythrocyte glycolysis and oxygen release for adaptation to high-altitude hypoxia*. Nat Commun, 2016. **7**: p. 12086.
155. Deng, D. and N. Yan, *GLUT, SGLT, and SWEET: Structural and mechanistic investigations of the glucose transporters*. Protein Sci, 2016. **25**(3): p. 546-58.
156. Thorens, B. and M. Mueckler, *Glucose transporters in the 21st Century*. Am J Physiol Endocrinol Metab, 2010. **298**(2): p. E141-5.
157. Wright, E.M., *Glucose transport families SLC5 and SLC50*. Mol Aspects Med, 2013. **34**(2-3): p. 183-96.
158. Feng, L. and W.B. Frommer, *Structure and function of SemiSWEET and SWEET sugar transporters*. Trends Biochem Sci, 2015. **40**(8): p. 480-6.
159. McCall, A.L., *Stress: Physiology, Biochemistry, and Pathology*. 2019: Academic Press.
160. James, D.E., et al., *Insulin-regulatable tissues express a unique insulin-sensitive glucose transport protein*. Nature, 1988. **333**(6169): p. 183-5.
161. Bogan, J.S., *Regulation of glucose transporter translocation in health and diabetes*. Annu Rev Biochem, 2012. **81**: p. 507-32.
162. Saltiel, A.R. and C.R. Kahn, *Insulin signalling and the regulation of glucose and lipid metabolism*. Nature, 2001. **414**(6865): p. 799-806.
163. Hresko, R.C., et al., *Mammalian Glucose Transporter Activity Is Dependent upon Anionic and Conical Phospholipids*. J Biol Chem, 2016. **291**(33): p. 17271-82.
164. Gould, G.W. and G.I. Bell, *Facilitative glucose transporters: an expanding family*. Trends Biochem Sci, 1990. **15**(1): p. 18-23.
165. Kumar, A., et al., *Glucose deprivation enhances targeting of GLUT1 to lipid rafts in 3T3-L1 adipocytes*. Am J Physiol Endocrinol Metab, 2004. **286**(4): p. E568-76.
166. Reed, B.C., et al., *3T3-L1 adipocyte glucose transporter (HepG2 class): sequence and regulation of protein and mRNA expression by insulin, differentiation, and glucose starvation*. Arch Biochem Biophys, 1990. **279**(2): p. 261-74.
167. Kitzman, H.H., Jr., et al., *Effect of glucose deprivation of GLUT 1 expression in 3T3-L1 adipocytes*. J Biol Chem, 1993. **268**(2): p. 1320-5.
168. Bieberich, E., *Lipid Rafts: Methods and Protocols*, in *Methods in Molecular Biology*, E. Bieberich, Editor., Humana.
169. Lima, S., et al., *TP53 is required for BECN1- and ATG5-dependent cell death induced by sphingosine kinase 1 inhibition*. Autophagy, 2018. **14**(6): p. 942-957.
170. Romero Rosales, K., et al., *Sphingolipid-based drugs selectively kill cancer cells by down-regulating nutrient transporter proteins*. Biochem J, 2011. **439**(2): p. 299-311.
171. Kim, S.M., et al., *Targeting cancer metabolism by simultaneously disrupting parallel nutrient access pathways*. J Clin Invest, 2016. **126**(11): p. 4088-4102.
172. Brown, K.A., *Erythrocyte Metabolism and Enzyme Defects*. Laboratory Medicine, 1996. **27**: p. 329-333.
173. van Wijk, R. and W.W. van Solinge, *The energy-less red blood cell is lost: erythrocyte enzyme abnormalities of glycolysis*. Blood, 2005. **106**(13): p. 4034-42.
174. Jacquez, J.A., *Red blood cell as glucose carrier: significance for placental and cerebral glucose transfer*. Am J Physiol, 1984. **246**(3 Pt 2): p. R289-98.
175. Lin, S. and J.A. Spudich, *Biochemical studies on the mode of action of cytochalasin B. Cytochalasin B binding to red cell membrane in relation to glucose transport*. J Biol Chem, 1974. **249**(18): p. 5778-83.
176. Hoffman, J.F., *The Interaction between Tritiated Ouabain and the Na-K Pump in Red Blood Cells*. J Gen Physiol, 1969. **54**(1): p. 343-53.
177. Chien, S., *Red cell deformability and its relevance to blood flow*. Annu Rev Physiol, 1987. **49**: p. 177-92.

References

178. Weed, R.I., P.L. LaCelle, and E.W. Merrill, *Metabolic dependence of red cell deformability*. J Clin Invest, 1969. **48**(5): p. 795-809.
179. Klepper, J., et al., *Glut1 Deficiency Syndrome (Glut1DS): State of the art in 2020 and recommendations of the international Glut1DS study group*. Epilepsia Open, 2020. **5**(3): p. 354-365.
180. Brownlee, M., *Biochemistry and molecular cell biology of diabetic complications*. Nature, 2001. **414**(6865): p. 813-20.
181. Schuster, D.P. and V. Duvuuri, *Diabetes mellitus*. Clin Podiatr Med Surg, 2002. **19**(1): p. 79-107.
182. Weykamp, C., *HbA1c: a review of analytical and clinical aspects*. Ann Lab Med, 2013. **33**(6): p. 393-400.
183. Wang, M. and T.M. Hng, *HbA1c: More than just a number*. Aust J Gen Pract, 2021. **50**(9): p. 628-632.
184. Symeonidis, A., et al., *Impairment of erythrocyte viscoelasticity is correlated with levels of glycosylated haemoglobin in diabetic patients*. Clin Lab Haematol, 2001. **23**(2): p. 103-9.
185. Lenters-Westra, E., et al., *Haemoglobin A1c: Historical overview and current concepts*. Diabetes Res Clin Pract, 2013. **99**(2): p. 75-84.
186. Little, R.R. and D.B. Sacks, *HbA1c: how do we measure it and what does it mean?* Curr Opin Endocrinol Diabetes Obes, 2009. **16**(2): p. 113-8.
187. Wang, Y., et al., *The Relationship between Erythrocytes and Diabetes Mellitus*. J Diabetes Res, 2021. **2021**: p. 6656062.
188. Venerando, B., et al., *Acidic and neutral sialidase in the erythrocyte membrane of type 2 diabetic patients*. Blood, 2002. **99**(3): p. 1064-1070.
189. Patel, K.V., et al., *Red blood cell distribution width and the risk of death in middle-aged and older adults*. Arch Intern Med, 2009. **169**(5): p. 515-23.
190. Xiong, X.F., et al., *Red cell distribution width as a significant indicator of medication and prognosis in type 2 diabetic patients*. Sci Rep, 2017. **7**(1): p. 2709.
191. Loyola-Leyva, A., et al., *Morphological changes in erythrocytes of people with type 2 diabetes mellitus evaluated with atomic force microscopy: A brief review*. Micron, 2018. **105**: p. 11-17.
192. Viskupicova, J., et al., *Effect of high glucose concentrations on human erythrocytes in vitro*. Redox Biol, 2015. **5**: p. 381-387.
193. Nojiri, T., et al., *Modulation of sphingosine-1-phosphate and apolipoprotein M levels in the plasma, liver and kidneys in streptozotocin-induced diabetic mice*. J Diabetes Investig, 2014. **5**(6): p. 639-48.
194. Sui, J., et al., *Sphingolipid metabolism in type 2 diabetes and associated cardiovascular complications*. Exp Ther Med, 2019. **18**(5): p. 3603-3614.
195. Vaisar, T., et al., *Type 2 diabetes is associated with loss of HDL endothelium protective functions*. PLoS One, 2018. **13**(3): p. e0192616.
196. Rapizzi, E., et al., *Sphingosine 1-phosphate increases glucose uptake through trans-activation of insulin receptor*. Cell Mol Life Sci, 2009. **66**(19): p. 3207-18.
197. Moon, M.H., et al., *Antiobesity activity of a sphingosine 1-phosphate analogue FTY720 observed in adipocytes and obese mouse model*. Exp Mol Med, 2012. **44**(10): p. 603-14.
198. Qi, Y., et al., *Loss of sphingosine kinase 1 predisposes to the onset of diabetes via promoting pancreatic β -cell death in diet-induced obese mice*. Faseb j, 2013. **27**(10): p. 4294-304.
199. Zhao, Z., et al., *FTY720 normalizes hyperglycemia by stimulating β -cell in vivo regeneration in db/db mice through regulation of cyclin D3 and p57(KIP2)*. J Biol Chem, 2012. **287**(8): p. 5562-73.
200. Oaks, J. and B. Ogretmen, *Regulation of PP2A by Sphingolipid Metabolism and Signaling*. Front Oncol, 2014. **4**: p. 388.

References

201. Kremmer, E., et al., *Separation of PP2A core enzyme and holoenzyme with monoclonal antibodies against the regulatory A subunit: abundant expression of both forms in cells*. Mol Cell Biol, 1997. **17**(3): p. 1692-701.
202. Chen, W., et al., *Cancer-associated PP2A Aalpha subunits induce functional haploinsufficiency and tumorigenicity*. Cancer Res, 2005. **65**(18): p. 8183-92.
203. Perrotti, D. and P. Neviani, *Protein phosphatase 2A (PP2A), a drugable tumor suppressor in Ph1(+) leukemias*. Cancer Metastasis Rev, 2008. **27**(2): p. 159-68.
204. Eichhorn, P.J., M.P. Creighton, and R. Bernards, *Protein phosphatase 2A regulatory subunits and cancer*. Biochim Biophys Acta, 2009. **1795**(1): p. 1-15.
205. Guo, F., et al., *Structural basis of PP2A activation by PTPA, an ATP-dependent activation chaperone*. Cell Res, 2014. **24**(2): p. 190-203.
206. Janssens, V. and J. Goris, *Protein phosphatase 2A: a highly regulated family of serine/threonine phosphatases implicated in cell growth and signalling*. Biochem J, 2001. **353**(Pt 3): p. 417-39.
207. Virshup, D.M., *Protein phosphatase 2A: a panoply of enzymes*. Curr Opin Cell Biol, 2000. **12**(2): p. 180-5.
208. Dobrowsky, R.T., et al., *Ceramide activates heterotrimeric protein phosphatase 2A*. J Biol Chem, 1993. **268**(21): p. 15523-30.
209. Kowluru, A. and S.A. Metz, *Ceramide-activated protein phosphatase-2A activity in insulin-secreting cells*. FEBS Lett, 1997. **418**(1-2): p. 179-82.
210. Chalfant, C.E., et al., *The structural requirements for ceramide activation of serine-threonine protein phosphatases*. J Lipid Res, 2004. **45**(3): p. 496-506.
211. Guenther, G.G., et al., *Ceramide starves cells to death by downregulating nutrient transporter proteins*. Proc Natl Acad Sci U S A, 2008. **105**(45): p. 17402-7.
212. Mukhopadhyay, A., et al., *Direct interaction between the inhibitor 2 and ceramide via sphingolipid-protein binding is involved in the regulation of protein phosphatase 2A activity and signaling*. FASEB J, 2009. **23**(3): p. 751-63.
213. Rahman, M.M., et al., *The phosphorylated form of FTY720 activates PP2A, represses inflammation and is devoid of S1P agonism in A549 lung epithelial cells*. Sci Rep, 2016. **6**: p. 37297.
214. Qadri, M., S. ElSayed, and K.A. Elsaid, *Fingolimod Phosphate (FTY720-P) Activates Protein Phosphatase 2A in Human Monocytes and Inhibits Monosodium Urate Crystal-Induced Interleukin-1beta Production*. J Pharmacol Exp Ther, 2021. **376**(2): p. 222-230.
215. Du, Y., A. Kowluru, and T.S. Kern, *PP2A contributes to endothelial death in high glucose: inhibition by benfotiamine*. Am J Physiol Regul Integr Comp Physiol, 2010. **299**(6): p. R1610-7.
216. Hojlund, K., et al., *Effect of insulin on protein phosphatase 2A expression in muscle in type 2 diabetes*. Eur J Clin Invest, 2002. **32**(12): p. 918-23.
217. Salzer, U. and R. Prohaska, *Stomatin, flotillin-1, and flotillin-2 are major integral proteins of erythrocyte lipid rafts*. Blood, 2001. **97**(4): p. 1141-3.
218. Tucker, D.F., et al., *Isolation of state-dependent monoclonal antibodies against the 12-transmembrane domain glucose transporter 4 using virus-like particles*. Proc Natl Acad Sci U S A, 2018. **115**(22): p. E4990-e4999.
219. Manel, N., J.L. Battini, and M. Sitbon, *Human T cell leukemia virus envelope binding and virus entry are mediated by distinct domains of the glucose transporter GLUT1*. J Biol Chem, 2005. **280**(32): p. 29025-9.
220. Manel, N., et al., *The ubiquitous glucose transporter GLUT-1 is a receptor for HTLV*. Cell, 2003. **115**(4): p. 449-59.

References

221. Jeya Paul, J., et al., *Inflammatory Conditions Disrupt Constitutive Endothelial Cell Barrier Stabilization by Alleviating Autonomous Secretion of Sphingosine 1-Phosphate*. *Cells*, 2020. **9**(4).
222. Thomas, N., et al., *Sphingosine-1-phosphate suppresses GLUT activity through PP2A and counteracts hyperglycemia in diabetic red blood cells*. *Nat Commun*, 2023. **14**(1): p. 8329.
223. Allende, M.L., et al., *Mice deficient in sphingosine kinase 1 are rendered lymphopenic by FTY720*. *J Biol Chem*, 2004. **279**(50): p. 52487-92.
224. Qi, H., et al., *Sphingosine Kinase 2 Phosphorylation of FTY720 is Unnecessary for Prevention of Light-Induced Retinal Damage*. *Sci Rep*, 2019. **9**(1): p. 7771.
225. Paugh, S.W., et al., *The immunosuppressant FTY720 is phosphorylated by sphingosine kinase type 2*. *FEBS Lett*, 2003. **554**(1-2): p. 189-93.
226. Juraszek, B. and K.A. Nalecz, *Protein phosphatase PP2A - a novel interacting partner of carnitine transporter OCTN2 (SLC22A5) in rat astrocytes*. *J Neurochem*, 2016. **139**(4): p. 537-551.
227. Liu, L., et al., *Protein phosphatase 2A activation mechanism contributes to JS-K induced caspase-dependent apoptosis in human hepatocellular carcinoma cells*. *Journal of Experimental & Clinical Cancer Research*, 2018. **37**(1): p. 142.
228. Guo, F., et al., *Structural basis of PP2A activation by PTPA, an ATP-dependent activation chaperone*. *Cell Research*, 2014. **24**(2): p. 190-203.
229. Xiong, Y., et al., *Erythrocyte-derived sphingosine 1-phosphate is essential for vascular development*. *J Clin Invest*, 2014. **124**(11): p. 4823-8.
230. Billich, A., et al., *Partial deficiency of sphingosine-1-phosphate lyase confers protection in experimental autoimmune encephalomyelitis*. *PLoS One*, 2013. **8**(3): p. e59630.
231. Ayzenberg, I., R. Hoepner, and I. Kleiter, *Fingolimod for multiple sclerosis and emerging indications: appropriate patient selection, safety precautions, and special considerations*. *Ther Clin Risk Manag*, 2016. **12**: p. 261-72.
232. Miller, L.H., et al., *Interaction between cytochalasin B-treated malarial parasites and erythrocytes. Attachment and junction formation*. *J Exp Med*, 1979. **149**(1): p. 172-84.
233. Bloch, R., *Inhibition of glucose transport in the human erythrocyte by cytochalasin B*. *Biochemistry*, 1973. **12**(23): p. 4799-4801.
234. Pinkofsky, H.B., et al., *Cytochalasin B binding proteins in human erythrocyte membranes. Modulation of glucose sensitivity by site interaction and partial solubilization of binding activities*. *J Biol Chem*, 1978. **253**(14): p. 4930-7.
235. Yan, Q., et al., *Mechanistic insights into GLUT1 activation and clustering revealed by super-resolution imaging*. *Proc Natl Acad Sci U S A*, 2018. **115**(27): p. 7033-7038.
236. Rungaldier, S., et al., *Stomatin interacts with GLUT1/SLC2A1, band 3/SLC4A1, and aquaporin-1 in human erythrocyte membrane domains*. *Biochim Biophys Acta*, 2013. **1828**(3): p. 956-66.
237. Gao, L., et al., *Super-resolution microscopy reveals the insulin-resistance-regulated reorganization of GLUT4 on plasma membranes*. *J Cell Sci*, 2017. **130**(2): p. 396-405.
238. Maraldi, T., et al., *Stem cell factor and H2O2 induce GLUT1 translocation in M07e cells*. *Biofactors*, 2004. **20**(2): p. 97-108.
239. Huang, J., T. Imamura, and J.M. Olefsky, *Insulin can regulate GLUT4 internalization by signaling to Rab5 and the motor protein dynein*. *Proc Natl Acad Sci U S A*, 2001. **98**(23): p. 13084-9.
240. Suzuki, K. and T. Kono, *Evidence that insulin causes translocation of glucose transport activity to the plasma membrane from an intracellular storage site*. *Proc Natl Acad Sci U S A*, 1980. **77**(5): p. 2542-5.

References

241. Cushman, S.W. and L.J. Wardzala, *Potential mechanism of insulin action on glucose transport in the isolated rat adipose cell. Apparent translocation of intracellular transport systems to the plasma membrane.* J Biol Chem, 1980. **255**(10): p. 4758-62.
242. Kim, F.J., et al., *HTLV-1 and -2 envelope SU subdomains and critical determinants in receptor binding.* Retrovirology, 2004. **1**: p. 41.
243. Ugi, S., et al., *Protein phosphatase 2A negatively regulates insulin's metabolic signaling pathway by inhibiting Akt (protein kinase B) activity in 3T3-L1 adipocytes.* Mol Cell Biol, 2004. **24**(19): p. 8778-89.
244. Li, J., et al., *Dysregulation of PP2A-Akt interaction contributes to Sucrose non-fermenting related kinase (SNRK) deficiency induced insulin resistance in adipose tissue.* Mol Metab, 2019. **28**: p. 26-35.
245. Mandavia, C. and J.R. Sowers, *Phosphoprotein Phosphatase PP2A Regulation of Insulin Receptor Substrate 1 and Insulin Metabolic Signaling.* Cardiorenal Med, 2012. **2**(4): p. 308-313.
246. Turchetti, V., et al., *Variations of erythrocyte morphology in different pathologies.* Clin Hemorheol Microcirc, 1997. **17**(3): p. 209-15.
247. Turpin, C., et al., *Enhanced oxidative stress and damage in glycated erythrocytes.* PLoS One, 2020. **15**(7): p. e0235335.
248. Chaurasia, B., et al., *Targeting a ceramide double bond improves insulin resistance and hepatic steatosis.* Science, 2019. **365**(6451): p. 386-392.
249. Sun, K., et al., *Elevated adenosine signaling via adenosine A2B receptor induces normal and sickle erythrocyte sphingosine kinase 1 activity.* Blood, 2015. **125**(10): p. 1643-52.
250. Figler, R.A., et al., *Links between insulin resistance, adenosine A2B receptors, and inflammatory markers in mice and humans.* Diabetes, 2011. **60**(2): p. 669-79.
251. Merighi, S., P.A. Borea, and S. Gessi, *Adenosine receptors and diabetes: Focus on the A(2B) adenosine receptor subtype.* Pharmacol Res, 2015. **99**: p. 229-36.
252. Resnick, L.M., et al., *Cellular ions in hypertension, diabetes, and obesity. A nuclear magnetic resonance spectroscopic study.* Hypertension, 1991. **17**(6 Pt 2): p. 951-7.

13 Erklärungen

13.1 Eidesstattliche Versicherung

Ich, Frau Nadine Thomas, versichere an Eides statt, dass die vorliegende Dissertation von mir selbstständig und ohne unzulässige fremde Hilfe unter Beachtung der “Grundsätze zur Sicherung guter wissenschaftlicher Praxis an der Heinrich-Heine-Universität Düsseldorf” erstellt worden ist.

Des Weiteren versichere ich, dass ich diese Dissertation nur in diesem und keinem anderen Promotionsverfahren eingereicht habe und dass diesem Promotionsverfahren kein gescheitertes Promotionsverfahren vorausgegangen ist.

Düsseldorf, den 18.05.2014

Unterschrift

13.2 Bemerkung / Remark

Diese Arbeit ist die Grundlage für einen wissenschaftlichen Artikel, der am 14.12.2023 in der Zeitschrift Nature communications veröffentlicht wurde. Thomas, Nadine et al. "Sphingosine-1-phosphate suppresses GLUT activity through PP2A and counteracts hyperglycemia in diabetic red blood cells." Teile der für diese Dissertation gesammelten Daten sind auch im veröffentlichten Manuskript zu finden.

This work is the basis for a scientific article published by the journal Nature communications on 14.12.2023. Thomas, Nadine et al. "Sphingosine-1-phosphate suppresses GLUT activity through PP2A and counteracts hyperglycemia in diabetic red blood cells." Data collected for this dissertation are partially be found in the published manuscript.